

ISSN 0385-2520

Rock Magnetism and Paleogeophysics

Volume 14
December 1987

DELP Publication No. 17



Edited by Rock Magnetism and Paleogeophysics Research Group in Japan

Published by the Japanese National Committee for the
Dynamics and Evolution of the Lithosphere Project (DELP)

Rock Magnetism and Paleogeophysics

Volume 14
December 1987

DELP Publication No. 17



Edited by Rock Magnetism and Paleogeophysics Research Group in Japan

Published by the Japanese National Committee for the
Dynamics and Evolution of the Lithosphere Project (DELP)

まえがき

本書は岩石磁気学・古地磁気学研究グループの1987年度の年次研究報告書であり、「国際リソスフェア計画フェア探査開発計画 (Dynamics and Evolution of the Lithosphere Project, DELP)」の成果報告 (DELP Publication) 第17号として刊行されるものである。

岩石磁気学・古地磁気学研究グループでは、以前から Annual Report として英文の報文集を刊行してきた。(Annual Progress Report of the Rock Magnetism (Paleogeophysics) Research Group in Japan, 1963, 1964, 1965, 1969; Rock Magnetism and Paleogeophysics, 1973-present)。これらの報文集は図書館などからの寄贈要請も多く、諸外国の関連分野の研究者によってかなり広く利用されている。このような経過からこの報文集もすべて英文によって編集された。日本国内の方々には幾分不自由をおかけすることになると思うが、以上の事情によることをご理解いただきたい。

DELP計画は昭和60年度から開始されすでに3年が経過した。我々の研究グループは課題5「日本列島の構造発達」に参加し、日本列島及びその周辺のテクトニックな発展の歴史を解明しようと努力を続けている。更に昨年度からグローバル・ジオサイエンス・トランセクトがとりあげられることになり、課題5の重要な研究目標となった。課題5の研究成果の一部は、7月20日-22日に筑波で開かれた研究会で発表された。この研究会のプログラムは目次の後に示されており、また、ここで発表された論文の多くは本研究報告に収められている。

なお、本書はあくまでも extended abstract 集であり、ここに収録された研究はいずれ正式の論文として発表されることになる。投稿中のものや投稿予定のはっきりしているものについては各報文の最後にそのことが示されているので引用される場合にはできるだけ正式の論文を参照していただくようお願いしたい。

本書の刊行及び研究会の開催については、文部省国際共同研究等経費「リソスフェア探査開発計画 (DELP)」(代表: 秋本俊一) より援助を受けた。ここに記して感謝の意を表す。

1987年12月

岩石磁気学・古地磁気学研究グループ

PREFACE

This volume is the annual progress report of the Rock Magnetism and Paleogeophysics Research Group in Japan for the year 1987. We have published annual reports with a title *Annual Progress Report of the Rock Magnetism (Paleogeophysics) Research Groups in Japan* four times between 1963 and 1967. In 1973, publication of the annual report was resumed with the present title of *Rock Magnetism and Paleogeophysics* and the reports have been published annually since then (except 1976).

As the previous reports were so, this volume contains a collection of summaries, extended abstracts or brief notes of the research works carried out in our group this year. Many of the reports contain materials which may undergo a significant change or may be revised as the research activity continues. In this respect, the readers are warned to regard them as tentative, and are also requested to refer from a complete paper if such is published as a final result. (Names of journals appear at the end of individual articles if they are in press, submitted, or in preparation for submission to some scientific journals).

This volume is published with a financial aid from Ministry of Education, Science and Culture for the Dynamics and Evolution of the Lithosphere Project (DELP). It is Publication No. 17 of the Japanese DELP Program. We thank other members of the Lithosphere Project for help and encouragements.

Tokyo
December 1987

Masaru Kono
Editor

Rock Magnetism and Paleogeophysics
Research Group in Japan

Table of Contents

まえがき	ii
Preface	iii
Table of Contents	iv
Rock Magnetism and Paleogeophysics Symposium 19	vii

ROCK MAGNETISM

M. Funaki, I. Taguchi, J. Danon, and T. Nagata	1
Magnetic Studies of the Bocaiuva Iron Meteorite	
Y. Fujiwara, P. Gautam, M. Yoshida and Y. Katsui	7
On the Nature of Remanence in the Andesite Pumice with Self-Reversed Magnetization from the Nevado del Ruiz, Colombia	
H. Morinaga, M. Kamino, H. Inokuchi, and K. Yaskawa	13
Remanent Magnetization of Synthetic Stalagmites	

PALEOMAGNETISM: QUATERNARY (JAPAN)

H. Morinaga, H. Inokuchi, and K. Yaskawa	18
Secular Variation of the Geomagnetic Field Deduced from Paleomagnetism of Stalagmites in Japan	
H. Kinoshita and T. Akimoto	23
Paleomagnetic Results of Izu and Hakone Volcanoes Conducted by Chiba University, 1980-1985	
E. Kikawa, M. Koyama and H. Kinoshita	24
Paleomagnetism of Quaternary Volcanics in the Izu Peninsula and Adjacent Areas, Japan, and Its Tectonic Significance	
A. Hayashida and T. Yokoyama	27
Brunhes/Matuyama Polarity Epoch Boundary in the Osaka Group, Southwest Japan	
H. Ueno, M. Nedachi, Y. Urashima, K. Ibaragi and R. Suzuki	31
Paleomagnetism of the Hishikari Gold Deposits; Preliminary Report	

H. Domen	36
Progress Note on Paleo/Rock Magnetic Study of Andesites from the Central Yamaguchi Prefecture, West Japan	
M. Miki, T. Matsuda and Y. Otofujii	38
Clockwise Rotation of the South Ryukyu Arc Inferred from Paleomagnetism	

PALEOMAGNETISM: TERTIARY AND OLDER (JAPAN)

C. Itota, H. Morinaga, H. Inokuchi, K. Yaskawa and S. Ishida	40
The Paleomagnetic Age-Determination of the Kobe Sedimentary Group	
Y. Itoh	42
Magnetostatigraphy of Neogene Rocks around the Yatsuo Area in Toyama Prefecture, Japan	
T. Nishitani and S. Tanoue	46
Paleomagnetic Investigation for the Oga Peninsula in Northeast Japan	
K. Kodama and T. Baba	52
A Magnetatigraphic Study of Cretaceous-Paleogene Deposits Amakusa-Shimajima, Kyushu, Southwest Japan	
M. Torii and H. Tsurudome	59
Paleomagnetic Results from the Late Cretaceous Koto Rhyolites, Southwest Japan (II)	

PALEOMAGNETISM: ASIA AND PACIFIC

H. Kinoshita and T. Furuta	66
Paleomagnetism of Hole 504B, Costa Rica Ridge: Rock Magnetism and Formation Magnetism	
P. Gautam and M. Yoshida	68
On the Secondary Magnetizations Observed in Nawakot Complex Rocks, Malekhu Area, Central Nepal	
Y. Adachi, H. Inokuchi, Y. Otofujii, N. Isezaki and K. Yaskawa	72
Rotation of the Philippine Sea Plate Inferred from Paleomagnetism of the Palau and the Yap Island	
H. Katao, H. Morinaga, M. Hyodo, H. Inokuchi, J. Matsuda and K. Yaskawa	75
Paleomagnetism and K-Ar Ages in Hiba-oa Island, Marquesas, French Polynesia	
Y. Otofujii, S. Funahara, J. Matsuo, F. Murata, T. Nishiyama, X. Zheng and K. Yaskawa	79
Paleomagnetic Evidence for Tectonic Deformation of the Narrow Zone Along the Indus-Zangbo Suture Between India and Eurasia	

Y. Otofuji	81
Large Northward Translation of East Asia During Last 20 My Inferred from Polar Wandering Path for East Asia	

M. Funaki, M. Yoshida and P.W. Vitanage	87
Paleomagnetic Study of Precambrian Rocks of Sri Lanka in View of Gondwana Reconstruction with Antarctica	

MAGNETIC ANOMALIES, CRUSTAL STRUCTURES

T. Yamazaki	92
Magnetization of Erimo Seamount	

H. Kinoshita and N. Matsuda	96
Magnetic Anomaly, Crustal Structure and Lithosphere Destruction	

H. Kinoshita, R. Morijiri and T. Nagao	97
Crustal Structure and Magnetic Anomaly in Southern Part of Boso Pen- insula, Chiba, Japan	

GEOMAGNETIC DYNAMO, RARE GASES

M. Kono and M. Hoshi	98
The Rikitake Two-Disk Dynamo System: Statistical Properties and Growth of Instability	

I. Kaneoka	106
Noble Gas Systematics in the Earth's Interior -- Classification of Noble Gas Components	

Author Index	114
--------------------	-----

ROCK MAGNETISM AND PALEOGEOPHYSICS SYMPOSIUM 19

The 19th Annual Symposium of Rock Magnetism and Paleogeophysics was held between 20th and 22nd of July, 1987, at Tsukuba Kenshu Center in Tsukuba Science City.

Monday 20 July Afternoon

1. N. Niitsuma (Shizuoka University)
Neogene Package, ODP Leg 117
2. Y. Okamura (Geological Survey of Japan)
Quaternary sea level change detected by seismic profiles and its geological significance
3. T. Yamazaki and Y. Okamura (Geological Survey of Japan)
Subducting seamount and deformation of forearc wedge around Japan
4. Y. Kobayashi (Tsukuba University)
On the echelon structure of the Japanese arc
5. P. Gautam and Y. Fujiwara (Hokkaido University)
On the self-reversal of pumice, Nerado del Ruiz volcano, Columbia
6. M. Koyama (Tokyo Institute of Technology)
Geology and 1986 eruptions of the Oshima Volcano
7. M. Ohno and Y. Hamano (University of Tokyo)
Paleomagnetism of Volcanic Rocks in Izu-Oshima Island (0-1500 B.P.)

Monday 20 July Evening

8. H. Uchimura and M. Kono (Tokyo Institute of Technology)
Paleomagnetic study of Nemuro group, Hokkaido
9. N. Ishikawa (Kyoto University)
Paleomagnetic study of Goto Island
10. A. Hayashida (Doshisha University)
Paleomagnetism of Setouchi Miocene series
11. H. Shibuya (University of Osaka Prefecture)
On presentation of a demagnetization diagram

Tuesday 21 July Morning

12. K. Uto (Geological Survey of Japan)
Temporal variations of Neogene alkaline magmatism in Southwest Japan
13. T. Sumii (Geological Survey of Japan)
Fission-track dating of volcanic ash layers: problems of the dating method itself and on the usage of FTD information
14. T. Tagami (Kyoto University)
Fission-track thermochronology: its principle and application

15. K. Hirooka (Toyama University)
Tectonism in Central Japan inferred from paleomagnetic study
16. N. Niitsuma (Shizuoka University)
Neogene Hawaiian hotspot trace and plate dynamics

Tuesday 21 July Afternoon

17. K. Heki (Radio Research Laboratories)
Measurement of ongoing plate motion by global VLBI
18. T. Seno (Building Research Institute)
On the recent topics of plate Kinematics: NUEVEL 1 and Okhotsk plate
19. M. Nakanishi (Electron Research Institute)
DC-SQUID magnetometer and its recent progress
20. Y. Okubo (Geological Survey of Japan)
Curie depth analysis using aeromagnetic data
21. Y. Hamano and M. Ohno (University of Tokyo)
Inner-hole magnetic field measurement at Mt. Futago in Izu-Oshima Island

Wednesday 22 July Morning

22. P. Gautam (Hokkaido University)
On the magnetic behaviour of Lesser Himalayan volcanic rocks of Tansen area, Nepal
23. M. Funaki (National Polar Research Institute)
Some paleomagnetic relationships between Antarctica and Sri Lanka
24. M. Okada (Shizuoka University)
Paleointensity from sedimentary rock based on ARM method
25. M. Ito (Tsukuba University)
Depositional systems developing Clinofolds
26. M. Kono (Tokyo Institute of Technology)
Solving Bullard-Gellman dynamo equations

MAGNETIC STUDIES OF THE BOCAIUVA IRON METEORITE

M. Funaki¹, I. Taguchi², J. Danon³, and T. Nagata¹

- 1: National Institute of Polar Research, 9-10 Kaga 1-chome, Itabashi-ku, Tokyo 173, Japan
- 2: National Museum of Japanese History, Jyonai 117, Sakura-shi, Chiba 285, Japan
- 3: National Observatory, 77 Rua General Jose, Cristino, São Cristovão, Rio de Janeiro, Brazil

1. Introduction

The Bocaiuva iron has been classified as a IAB meteorite and is unique in its structure which contains about 10 to 15% by volume of silicate inclusions, surrounded by kamacite (6.5wt% Ni), (Desnoyers et al., 1985). Taenite, plessite, chromite, schreibersite and pyrrhotite have been reported. A Widmanstätten pattern of 0.1-0.3 mm wide kamacite bands and Neumann bands are present. Magnetite, probably maghemite and goethite are often found at the metal-silicate boundaries and are observed to fill the cracks in metal and silicates. The Mössbauer spectra of a thin slice sample and an extracted sample by HCl from Bocaiuva shows only the presence of kamacite and disordered taenite from 33 to 36% Ni contents respectively (Araujo et al., 1983). Scorzelli and Danon (1986) reported the taenite and schreibersite in the extracted materials by HCl. There is no evidence for the presence of ordered FeNi tetrataenite phase by Mossbauer spectroscopy, which suggests a rather fast cooling rate of the meteorite. In the present paper Bocaiuva was investigated magnetically and metallographically in order to understand the stability of its natural remanent magnetization (NRM).

2. Natural remanent magnetization (NRM), AF and thermal demagnetizations

The original NRM of a bulk sample A of Bocaiuva has been found to be 1.519×10^{-2} Am²/kg. It was demagnetized up to 50 mT by 3 axes AF demagnetizer. The original NRM intensity, decreased steeply by 5 mT, then gradually to 50 mT. The variations of NRM components using a Zijderveld projection are shown in Fig. 1. The components decompose to 3 stages; the first stage is a relatively soft magnetic component up to 10 mT characterized by a large demagnetization of vertical component; the second stage is a stable one from 10 to 40 mT shifting toward zero for the horizontal components and shifting horizontally for the vertical component; the third stage is a relatively stable one from 40 to 50 mT shifting flat for the both components. The median demagnetization field (MDF) value of this sample is about 5 mT.

The samples B and C were thermally demagnetized from 50 to 750°C in steps 50°C. The sample B, having only stable NRM component by carrying out of AF demagnetization to 15 mT, has relatively stable NRM between room temperature and 550-600°C; the intensity (4.760×10^{-3} Am²/kg) decreases smoothly to 550°C and the directions change within a small area up to 600°C. However, unstable NRM is observed from 550-600 to 750°C. A NRM blocking temperature is defined at 550°C. Sample C is a original sample having 3.045×10^{-2} Am²/kg which is stronger about 10 times than sample B. The variations of NRM intensity are very small from room temperature to 300°C but then decrease abruptly from 300 to 500°C. Change of the directions is small up to 500°C and become large from 550 to 750°C. The NRM blocking temperature is clearly at 550°C.

3. Distribution of NRM directions

A total of 22 samples with an orientation, ranged from 0.071 to 2.8g in

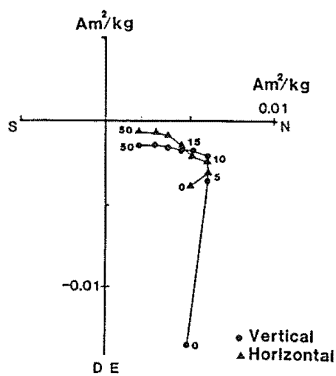


Fig. 1

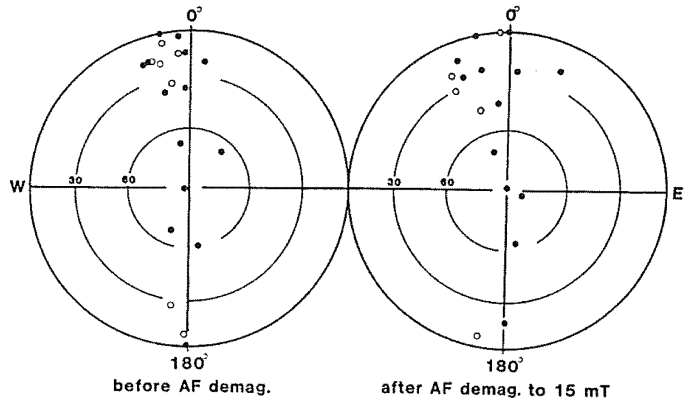


Fig. 2

Fig. 1: AF demagnetization curves of a bulk sample of Bocaiuva. Zijdeveld projection of NRM components.

Fig. 2: Distributions of NRM directions for bulk samples before and after AF demagnetization to 15mT.

weight, were prepared from a block sample of Bocaiuva. The original NRM of every sample was measured and then 18 samples were AF demagnetized by 15mT, which is the optimum AF demagnetization field intensity, by taking away the relatively soft NRM components (the first stage of AF demagnetization).

The variations of the NRM intensities are fairly large among the samples such as 1.1×10^{-1} to 4.6×10^{-3} Am²/kg for the original samples and 1.4×10^{-2} to 4.4×10^{-3} Am²/kg after the AF demagnetization. The respective average intensities are of the order of 10^{-2} and 10^{-3} Am²/kg. The samples with the weaker or stronger NRM intensities distribute at random in the block sample. The NRM directions before and after demagnetization are distributed as shown in Fig. 2. The distribution shows a tendency of approximately alignment along a great circle over a hemisphere. This tendency does not change by demagnetization, although the NRM directions of a few samples shift widely within the great circle by the demagnetization. This indicates that both of the hard and the relatively soft magnetic components of Bocaiuva have been magnetized in a same plain.

4. Magnetic hysteresis properties and thermomagnetic curves

Magnetic hysteresis properties and thermomagnetic (I_S -T) curves have been measured with the bulk of the 1 and 2 samples and with an extracted sample by HCl from the Bocaiuva meteorite. Magnetic hysteresis properties, saturation magnetization (I_S), saturation remanent magnetization (I_R), coercive force (H_C) and remanence coercive force (H_{RC}) were determined using the magnetization curve from -1.4 to +1.4 T in a steady magnetic field at room temperature. These values before and after heating up to 850°C are listed in Table 1, whereas the values H_{RC} could not be obtained due to the weak magnetization as compared with the noise level (about 5 mT). The principal magnetic mineral in both bulk samples appears to be FeNi with low Ni content from their large I_S values (205.5 and 201 Am²/kg for samples 1 and 2 respectively). Small values of I_R and H_C values may suggest multidomain structure of the principal magnetic minerals. These magnetic characteristics do not change obviously by heating treatment to 850°C. For the extracted samples, however, large values of H_C and H_{RC} (23.5 and 66.7 mT respectively) has been observed, which decreases markedly ($H_C=1.0$ and $H_{RC} < 5$ mT) after heating the sample to 650°C. These marked changes of H_C and H_{RC} by heat treatment are explained by existence of tetrataenite phase in the extracted sample.

Table 1. Magnetic hysteresis properties and Curie Points of Bocaiuva.

Sample	Heating	I_S Am ² /kg	I_B Am ² /kg	H_C mT	H_{RC} mT	Tc heating °C	Tc cooling °C
Bulk 1	before	205.5	0.5	4	< 5	760	610 -450
	after	209	0.02	1.5	< 5	725	605
Bulk 2	before	201	0.035	2.5	< 5	745	605
	after	212	0.04	1.0	< 5	735	605
Lamella	before	87.5	1.5	23.5	66.7	310 550	255
	after	82.5	0.005	1.0	< 5	290	260

Thermomagnetic curves (I_S -T curves) were obtained from room temperature up to 850°C under 10^{-2} Pa atmospheric pressure, 200°C/h of heating and cooling rates and 600 mT of steady magnetic field. The 1st and 2nd run curves are shown in Fig. 3 and the Curie points are listed in Table 1. The 1st run I_S -T curve of bulk 1 sample shows a phase transition temperature from bcc to fcc ($\alpha \rightarrow \beta$) at 760°C and from fcc to bcc ($\beta \rightarrow \alpha$) at 610°C suggesting 6% Ni FeNi alloy for the main magnetic mineral. Small change of the Curie point at around 450°C was observed in the cooling curve. In the 2nd run I_S -T curves, the phase transition temperatures decrease to 725°C ($\alpha \rightarrow \beta$) and to 605°C ($\beta \rightarrow \alpha$) suggesting an increase of the Ni content to 8% in kamacite by the heat treatment. The Curie point observed at about 450°C in the 1st run cooling curve disappears in that of 2nd run curve, suggesting that it is due to an unstable phase. In case of the bulk sample 2, the phase transitions were observed at temperature of 745°C ($\alpha \rightarrow \beta$) and 605°C ($\beta \rightarrow \alpha$) for the 1st run cycle and 735°C ($\alpha \rightarrow \beta$) and 605°C ($\beta \rightarrow \alpha$) for the 2nd run cycle. This suggests that the bulk sample 2 consists of 7wt% Ni kamacite originally and 8wt% Ni kamacite after heating to 850°C.

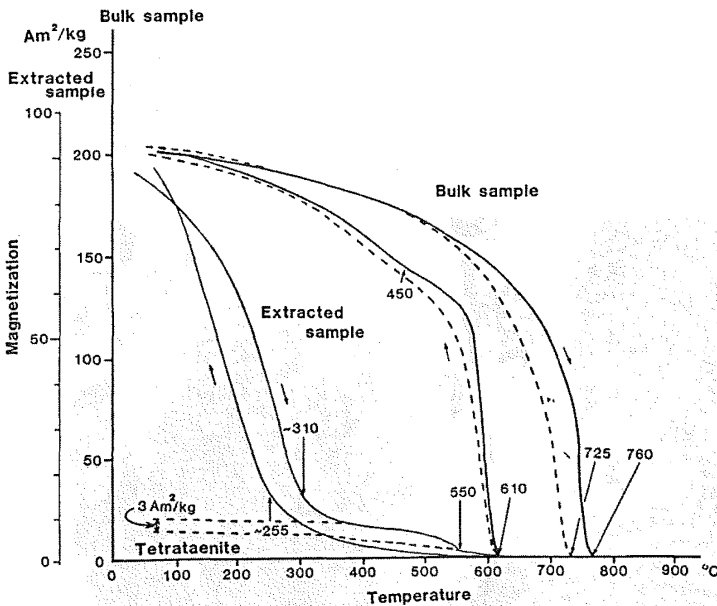


Fig. 3. Thermomagnetic (I_S -T) curves of a bulk sample and an extracted sample by HCl obtained by 0.6T external magnetic field. Solid curves: 1st run I_S -T curves, Dotted curves: 2nd run I_S -T curves.

The I_S -T curves of the extracted samples are irreversible with Curie points at about 310 and 550°C in the heating curve and at about 255°C in cooling curve. The main Curie points observed at about 310 and 255°C can be attributed to the taenite with 34-36% Ni. It is also possible the Curie points results from schreibersite, since this mineral has a Curie point of about 300°C. The I_S -T curve shows a very flat behaviour from 350 to 500°C then decreases abruptly up to 550°C, while there is no significant Curie point around 550°C in the cooling curve. Characteristics of the I_S -T curves between 350 to 550°C are typical of the tetraenaite phase.

The weight of the extracted sample of 0.01305g (2.7%) was obtained from 0.482g of the bulk Bocaiuva sample. If the Is-T curves result from the tetrataenite phase, the magnetization intensity of the phase can be estimated to be about $3 \text{ Am}^2/\text{kg}$. Since the saturation magnetization of a 50%Fe 50%Ni alloy is $85.5 \text{ Am}^2/\text{kg}$, the calculated amount of tetrataenite phase is found to be about 0.1% in weight, if this phase supposed to be saturated at an external magnetic field of 0.6T. Usually tetrataenite does not saturate at 0.6T, but the magnetization shows more than half of the saturation magnetization is attained. It may therefore be concluded that Bocaiuva contains the tetrataenite phase with less than 0.2wt% in the bulk sample.

5. Identifications of NRM carrier by the Bitter pattern method.

In order to study the magnetic carriers in Bocaiuva we used the Bitter pattern method by magnetic fluid. Figure 4 shows the Bitter pattern configuration of magnetic domains on the surface of kamacite. The domain structure of kamacite (5-20 μm in wide and 5-20 μm in length of each laths) shows parallel alignments or eddy patterns being composed of straight laths. After thermal demagnetization to 750°C, these systematic ordering configurations of domain structures collapse. The domain on schreibersite (under 10 μm in wide and 100 μm in length) shows parallel alignment having internal zigzag deformations. No correlation is observed between these domain configurations of kamacite and schreibersite and the NRM directions of Bocaiuva. Small concentration of the magnetic fluid appear on the magnetite veins, although no magnetic fluid concentration appears on the iron-sulphide grains.

The magnetic fluid concentrate heavily along the borders of some taenite lamellae suggesting strong NRM carrier. It consists of linking together of elliptical speckles which have no internal structures as magnetic domains of kamacite. From the speckles fine twings of the concentration branched out into the kamacite field along the kamacite domain walls. The dominant direction of these lamellae is almost parallel to the NRM direction. These taenite grains taking strong NRM disappear after heat treatment at 650°C. The phenomenon is similar to the thermal disordering of tetrataenite lamellae in Toluca iron meteorite reported by Funaki et al. (1986).

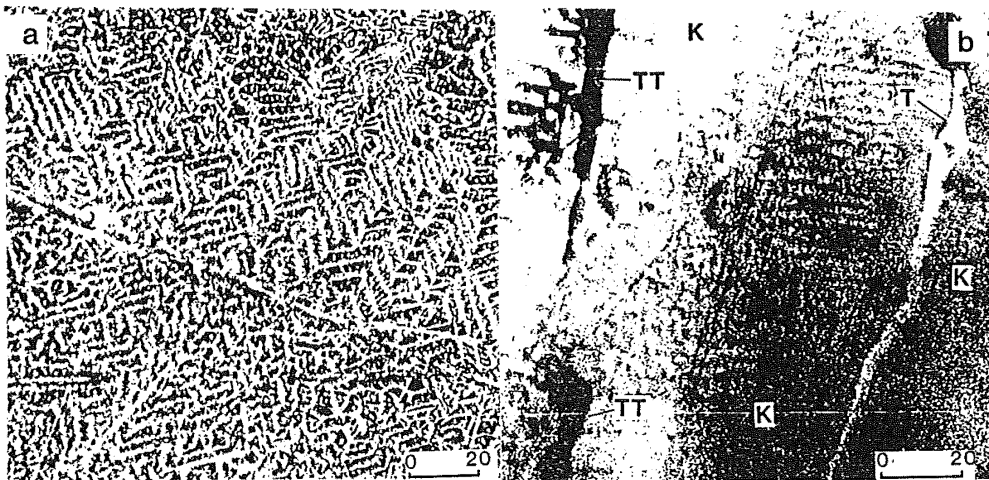


Fig. 4: Features of strong NRM regions of Bocaiuva by the Bitter pattern method. Scale: μm , (a): configurations of magnetic domains of kamacite under dark fields. (b): branched out of extremely twings (tetrataenite) into the kamacite field through domain walls from tetrataenite lamella. K: kamacite, T: taenite, TT:tetrataenite.

6. Discussion

Bulk samples of Bocaiuva exhibit very small coercivity ($H_C=1.5-4.0$ and $H_{RC} < 5$ mT). From the I_S-T curves the main magnetic minerals is found to be kamacite with 6-7wt% Ni. The secondary magnetic minerals, such as taenite, plessite, magnetite and schreibersite which exist in Bocaiuva were investigated by microscopic observations using the Bitter pattern method. Pyrrhotite may be nonmagnetic at room temperature due to absence of characteristic of ferrimagnetic pyrrhotite in I_S-T curves and evidence of concentration of magnetic fluid.

However, extracted samples of Bocaiuva exhibit extremely high coercivities ($H_C=23.5$ and $H_{RC}=66.7$ mT) which decrease to small ($H_C=1$ and $H_{RC} < 5$ mT) by heat treatment at 650°C . This coercivity change is characteristic of the tetrataenite (Nagata et al., 1986). The I_S-T curves of the extracted samples show a main Curie point at 310°C which probably due to an overlap of the Curie points of taenite with 34-36wt% Ni and schreibersite. We used same method for obtaining the extracted samples as that of Scorzelli and Danon (1986) which observed an overlap pattern of the Mossbauer spectrum of taenite and schreibersite.

The I_S-T curves of the extracted samples show a minor amount of tetrataenite phase which, is characterized by flat heating curves from 300 to 550°C with Curie point at 550°C in only heating curves. The Bitter pattern configurations on magnetic grains showed very strong NRM to high nickel taenite lamellae. Funaki et al., (1986) reported the extremely strong NRM of tetrataenite extracted from lamellae of Toluca iron meteorite. Its magnetic characteristics and those observed with Bocaiuva are essentially consistent.

Our results indicate that Bocaiuva includes a small amount of tetrataenite (less than 0.2wt%), as discussed before. No detection of tetrataenite in the bulk samples is due to the very small amount of tetrataenite, as compared with that of kamacite. Even in the extracted samples, tetrataenite may not been detected by previous Mossbauer measurements Araujo et al., 1983; Scorzelli and Danon, 1986) because of overlapping with the much more intense lines of the Ni rich disordered taenite phase.

The NRM in Bocaiuva is very stable against AF demagnetization suggesting a relation with high coercivity magnetic minerals. The NRM decays completely by thermal demagnetization at 550°C , supposing the assumption that it results mainly from tetrataenite. Brecher and Albright (1977) pointed out that all magnetization directions in octahedrites appear to be preferentially associated with the octahedral (111) crystallographic planes. The NRM directions of 22 block samples of Bocaiuva are almost parallel to a dominant plain of lamellar tetrataenite development of the (111) plain. DuBois (1965) studied the magnetic domain configurations of kamacite and schreibersite in Odessa (coarsest octahedrite) and reached the conclusion that the NRM and the domain configuration are roughly related. However, no obvious correlations between the domain configurations and the NRM directions are observed with Bocaiuva. These experimental results of NRM tends to support the assumption that tetrataenite is the NRM carrier for Bocaiuva.

The amount of kamacite is much higher than that of other magnetic minerals in Bocaiuva. On the surface of the kamacite the magnetic multi-domain structures appear clearly by the Bitter pattern method. One would expect that kamacite should contribute to the NRM of Bocaiuva. However, it does not appear that the NRM from kamacite of the multidomain structures affects Bocaiuva strongly due to its good NRM stability.

Among the octahedrite meteorites having kamacite as main magnetic mineral, relatively stable NRM against AF demagnetization have been observed with Y-75031, Y-75105 and ALH-762 (Nagata, 1979), whereas their coercivities are very small. As the former 2 meteorites have a small size, they probably acquired the stable NRM through the earth's atmosphere in presence of the geomagnetic field. ALH-762 is however are relatively large meteorite and the

measurements were effected with samples obtained sufficiently away from its fusion crust, suggesting that they were not affected by heating through the passage in the earth's atmosphere. The samples of Bocaiuva were extracted from inside of the meteorite and the NRM characteristics are very similar to that of ALH-762 meteorite. On the other hand, Toluca (medium octahedrite) has extremely unstable NRM, although it consists relatively large amount of Tetrataenite as compared to Bocaiuva. These experimental evidences suggest that the contribution of kamacite to NRM differs among the octahedrite meteorites.

In case of Bocaiuva, the reason of the weak contribution of kamacite to NRM seems to be due to the fact that the NRM directions of kamacite magnetic domains are completely random, and consequently the integrated NRM is negligible as compared to that arising from tetrataenite.

Desnoyers et al. (1985) indicated that the Bocaiuva cooled rapidly from 1100°C to the temperature where the diffusion in the silicates is stopped, then it must cool down slowly up to 600°C as indicated by the presence of Widmanstätten patterns. From our magnetic and metallographical results, the existence of small amount of tetrataenite phase in Bocaiuva suggest that this meteorite further cooled slowly under 300°C. Bocaiuva exhibit many Neumann bands in the kamacite field due to shocks produced by collisions of the meteorite. Originally tetrataenite could be discovered by temperature increase due to these shock effects and subsequently reformed again by further cooling of the meteorite. Poor development of the tetrataenite phase may result by these type of events.

7. Conclusions

Bocaiuva exhibit a very stable NRM against AF demagnetization, contrasting with low H_C and H_{RC} values. The NRM directions align to a plain related to the octahedrite structure. The NRM is broken down by thermal demagnetization at 550°C. Extremely strong NRM lamellae are observed by the Bitter pattern method but they disappear after heat treatment at 600°C. Extracted lamellae have large H_C and H_{RC} values and present a Curie point at 550°C and the coercivity decreases to small values after heating at 600°C. This magnetic behavior is consistent with that of typical tetrataenite. Probably fine tetrataenite exists in small amounts dispersed in kamacite domain walls besides some tetrataenite in lamellae. One concludes from these results that Bocaiuva cooled down slowly around 300°C, producing the tetrataenite phase in the high Ni regions.

References:

- Araujo, S.I., Danon, J., Scorzelli, R.B. and Azevedo, I.S. (1983), *Meteoritics*, 18, 261.
- Brecher, A. and Albright, L. (1977), *J. Geomag. Geoelectr.*, 29, 379-400.
- Desnoyers C., Christophe Michel-Levy, M. Azevedo, I.S., Scorzelli, R.B., Danon, J. and Galvao da Silva, E. (1985), *Meteoritics*, 20, 1, 113-124.
- DuBois, R.L. (1965), *J. Geomag. Geoelectr.*, 17, 381-390.
- Funaki, M., Nagata, T. and Danon, J. (1986), *Mem. Natl. Inst. Polar Res. Spec. Issue*, 41, 382-393.
- Nagata, T. (1979), *Mem. Natl. Inst. Polar Research, Spec. Issue*, 12, 238-249.
- Scorzelli, R.B. and Danon, J. (1986), *Meteoritics*, 21, 2, 509.

ON THE NATURE OF REMANENCE IN THE ANDESITE PUMICE
WITH SELF-REVERSED MAGNETIZATION
FROM THE NEVADO DEL RUIZ, COLOMBIA

Yoshiki FUJIWARA, Pitambar GAUTAM, Mitsuo YOSHIDA
and
Yoshio KATSUI

Department of Geology & Mineralogy, Faculty of Science,
Hokkaido University, Sapporo 060, Japan

1. Introduction

The occurrence of self-reversal of remanent magnetization in the Nevado del Ruiz 1985 pumice have already been described by Heller et al. (1986). In their study, they demonstrated the reverse nature of the NRM in the pumice and showed that the NRM suddenly changes its polarity from reverse to normal at 120°C, with complete demagnetization of the reverse component around 150-160°C. The remaining normal component disappeared at temperatures from 350 to 400°C on further heating. They observed that the self-reversibility of the remanence in the laboratory conditions was very sensitive to the maximum demagnetization temperatures of 160 - 190°C during which the higher the temperature raised the more suppressed was the reverse component. The two opaque oxide phases of titanomagnetite and ilmenohematite observed were attributed to correspond to the major and minor phases of saturation magnetization with Curie temperatures of 370-410°C and 180-200°C respectively. The titanomagnetite was considered solely to be responsible for the normal component whereas the reverse component was attributed to be the effect of exchange interaction between two intimately mixed phases of ilmenohematite within the lower Curie temperature range. The exact mechanism controlling the self-reversal, however, was not made clear.

This study was initiated with an aim of better understanding of the nature of the remanence in the pyroclastics of the Nevado del Ruiz eruption. We report here some of the preliminary findings concerning the multi-component nature of the remanence. An elaborate discussion is believed to be possible in future as the work progresses further.

2. Samples

The main object of this study is the 1985 Nevado del Ruiz pumice, sampled during the field survey of Ruiz volcano as a part of the Natural Disaster Scientific Research Expedition organized by one of us (Y. K.). The pumice is hornblende-titaniferous phlogopite-orthopyroxene-clinopyroxene andesite in composition and occurs as mostly white (SiO₂ 63%) but partly gray (SiO₂ 60%) varieties (Katsui et al., 1986). Cylindrical specimens (2.54cm in diameter and 2.5cm in length) were drilled

from two pumice samples (R5 and R15) and also from a prehistoric lava (R4) for standard magnetic measurements on a Schonstedt SSM-1A spinner magnetometer.

3. Experimental procedures and results

Magnetic measurements included: measurements of natural remanent magnetization (NRM) of the standard specimens, stepwise thermal demagnetization of specimens with heating in air with steps ranging from 5 to 50°C from room temperature up to 500 - 600°C, partial thermo-remanent magnetization (TRM) acquisition experiments at the ambient geomagnetic field at the laboratory, thermomagnetic analysis of whole-rock (chip) samples, magnetic fractions and heavy fractions (obtained by heavy-liquid separation using Bromoform). In addition, the sample R5 was examined in polished thin section by using reflection microscopy and electron probe micro analysis (EPMA).

a) Remanence and polarity

Table 1 shows the initial NRM and the total laboratory-induced TRM intensities with the polarities for the representative specimens. It is evident that the gray pumice has NRM intensity comparable to that of the lava whereas it is about 5 times higher compared to that of the white pumice. The total TRM intensity is surprisingly same to that of NRM for the gray pumice, implying that the original NRM was also a TRM.

Table 1 Samples and Magnetization Intensity Data

Sample	Description	NRM Intensity ($\times 10^{-3}$ A m $^{-1}$)	TRM	
			Intensity ($\times 10^{-3}$ A m $^{-1}$)	Polarity
R5	Andesite pumice, white	141	167	Reverse
R15-W	Andesite pumice, dominantly white	150	42	Reverse
R15-G	Andesite pumice, dominantly gray	617	617	Reverse
R4	Lava, prehistoric	642	3100	Normal

All pumice specimens acquired TRM in a direction antiparallel to the applied field showing their reverse nature by which it was inferred that the NRM directions were of reverse nature as well (the samples were not field-oriented so that judging from the direct measurements was not possible!). The lava, in contrast, was magnetized parallel to the applied field.

b) Demagnetization behavior

Results of the thermal demagnetization studies for specimen R15-G are presented in Fig. 1. It can be observed that the region from room temperature to about 225°C is reverse-dominated whereas the region above it is dominated by normal polarity. The difference curve clearly indicates the presence of four regions during which either reverse or normal components are being removed. These regions are: 1) reverse, poorly defined (20 to 50°C), 2) normal (100 to 125°C), 3) reverse (150 to 275°C), and 4) normal (350 to 425°C). The white pumice specimens (R5 and R15-W) also exhibited similar component-regions with the only difference that the proportion of intensities carried out by each of these components varied. TRM acquisition curves showed clearly the presence of three regions corresponding approximately to the last three component-regions derived from the difference curves.

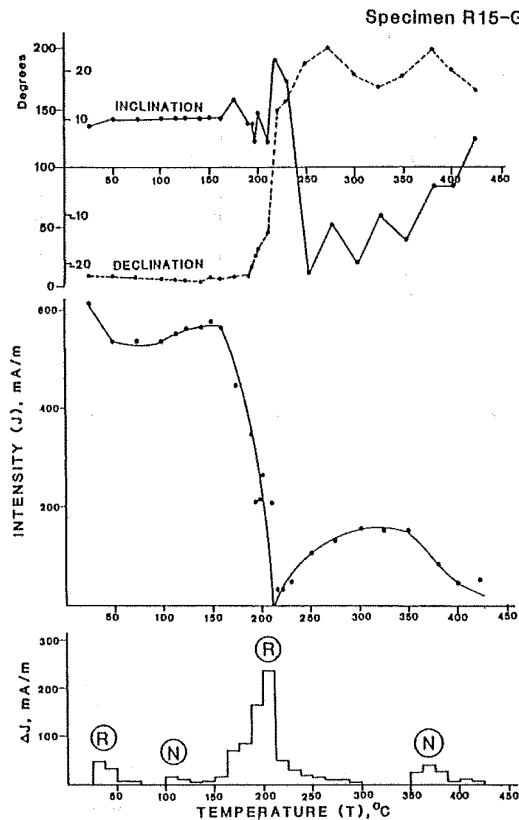


Fig. 1 Results of stepwise thermal demagnetization of R15-G.

Top: Changes in declination, inclination of the remanent vector.

Middle: Variation in intensity of remanent magnetization.

Bottom: Difference intensity curve deduced from the intensity response curve (middle) to show the amount of the intensity removed during successive temperature interval. Only absolute value is plotted. R and N enclosed by circles denote reverse and normal polarity regions, respectively.

Table 2 Representative Electron Probe Microanalysis Data for Titanomagnetite and Titanohematite from Sample R5

Oxides, conc. %	Titanomagnetite		Titanohematite	
	TM-6	TM-10	TH-4	TH-7
SiO ₂	0.08	0.13	0.01	0.02
TiO ₂	7.96	8.56	37.88	38.67
Al ₂ O ₃	1.88	1.95	0.33	0.28
Cr ₂ O ₃	0.38	0.04	0.07	0.11
FeO*	81.42	80.85	55.58	54.04
MnO	0.33	0.34	0.34	0.34
MgO	2.13	2.25	2.79	3.03
CaO	0.01	0.02	0.01	0.04
NiO	0.06	0.06	0.04	0.07
Sum	94.25	94.20	97.05	96.60
Recalculated analysis:				
Fe ₂ O ₃	51.57	50.53	29.87	27.89
FeO	35.02	35.38	28.70	28.94
Total	99.42	99.26	100.04	99.39
Cations on 32 Oxygen basis		Cations on 3 Oxygen basis		
Si	0.023	0.038	0.000	0.001
Ti	1.793	1.925	0.713	0.731
Al	0.663	0.689	0.010	0.008
Cr	0.091	0.009	0.001	0.002
Fe ³⁺	11.615	11.377	0.562	0.527
Fe ²⁺	8.765	8.853	0.601	0.608
Mn	0.083	0.086	0.007	0.007
Mg	0.948	1.004	0.104	0.114
Ca	0.004	0.006	0.000	0.001
Ni	0.014	0.014	0.001	0.001
Total	23.999	24.001	1.999	2.000
Molar fractions: X _{Usp}		Molar fractions: X _{Iilm}		
	0.227	0.245	0.713	0.731

* Total Fe calculated as FeO

Table 3 Average Compositions of Titanomagnetite and Titanohematite in Sample R5 (from EPMA Data)

Classification of grains	Analyzed grains		Mineral	Molar proportion	
	Size, (μm)	No. of grains		Mean value	Standard deviation
Grains with low brownish white reflection with well-developed cracks.	10 - 140	10	Titano-magnetite	X _{Usp} : 0.231	0.021
Grains with high yellowish white reflection with almost absence of cracks.	20 -250	8	Titano-hematite	X _{Iilm} : 0.716	0.010

c) Thermomagnetic analysis

Fig. 2 shows a set of thermomagnetic curves (analyses in vacuum close to 0.26 Pa., heating rate 10°C/min.) for the heavy fraction constituting sample R15. Whole-rock analyses showed only single Curie-point (higher one) curves as opposed to the clear double Curie-points character for magnetic and heavy fractions. Repeated runs for the same sample with varying applied field values showed the clear field-dependence especially well-expressed for the right part of the curve. The repeated heatings in the same applied field yield completely reversible curves.

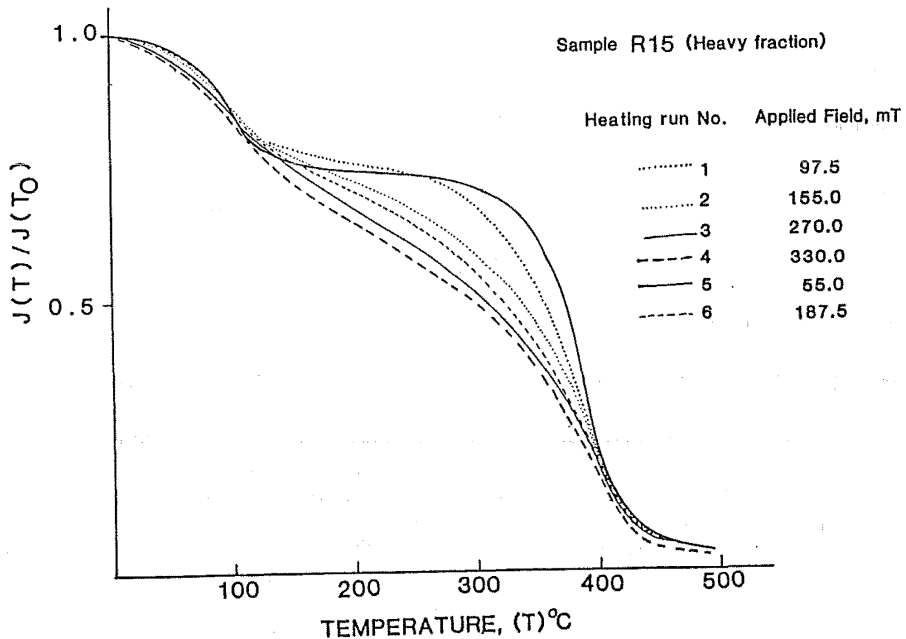


Fig. 2 Double Curie-point thermomagnetic curves showing dependance of the shape on the applied Field.

d) Microscopic and EPMA data

Optical examination of sample R5 revealed the presence of two types of opaques with contrasting reflectivity occurring mostly in isolation to each other but very rarely as twins. Representative EPMA data (analyses by JEOL JXA-733, standard ZAF corrections applied) and relevant information on grains with results of recalculated analyses applying the scheme by Carmichael (1967) are given in Tables 2 & 3. These data suggested the mineralogical phases to be titaomagnetite (X_{Usp} range: 0.704 to 0.731) and titanohematite (X_{Ilm} range: 0.176 to 0.251).

4. Interpretation and discussion

Fig. 3 summarizes the temperature data. Calculated Curie temperatures are based on the assumption of linear variation of the values from -153°C to 578°C for titanomagnetite series and from -200°C to 675°C for titanohematite series members (Collinson, 1983).

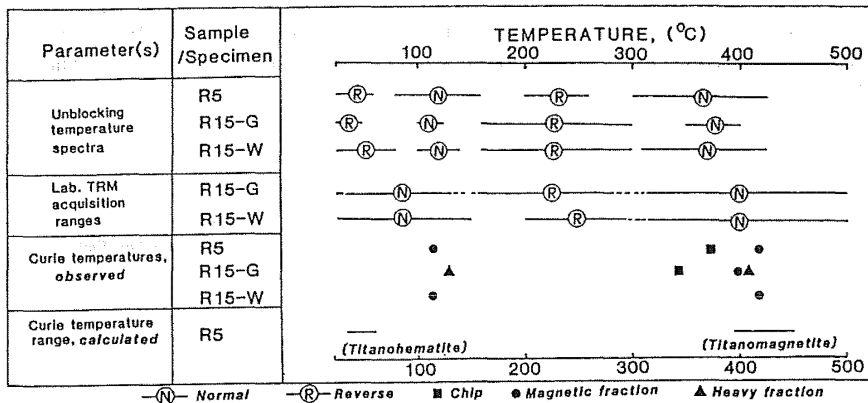


Fig. 3 Summary of the temperature data.

It can be definitely said that the major normal component is carried out by the titanomagnetite phase with variable chemistry having Curie-temperatures close to 400°C . There is a definite correlation between the observed lower Curie-temperature and the minor normal component demagnetization spectra. The major reverse component has a peak demagnetization and acquisition range between $200-225^{\circ}\text{C}$ but no such mineral phase could be detected by thermomagnetic analysis. The exact contribution of the Titanohematite phase also remains open.

In conclusion of this study, we would like to point out that the exact nature of the remanence and the mineral chemistry in the 1985 Nevado Del Ruiz pumice seems to be rather complex. One of the clear differences in previous data (Heller et al., 1986) and ours is that the major reverse magnetization component has higher unblocking temperatures than mentioned earlier. The fact that the titanomagnetite phase contributes to the major normal component and has probably no relation to the reverse magnetization, however, is supported also by our study.

References

- Carmichael, Ian S. E. (1967), *Contr. Mineral. and Petrol.* 14, 36-64.
- Collinson, D. W. (1983) *Paleomagnetism. Techniques and instrumentation* (Chapman & Hall, London), 502.
- Heller, F., J. C. Carracedo and V. Soler (1986) *Nature*, 324, 20, 241-242.
- Katsui, Y., T. Takahashi, S. Egashira, S. Kawachi and H. Watanabe (1986) *Rep. Nat. Disaster Sci. Res., Japan*, B60-7, 102 (in Japanese with abstract in English).

REMANENT MAGNETIZATION OF SYNTHETIC STALAGMITES

Hayao MORINAGA, Masaki KAMINO, Hiroo INOKUCHI,
and Katsumi YASKAWA

Faculty of Science, Kobe University, Nada, Kobe 657, Japan

Natural stalagmite is one of speleothems in limestone caves and grows upward from cave floors as crystals of calcite (CaCO_3). The growth takes place through degassing of carbon dioxide (CO_2) from calcium bicarbonate solution after dropping of the solution from cave ceiling.

Natural stalagmites have very stable remanent magnetizations and keep continuous records of the past geomagnetic field directions as the primary components. It was suggested that directions of the natural remanent magnetization (NRM) are not affected by surface conditions of natural stalagmites (Latham et al., 1979; Morinaga et al., 1987). Palaeomagnetic direction records obtained from natural stalagmites in Japan showed "internal consistencies" within one stalagmite and between two stalagmites from the same limestone cave. The records obtained from three stalagmites in Japan overlapped for the last about 1000 years and were concordant with each other within this interval, also showing "regional consistency".

The directional variation curve obtained from these three stalagmites agreed well with the cave for the last 2000 years obtained from archaeomagnetism (Hirooka, 1971 & 1983) in Japan and did not contradict the curve for the last about 9000 years obtained from palaeomagnetism of a unconsolidated sediment core (Muroi & Yaskawa, 1977; Hyodo & Yaskawa, 1986) in Japan (Morinaga et al., 1987). Subsamples near the surface of natural stalagmites, which were assumed to generate nearly recently, kept almost the same remanent direction as that of the present geomagnetic field in Japan (Morinaga et al., 1987).

We describe here features of remanent magnetization and timing of remanence acquisition for stalagmite-like deposits synthesized using sodium thiosulfate ($\text{Na}_2\text{S}_2\text{O}_3$), and also indicates indirect evidences that natural stalagmites have highly reliable records of the geomagnetic field, through comparison of the remanence with that of synthetic stalagmites.

Sodium thiosulfate is a crystal in room temperature and melts at 48.45°C . A small amount of cave sediments, whose thermomagnetic curve was almost the same as that of

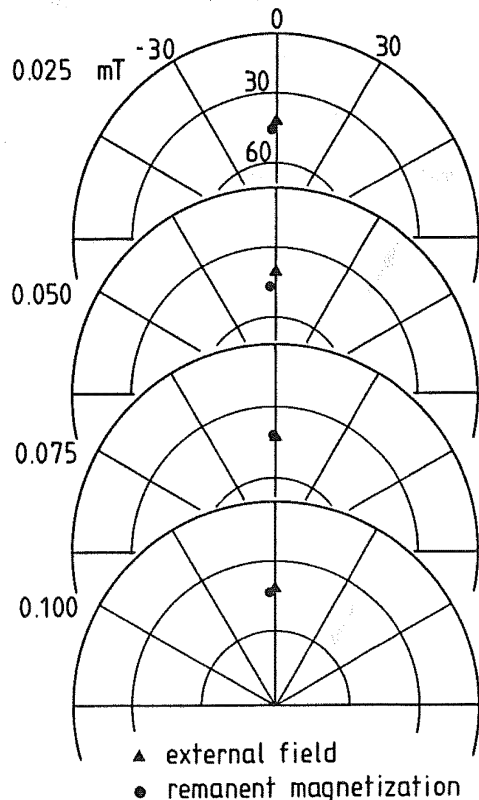


Fig.1 Remanent directions of four synthetic stalagmites made in four steps of controlled direct field.

magnetic particles separated from natural stalagmites (Morinaga et al., 1986), were added to the molten sodium thiosulfate at about 50°C. Then, the melt containing cave sediments was mixed well and was used to synthesize stalagmite-like deposits. The mixture was dropped onto the base of various shaped specimen cases which were placed in the centre of controlled direct field. The specimen case and a Helmholtz coil for direct field control were held in a μ -metal which shields the ambient field. The ambient field at the position of the specimen case was restrained below 50 nT owing to the μ -metal. The dropped mixture crystallized for several tens of minutes in case that no water was added to the mixture. The controlled direct field was kept constant until completion of the crystallization.

Stalagmite-like deposits (synthetic stalagmites) were made of the dropped melt in four steps of the controlled direct fields, which were on the same order of the geomagnetic field intensity. Directions of each remanent magnetization are shown in Fig.1. Triangles denote the directions of the direct fields and circles denote those of the remanent magnetizations.

There are no systematic offsets between the directions of the remanent magnetizations and the direct fields which brought about the remanences. The offsets by several degrees, therefore, are due to the experimental errors which arose from the inaccuracies in emplacement of the specimen cases within the direct field and from viscous secondary components acquired until each magnetic measurement. Taking account of these inaccuracies, the remanent directions are regarded as being fairly parallel to those of the direct fields despite of the low mobility of magnetic particles in the melt. Synthetic stalagmites kept almost constant remanent magnetization with only a weak viscous component even after storage investigated during a few months.

The presence of the stable remanent magnetization and concordance of the remanent direction to that of the controlled direct field explain the

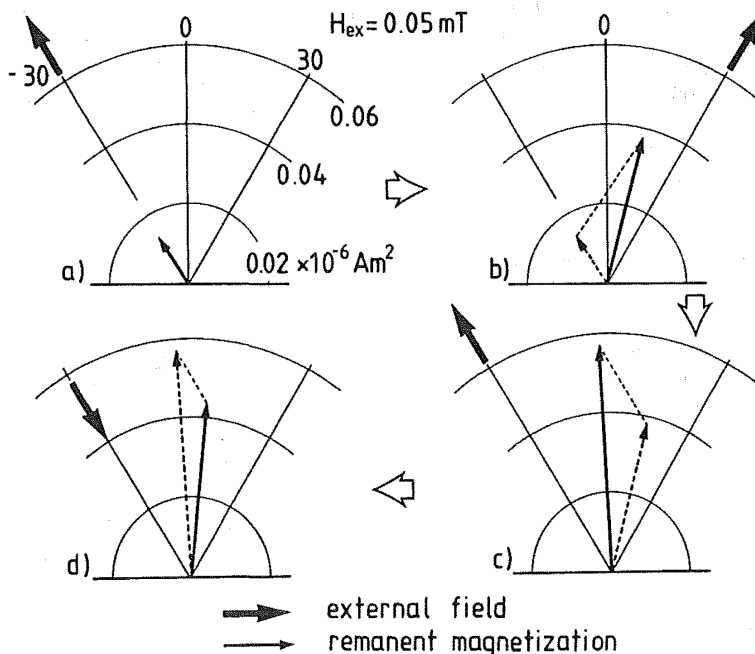


Fig.2 Remanent magnetization (direction and intensity) of a synthetic stalagmite consisting of several layers.

fact that thin films at the surface of natural stalagmites possessed a stable remanent magnetization whose direction is almost the same as the present geomagnetic field direction at the sampling site (Morinaga et al., 1986).

It was clarified that synthetic stalagmites consisting of several layers have a remanent magnetization composed of remanences of each layer as vectors. A small amount of deposit was made through crystallization of the dropped melt within a field (0.05 mT) directed in the direction of -30° as compared with a certain fixed one. The direction of the remanent magnetization is parallel to that of the direct field (Fig.2-a). Then, within a field (0.05 mT) directed in the direction of $+30^\circ$ as compared with the fixed one, a deposit consisting of two different layers was made through further dropping and crystallization of the melt. The resultant remanent direction and intensity correspond to those composed of the different remanent magnetizations recorded in the two layers as vectors (Fig.2-b). This implies that the remanence of the lower layer and was unaffected by the remanence acquisition for the upper layer and was kept constantly. In the same way, it was confirmed through further treatments that composition of the remanent magnetizations as vectors really occurs for synthetic stalagmites (Fig.2-c and -d). This is a strong evidence as supporting that natural stalagmites keep continuous records of the past geomagnetic direction without any magnetic deformation, owing to their successive growth.

Figure 3 shows behaviours of the remanent magnetizations during progressive alternating-field (AF) demagnetization, for a natural stalagmite specimen (left) and a synthetic stalagmite specimen (right). Both natural and synthetic specimens have viscous components which can be removed at the AF levels below 10 mT, and reveal much the same intensity decay curves; that is, coercivity spectra (upper figures). The remanent directions of both specimens scarcely change up to the AF level of 40 mT. Acquisition curves of isothermal remanent magnetization (IRM) for both stalagmites are very

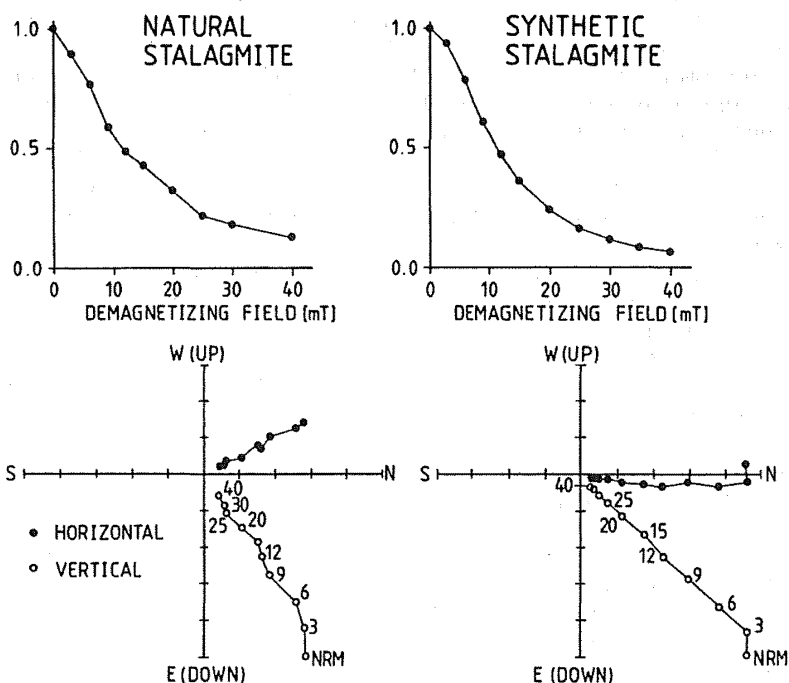


Fig.3 Behaviours of remanent magnetizations for natural (left) and synthetic (right) stalagmites during progressive AF demagnetization.

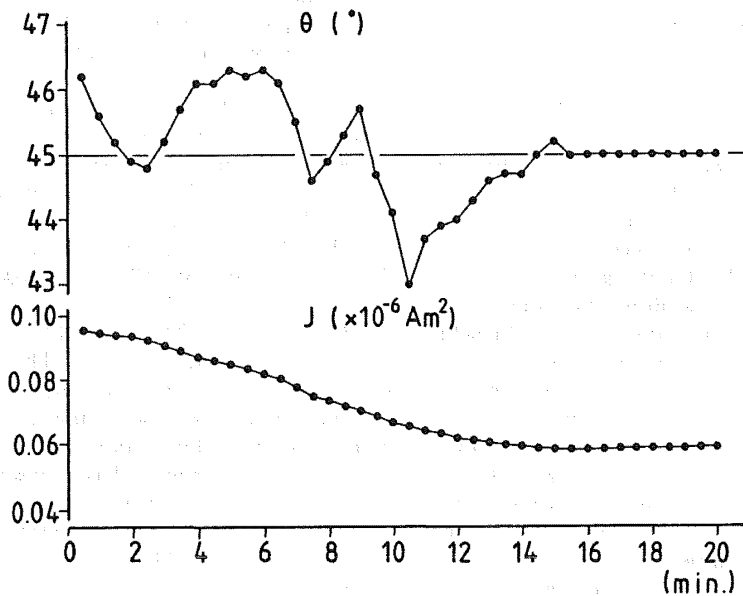


Fig.4 Remanence acquisition process for a synthetic stalagmite.

similar to each other. These similarities imply that the magnetic particles were fixed among and/or within the crystals of both stalagmites through very similar processes to one another.

A chain of behaviors of the magnetization for a synthetic stalagmite specimen until the fixation of magnetic particles were traced within a cryogenic magnetometer trapping a laboratory field (about 0.05 mT). The exact direction of the laboratory field trapped in the magnetometer was unknown. A specimen case, onto which sodium thiosulfate melt containing cave sediments was dropped, was quickly inserted into the magnetometer. Then the magnetic measurements of both horizontal and vertical components were repeated every thirty minutes. Changes in an angle between the measured horizontal and vertical components (θ), and an intensity calculated from both components (J) are shown against time after inserting of the specimen in Fig.4.

The intensity (J) reaches a constant value (about $0.06 \times 10^{-6} \text{ Am}^2$) after about fifteen minutes as uniformly decreasing. The angle (θ) also becomes a constant value (45°) after the same period as fluctuating.

This period (about fifteen minutes) requiring to fix the remanent magnetization seems to experimentally correspond to a period requiring to accomplish crystallization of the sodium thiosulfate melt. The resultant angle (45°) is assumed to correctly reflect the direction of the direct field trapped in the magnetometer, because the present inclination value in Japan is about 48° . The remanent magnetization of synthetic stalagmites, therefore, must be acquired through the fixation of the magnetic particles in the direction of an ambient field, which occurs among and/or within the crystals at the time of accomplishment of the crystallization.

Experiments synthesizing stalagmite-like deposits using sodium thiosulfate show the presence of a stable remanent magnetization acquired in the direction of an ambient field during the crystallization. Several similarities of the remanence features to those of natural stalagmites indicate that the remanence acquisition for natural stalagmites must have been reproduced through a series of experiments for the synthetic

stalagmites.

Natural stalagmites, as observed in the laboratory experiments, seem to acquire the remanences through the fixation of the magnetic particles in the direction of the geomagnetic field, which occurs among and/or within the crystals at the time of formation. Magnetic particles in natural stalagmites seem to align not only in the direction of the geomagnetic field but also in proportion to the intensity of the geomagnetic field.

References

- Hirooka, K. (1971) Mem. Fac. Sci. Kyoto Univ., Ser. Geol. Mineral., 38, 167.
Hirooka, K. (1983) Geomagnetism of Baked Clays and Recent Sediments (eds Creer, K. M. et al., Elsevier, Amsterdam), 150.
Hyodo, M. & Yaskawa, K. (1986) Geophys. J. R. astr. Soc., 86, 41.
Latham, A. G., Schwarcz, H. P., Ford, D. C. & Pearce, G. W. (1979) Nature, 280, 383.
Morinaga, H., Inokuchi, H. & Yaskawa, K. (1986) J. Geomag. Geoelectr., 38, 27.
Morinaga, H., Inokuchi, H. & Yaskawa, K. (1987) submitted to Geophys. J. R. astr. Soc.
Muroi, I. & Yaskawa, K. (1977) Rock Mag. Paleogeophys, 4, 76.

(To be submitted to Geophys. J. R. astr. Soc.)

SECULAR VARIATION OF THE GEOMAGNETIC FIELD DEDUCED FROM PALAEOMAGNETISM OF STALAGMITES IN JAPAN

Hayao MORINAGA, Hiroo INOKUCHI, and Katsumi YASKAWA

Faculty of Science, Kobe University, Nada, Kobe 657, Japan

Stalagmite, which is one of speleothems, has very stable remanent magnetization due to the presence of magnetite (Morinaga et al., 1986). Owing to their successive growth, low-priced sample collection and simple preparation of subsamples for magnetic measurements, stalagmites play a very important role as a recorder of the past geomagnetic field. We demonstrate here the reliability of NRM recorded in stalagmites, which is verified from results of new palaeomagnetic investigations in addition to the published one (Morinaga et al., 1985 & 1986). We also present a provisional secular variation curve of the geomagnetic field in West Japan, which is deduced from NRM's of three stalagmites.

Two stalagmites were collected from Komori-Ana cave ($34^{\circ}13'N$, $131^{\circ}19'E$) in Akiyoshi Plateau, Yamaguchi Prefecture, West Japan. The Palaeomagnetic, palaeo-climatic and other investigations have been already performed for one of them, KM1 (Morinaga et al., 1985 & 1986). Nine parallel (time-equivalent) samples were scooped out from the mound-like stalagmite body (Fig.1-a). The other stalagmite (KM2) was in the conical shape of diameter less than 20 cm and height of 25 cm. Six parallel (time-equivalent) samples were scooped out horizontally from outer portion of this stalagmite (Fig.1-b). They were in the cylindrical form of 1 inch diameter and 4 to 5 cm long. The parallel samples scooped out from two stalagmites have similar growth layers' pattern to each other every stalagmite, so that simultaneous growth layers can be identified among the samples through observation by eye.

Another stalagmite (RYU) was collected from Ryuga-Do cave ($33^{\circ}36'N$, $133^{\circ}45'E$) in Kochi Prefecture, South-west Japan. This stalagmite was in the

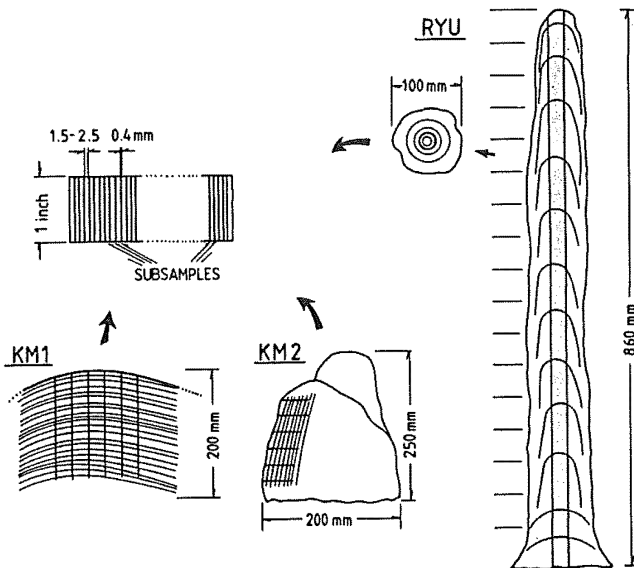


Figure 1. Schematic views of three stalagmites, KM1, KM2 and RYU, their growth layers' patterns and subsamples for magnetic measurements.

columnar shape of about 10 cm diameter and 86 cm high. Seventeen successive (time-serial) samples were cored in the cylindrical form of 1 inch diameter and 5 cm long from the vertical centre part of this stalagmite (Fig.1-c). These three stalagmites have grown up till their collection.

All samples taken from three stalagmites were divided into thin disk subsamples of 1.5 to 2.5 mm thick, for magnetic measurements. Numbers of the disk subsamples are 311, 68, 309 for KM1, KM2 and RYU stalagmites, respectively. These disk subsamples may possess an average record of the geomagnetic field for the period below 50 years.

Magnetic measurements were carried out using a cryogenic magnetometer whose sensitivity is 10^{-11} Am² (10^{-8} emu). The progressive alternating-field (AF) demagnetization was performed on all disk subsamples in order to examine the magnetic stability and to find a primary component of their magnetization. The NRM intensities of disk subsamples before the AF demagnetization fell in the range of 10^{-5} to 10^{-7} Am²/Kg (emu/g). All the subsamples had little secondary components which were able to be removed at the AF levels up to about 10 mT.

The results of magnetization measurements obtained from three stalagmites are shown in Figures 2 and 3 for declination and inclination, respectively. In the case of the parallel samples scooped out from two stalagmites; KM1 and KM2, correlation among positions of disk specimens taken from each cylindrical sample was determined by observation and comparison of the growth layers' pattern. The positions of all subsamples were then adjusted to distance from the surface of "master" sample selected for each stalagmite through their stretch and compression.

Variation curves of declination, inclination and NRM intensity of six parallel samples consist well with each other, showing "internal consistency" within one stalagmite. The internal consistency indicates that the remanent magnetizations are attributed to an identical source outside of this stalagmite.

Sequential five-point moving average curves of direction (declination and inclination) obtained from two Komori-Ana stalagmites; KM1 and KM2 are shown in Figures 4-a and 4-b, respectively. The curves are

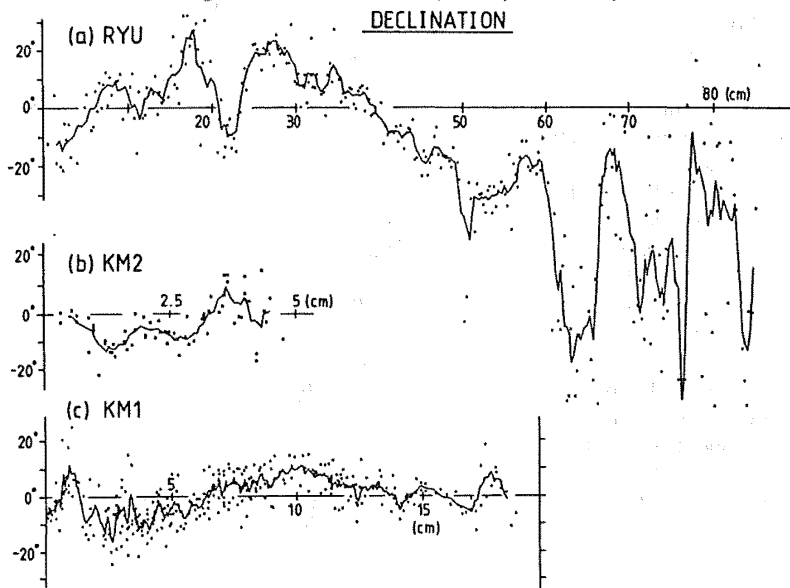


Figure 2. The AF-cleaned declinations for three stalagmites against distance from the top or the surface (dots and squares). Sequential five-point moving vector averages are also shown (lines).

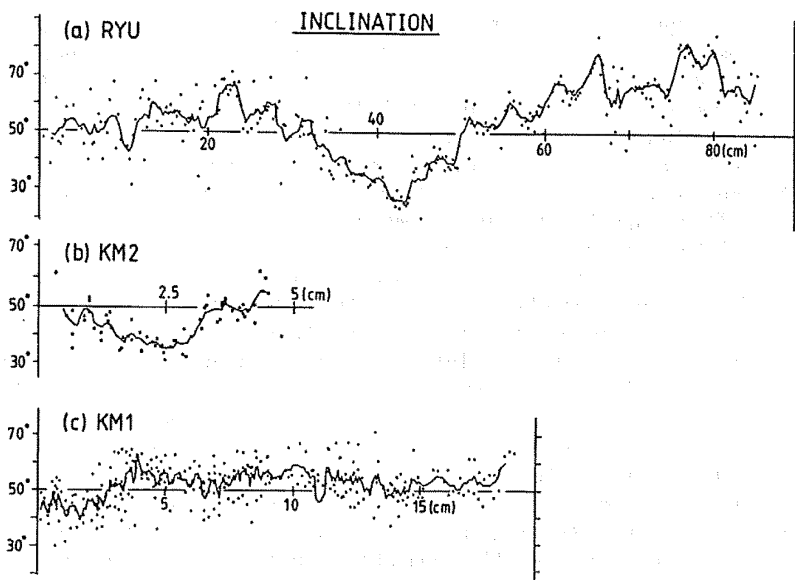


Figure 3. The AF-cleaned inclinations for three stalagmites against distance from the top or the surface (dots and squares). Sequential five-point moving vector averages are also shown (lines).

concordant with each other on their amplitude and variation, showing consistency between two stalagmites in the same limestone cave. The comparison between two stalagmites was made through observation by eye so as not to bring about great discrepancies in the growth rates of two stalagmites.

The consistency between the results of two stalagmites indicates that the magnetization of stalagmites is not subject to depositional errors, which arise from interactions between the magnetic carriers and the substrata at the sediment/water interface in the case of sediments (Verosub 1977). Because KM1 and KM2 samples were scooped out from positions of lateral and upward growth of respective stalagmites. This supports the results by Latham et al. (1979), which the NRM's were unaffected by surface conditions.

The variation curves of direction (declination and inclination) obtained from RYU and KM1 stalagmites are shown in Figures 5-a and 5-b, respectively. The curves are drawn with

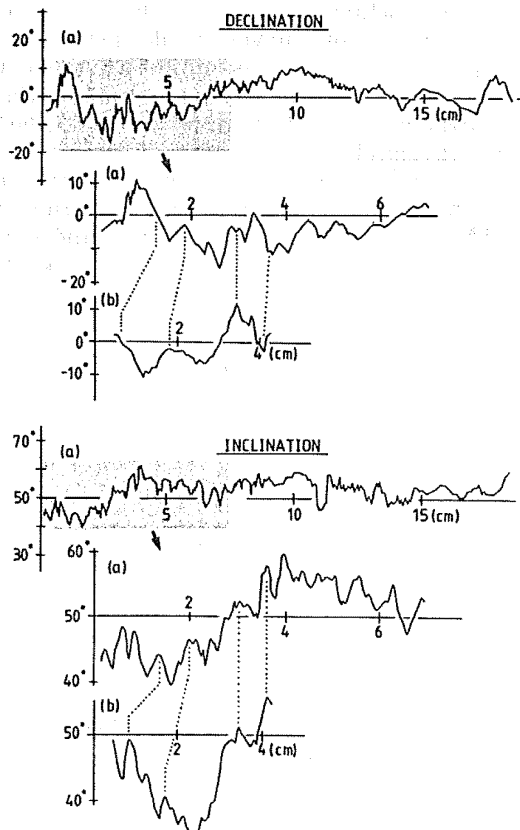


Figure 4. Correlation between the palaeomagnetic results of two stalagmites from the same limestone cave, Komori-Ana cave. This shows consistency within the limestone cave.

sequential five-point moving averages as a function of distance from the top or from the surface. These curves agree with each other, showing "regional consistency" between two different limestone caves. This comparison was also made through observation by eye so as not to bring about great discrepancies in the growth rate of two stalagmites. The regional consistency indicates that remanent magnetizations kept in stalagmites surely reflect the past geomagnetic field. Based on palaeomagnetic results of three investigated stalagmites, provisional variation curves of the past geomagnetic field direction in West Japan were obtained (Fig.6-a) as a function of distance from the top of the RYU stalagmite.

Figure 6 shows variation curves of the past geomagnetic field direction (declination and inclination, respectively) in South-west Japan obtained from (a) palaeomagnetic results of three stalagmites and (b) archaeomagnetic results (Hirooka 1971 & 1983). The curves of the latter results are drawn with average values every 50 years. Both declination and inclination curves are in good agreement with each other. This concordance still more ensure that the remanent magnetization kept in the stalagmites reflect the past geomagnetic field and that stalagmites are an excellent recorder of the geomagnetic field. From this concordance, these curves of the declination and the inclination are considered to represent secular variation of the geomagnetic field direction, although the absolute ages of these investigated stalagmites are not able to be determined at present. The extrapolated age of the oldest position in the curves is about 15000 years BP, based on this concordance.

References

- Hirooka, K. (1971) Mem. Fac. Sci. Kyoto Univ., Ser. Geol. Mineral., 38, 167.
 Hirooka, K. (1983) Geomagnetism of Baked

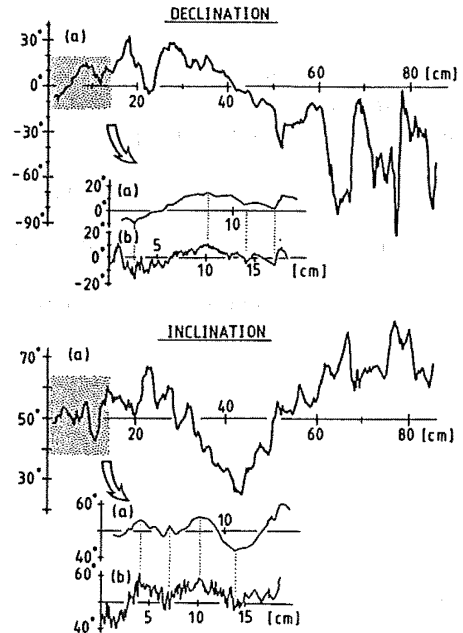


Figure 5. Correlation between the palaeomagnetic results of two stalagmites from different limestone caves, (a) Ryuga-Do cave and (b) Komori-Ana cave. This shows "regional consistency" between the different limestone caves.

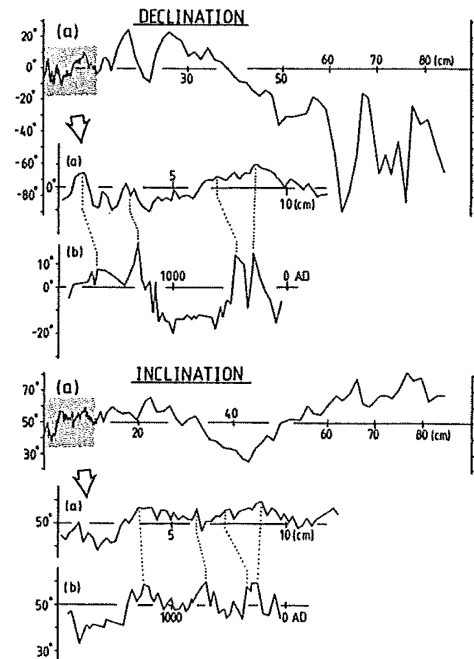


Figure 6. Correlation between (a) provisional secular variation curves obtained from three stalagmites and (b) archaeomagnetic curves (Hirooka 1971 & 1983). This ensures the reliability of remanent magnetizations recorded in the stalagmites.

Clays and Recent Sediments (eds by Creer, K. M., Tucholka, P. & Barton, C. E., Elsevier, Amsterdam), 150.

Latham, A. G., Schwarcz, H. P., Ford, D. C. & Pearce, G. W. (1979) *Nature*, **280**, 383.

Morinaga, H., Inokuchi, H. & Yaskawa, K. (1985) *J. Geomag. Geoelectr.*, **37**, 823.

Morinaga, H., Inokuchi, H. & Yaskawa, K. (1986) *J. Geomag. Geoelectr.*, **38**, 27.

Verosub, K. L. (1977) *Rev. Geophys. Space Phys.*, **15**, 129.

(Submitted to *Geophys. J. R. astr. Soc.*)

PALEOMAGNETIC RESULTS OF IZU AND HAKONE VOLCANOES
 CONDUCTED BY CHIBA UNIVERSITY, 1980 - 1985

Hajimu KINOSHITA and Takatoshi AKIMOTO*

Department of Earth Sciences, Faculty of Science
 Chiba University, Chiba 260

Series of paleomagnetic studies on late Tertiary and Quaternary volcanic bodies around Izu Peninsula, Shizuoka, Japan has been conducted by students of Chiba University. Locations of sampling site (volcanic body) and the age distribution of these rock samples are shown in Figs. 1 and 2. The data are listed in a form of what was used by Irving (1964) or Kinoshita (1970) to fit paleomagnetic reference in various field of geosciences.

List of data will be presented in a future issue of Journal of Geomagnetism and Geoelectricity (Kinoshita et al, 1988). Some tectonic implications are deduced from these data (Kikawa, 1984) and it will be presented also in a future volume of J.G.G. (Kikawa et al 1988).

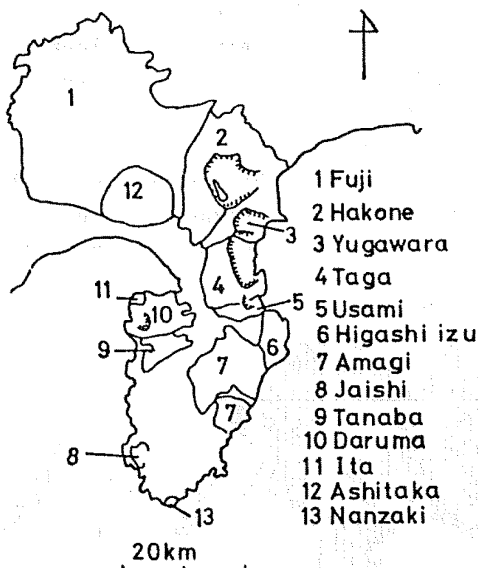


Fig. 1 (left) Locality of volcanic bodies samples by present authors and their colleague.

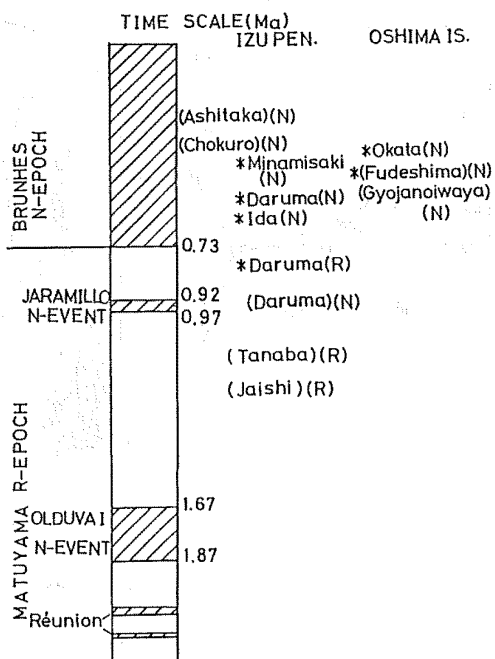
Fig. 2 (bottom) Ages of volcanic bodies from Fig. 1.

References

Irving, E. (1964) John Wiley & Sons

Kikawa, E. (1984) MC thesis, Chiba University
 Kikawa, E., Koyama, M. and Kinoshita, H. (1988) Submitted to J.G.G.
 Kinoshita, H. (1970) J.G.G., v.22, 507-550
 Kinoshita, H. and Akimoto, T. (1988) Submitted to J.G.G.

* Present address: Makuhari-Kita High-school, Makuhari, Chiba 281



PALEOMAGNETISM OF QUATERNARY VOLCANICS IN THE IZU PENINSULA
AND ADJACENT AREAS, JAPAN, AND ITS TECTONIC SIGNIFICANCE

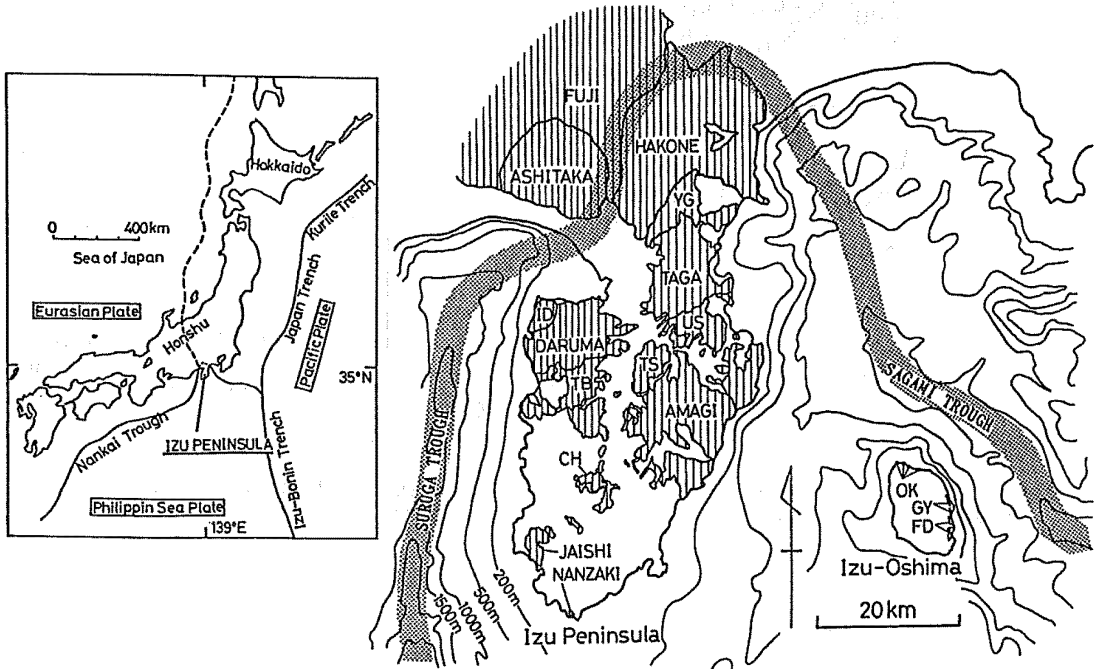
KIKAWA, Eiichi*, KOYAMA, Masato** and KINOSHITA, Hajimu***

* Earthquake Research Institute, The University of Tokyo,
Bunkyo-ku, Tokyo 113, Japan

** Department of Applied Physics, Tokyo Institute of Technology,
Meguro-ku, Tokyo 152, Japan

*** Department of Earth Sciences, Chiba University,
Yayoi-cho, Chiba 260, Japan

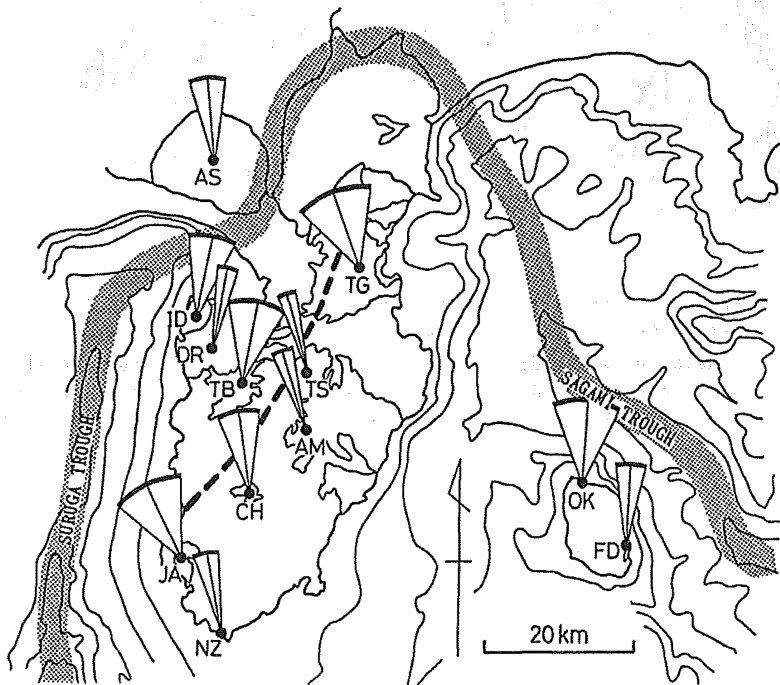
A paleomagnetic investigation was made on the Quaternary volcanics in the Izu Peninsula and the adjacent Ashitaka and Izu-Oshima areas located on the northern tip of the Philippine Sea plate, Central Japan. This study aims to evaluate the deformation associated with the collision of the Izu block with Honshu. About 900 volcanic rock samples of ages from 0.2 to 1.5 Ma, were measured. Alternating field demagnetizations indicate that these samples have stable natural remanent magnetizations. Fine grained titanomagnetite was identified as the carrier of the remanent magnetizations by thermomagnetic analyses and microscopic observations.



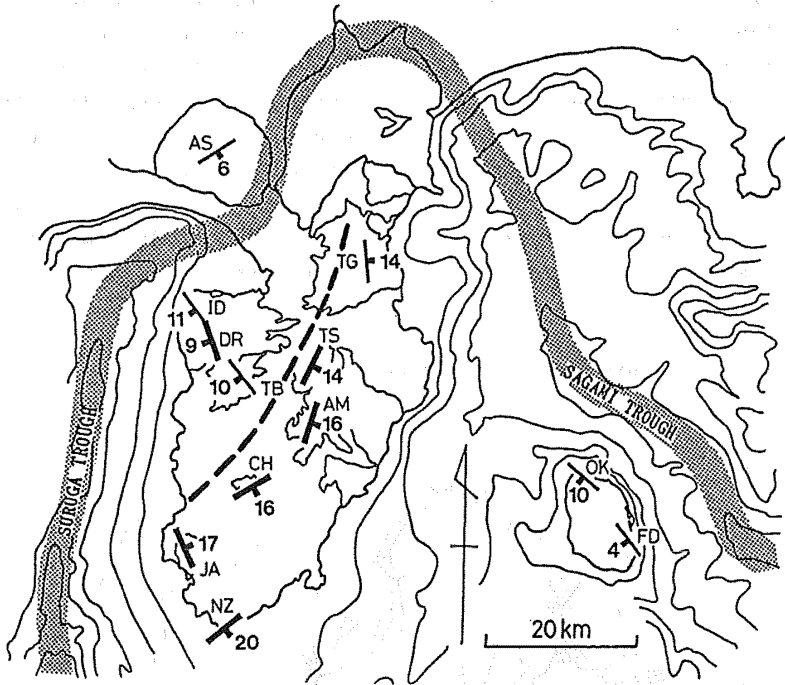
Distribution of the Quaternary volcanics in the Izu Peninsula and adjacent areas. The name of the major Quaternary volcanoes are also shown. ID: Ida Volcano, TB: Tanaba Volcano, CH: Chokuro Volcano, TS: Tenshi Volcano, US: Usami Volcano, YG: Yugawara Volcano, OK: Okata Volcano, GY: Gyojanoiwaya Volcano, FD: Fudeshima Volcano. Shaded belt: material boundary between the Philippine Sea plate and Honshu (Nakamura et al., 1984).

The paleomagnetic directions both from Ashitaka Volcano and from the Izu-Oshima island, which are located on the north and to the east of the Izu Peninsula, respectively, are not significantly different from that of the present axial geocentric dipole field. In contrast, the mean directions from the northwestern Izu Peninsula show ca. 10° clockwise deflections, whereas the directions from the northeastern to southern Izu Peninsula show 8° to 25° counterclockwise deflections. These deflections of paleomagnetic directions are probably caused by tectonic movement since 1.5 Ma. A deformation model is proposed and discussed to account for these paleomagnetic directions.

(submitted to J. Geomag. Geoelectr.)



Mean direction of paleomagnetic declination and its confidence limit for each volcanoes. AS(Ashitaka Volcano), ID(Ida Volcano), DR(Daruma Volcano), TB(Tanaba Volcano), CH(Chokuro Volcano), JA(Jaishi Volcano), NZ(Nanzaki Volcano), OK(Okata Volcano) and FD(Fudeshima Volcano) are obtained by this study. TG(Taga Volcano), TS(Tenshi Volcano) and AM(Amagi Volcano) are by the previous works (Table 3). All the directions with reversed polarity were converted to those with normal polarity. The locality of each volcano is approximately on the center of the sampling sites of each volcano. Broken line: approximate boundary between the declination deflections in the Izu Peninsula (see text)



Estimated tilting direction and angle for each volcano in the tilting model (see text). The reliability of each data is shown with symbols. Thick symbol: the data of which direction is significantly deflected from that of the present axial geocentric dipole field, thin symbol: the data of which direction agrees with that of the present axial geocentric dipole field within the confidence limit.

BRUNHES/MATUYAMA POLARITY EPOCH BOUNDARY IN THE OSAKA GROUP, SOUTHWEST JAPAN

Akira HAYASHIDA and Takuo YOKOYAMA

Laboratory of Earth Science, Doshisha University, Kyoto 602, Japan

The Osaka Group, distributed in underground and surrounding hills of the Osaka Bay area, is a sequence of mud, sands and gravels of the Pleistocene age. The upper part of the Osaka Group consists of alternations of fluvio-lacustrine deposits and 'marine clay' beds. The marine clay beds, called Ma 1, Ma 2, ..., Ma 13, show some characteristic features, such as precipitation of sulfate, distinguishing them from other non-marine mud layers. The marine clay beds seem to have been deposited in shallow marine environments, possibly associated with transgression in inter-glacial periods. Chronological framework of the Osaka Group has been given using paleomagnetic polarity data mainly from volcanic ash layers. Pioneer workers (Ishida et al., 1969) reported magnetic polarity data of several volcanic ashes in the Osaka Group, and suggested that the marine/non-marine cycles had initiated prior to the Jaramillo event in the Matuyama chron. The Matuyama/Brunhes boundary, now dated at 0.73 Ma (Mankinen and Dalrymple, 1979), was assumed between the Ma 3 and Ma 4 beds. While subsequent researches (Torii et al., 1974; Nishida and Ishida, 1975) approved this assignment, exact horizons of the polarity epoch boundaries have not been determined so far. The horizon of the Brunhes/Matuyama boundary has a great importance in Pleistocene chronology; its uncertainty in the Osaka Group has been prevented exact correlation with other records of global climatic changes.

We performed a detailed paleomagnetic study of a core sample of the Osaka Group, attempting to clarify the horizon of the Brunhes/Matuyama boundary. The core sample was obtained from the east of the Senriyama Hills, Osaka Prefecture, around which the typical sections of the upper Osaka Group were well observed before 1970's. The drilled sequence, about 53 m thick, includes four mud layers corresponding to the Ma 3, Ma 4, Ma 5 and Ma 6 marine clay beds. Volcanic ashes, found at the depth of 15.2 m and 13.7 m, and identified as the Hacchoike I and Hacchoike II volcanic ashes, respectively.

We tried to collect oriented core samples from the four mud layers, using a new type of core sampler; the thin-wall core liner has a V-shape groove, and is devised to be kept free of rotation within the rotary core bit. First, the core sampler was slowly lowered to the bottom of the bore hole, with the groove of the liner kept to face towards north. Second, the toe of the liner, preceding the core bits, was inserted into and fixed in bottom sediments. Then, the outer core bit began to be rotated to drill the sediments. The core liner is expected to be pushed down without rotation, if the friction between the sediments and the liner was enough. Although the samples were expected to have been fixed in the core liner, about half of 61 samples appeared to have been disturbed. They were coated with slime on lateral surfaces or having biscuit structure and cracks. It is evident that these core had been rotated or broken within the core liner during the drilling operation.

The core samples recovered were first split into working and archive halves along the north-south plain suggested by the V-groove. Then, cubic specimens for magnetic measurements were collected from the split

face of the working half, by inserting polycarbonate cases of about 10 cm³ at intervals of about 5 cm. The split face was about 1 cm off the core axis, so that the paleomagnetic samples located at the center of the core. We obtained a total of 422 specimens from 58 oriented cores of mud or very fine sands. Measurement of remanent magnetization was made using a cryogenic magnetometer (ScT, C-112). Prior to magnetic cleaning, we measured magnetization of all the specimens, of which intensity ranged from 1.6×10^{-2} to 1.5×10^{-4} A/m². One pilot specimen from each core was subjected to stepwise demagnetization by alternating field (AF) or thermal method. The progressive demagnetization revealed that most specimens contain soft magnetic component which is decreased by low AF (about 10 mT) or low temperature (about 200°C) demagnetization. This component seems to have been originated from viscous remanent magnetization (VRM). The stable components were not fully characterized on higher demagnetization levels than 50 mT or 400°C, possibly due to weak magnetic intensity or due to production of an unstable magnetic phase in high temperature demagnetization. Assuming the stable magnetization represents the primary component, other specimens were routinely demagnetized in peak AF at 20 mT. Intensity of the magnetic moment after AF treatment at 20 mT ranged from 2.2×10^{-3} to 2.5×10^{-5} A/m². Mean magnetic directions and precision parameters were calculated for each core, which comprises 2 to 8 specimens. Specimens from disturbed cores, which was supposed to have been broken in drilling, showed highly scattered magnetic directions, sometimes distributed along a circular girdle around the projection center. Most of undisturbed cores, especially from the Ma 6 and Ma 5 beds, showed concentrated magnetic directions which trend in north-south direction.

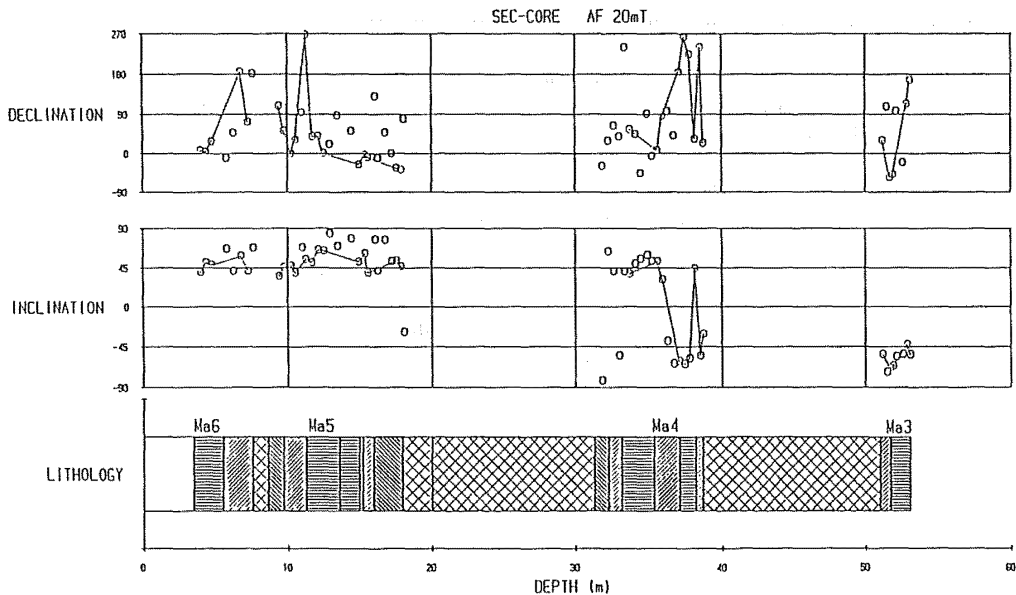


Figure 1 Mean inclinations and declinations plotted against depth of the core. Data from undisturbed cores are connected by lines. The lithology column shows horizon of four marine clay beds, Ma 6, Ma 5, Ma 4 and Ma 3.

All the mean magnetic directions of the Ma 6 and Ma 5 beds have downward inclinations, and those of Ma 3 have upward inclination. These data are concordant with previous results of paleomagnetic study of the Osaka Group, that is, the Brunhes/Matuyama polarity epoch boundary bed has been assumed between the Ma 3 and Ma 4 beds (Ishida et al., 1969; Maenaka et al., 1977; Nishida and Ishida, 1975). It was now revealed, however, that some cores from the Ma 4 bed have reversed magnetic polarity, as shown by downward inclinations and southerly declinations in part. Plot of the magnetic directions in respect to the depth of the core (Figure 1) shows that a geomagnetic polarity change was recorded at the depth about 36 m. Thus, the Brunhes/Matuyama boundary is suggested to occur within the lower part of the Ma 4 bed. Analysis of diatom assemblages and sulfate contents in sediments, which were performed on the present core samples (Koizumi and Yokoyama, 1987; Yokoyama and Sato, 1987), revealed that the Ma 4 and Ma 5 beds respectively contain a record of marine transgression and subsequent regression. While the lowermost part of the Ma 4 bed yielded fossil diatoms only of fresh water origin, brackish or marine diatom fossils were commonly found in most parts of Ma 4. The abundance of marine species increased in the upper part (Koizumi and Yokoyama, 1987). The Brunhes/Matuyama boundary at the depth of 36 m is included within the zone including brackish diatoms. It is suggested, therefore, that the geomagnetic polarity change occurred in the beginning of transgression.

Timing of the Brunhes/Matuyama polarity transition in respect to the global climatic change is not fully clarified yet. Oxygen isotope records of deep-sea sediments reflect changes in the continental ice volume (Shackleton and Opdyke, 1973), and also provides the most precise time scale especially for the Brunhes epoch (Prell et al., 1986). While paleomagnetic studies combined with oxygen isotope stratigraphy were made on several deep-sea cores, the Brunhes/Matuyama boundary has not yet calibrated precisely against the oxygen isotope stage (Niitsuma, 1977). For example, the Brunhes/Matuyama boundary was found at the depth of 1200 cm within interglacial stage 19 in a Pacific deep-sea core, V28-238 (Shackleton and Opdyke, 1973), while it was at 726 cm within glacial stage 20 in V28-239 from the vicinity (Shackleton and Opdyke, 1976). Niitsuma (1977) explained this discrepancy as caused by a time lag of fixation of remanent magnetization in deep-sea sediments; magnetization of sediments is not acquired at the time of deposition, but is fixed below the sediment surface as post-depositional detrital remanent magnetization (post-depositional DRM). Niitsuma (1977) estimated, assuming the depth-lag of post-depositional DRM about 40 cm, that the Brunhes/Matuyama polarity transition occurred in oxygen isotope stage 18. A detailed paleomagnetic study of a hydraulic piston core at DSDP Site 607 showed that the Brunhes/Matuyama boundary is situated within stage 18 in sediments of higher accumulation rate.

The assignment of the Brunhes/Matuyama boundary into glacial stage 18 seems discordant with the present result that the polarity epoch boundary was found in the transgression sequence of Ma 4 in the Osaka Group. Detailed study of oxygen isotope stratigraphy, however, revealed that fluctuations in the isotope ratio occurred during stage 18. It is possible, therefore, to assign the Ma 4 bed to a short interglacial period in stage 18, during which the sea level could be raised to some amount. This correlation implies that all the 'marine clay' beds of the Osaka Group could not be assigned to the major interglacial periods with about 10^5 year cycles. An alternative interpretation may be possible, assuming the Ma 4 bed to be associated with a major interglacial stage 17. Then, the Brunhes/Matuyama boundary should correspond to the beginning of stage 17 rather than stage 18. It is desired that more detailed stratigraphy,

combined both oxygen isotope analysis and paleomagnetism, is studied on continuous sections which was deposited with high accumulation rates.

References

- Ishida, S., Maenaka, K. and Yokoyama, T. (1969) *J. Geol. Soc. Japan*, 75, 183-197.
- Koizumi, I. and Yokoyama, T. (1987) *In preparation*.
- Maenaka, K., Yokoyama, T. and Ishida, S. (1977) *Quaternary Res.*, 7, 341-362.
- Mankinen, E. A. and Dalrymple, G. B. (1979) *J. Geophys. Res.*, 84, 615-626.
- Niitsuma, N. (1977) *Rock Magnetism and Paleogeophysics*, 4, 65-71.
- Nishida, J. and Ishida, S. (1975) *Rock Magnetism and Paleogeophysics*, 3, 32-35.
- Prell, W. L., Imbrie, J., Martinson, D. G., Morley, J. J., Pisias, N. G., Shackleton, N. J. and Streeter, H. F. (1986) *Paleoceanography*, 1, 163-180.
- Shackleton, N. J. and Opdyke, N. D. (1973) *Quaternary Res.*, 3, 39-55.
- Shackleton, N. J. and Opdyke, N. D. (1976) *Geol. Soc. Am. Mem.*, 145, 449-464.
- Torii, M., Yoshikawa, S. and Itihara, M. (1974) *Rock Magnetism and Paleogeophysics*, 2, 34-37.
- Yokoyama, T. and Sato, M. (1987) *J. Geol. Soc. Japan*, 93, 667-679.

(Submitted to *Paleogeography, Paleoclimatology, Paleoecology*)

PALEOMAGNETISM OF THE HISHIKARI GOLD DEPOSITS;
PRELIMINARY REPORT

Hiroto UENO*, Munetomo NEDACHI**, Yukitoshi URASHIMA**,
Kenzo IBARAGI*** and Ryoichi SUZUKI***

* Institute of Mineralogy, Petrology and Economic Geology,
Faculty of Science, Tohoku University, Sendai 980

** Department of Geology, College of Liberal Arts,
Kagoshima University, Kagoshima 890

*** Sumitomo Metal Mining Co., Ltd, 11-3 Shinbashi 5 Chome,
Minato-ku, Tokyo 105

Introduction

The Hishikari mine (32°05'N, 130°41'E) is situated at the Hishikari-cho, Kagoshima Prefecture, Kyushu (Fig. 1). The Hishikari gold deposits was discovered in 1981. The high grade of gold and large size of the mine are remarkable. Estimated ore reserves are 1.5 million tons containing 80 g/ton Au and equivalent Ag (Kondoh, 1986; Suzuki and Ibaragi, 1987). In addition, age of mineralization is Pleistocene against common sense that epithermal mineralization is Miocene in age.

About one hundred data of absolute ages concerning the mine were accumulated (Nishizawa and Ibaragi, 1985; Abe et al., 1986; Metal Mining Agency of Japan and Sumitomo Mining Co., Ltd., 1987; Urashima and Ikeda, 1987). Although magnetic measurements are not completed until now, the polarity sequence in light of absolute ages are briefly described in this paper.

Geological Setting

The sequences in the area are in two main groups: the Shimanto Supergroup of Cretaceous and volcanic rocks of Pleistocene.

Shimanto Supergroup. The Shimanto Supergroup in the area consists of alternations of shale and sandstone, and is correlated with the Cretaceous based on rock facies (Ishihara, 1986). Ore veins of the mine are mainly embedded in this unit.

The Pleistocene volcanic rocks are divided into five units in ascending order (Metal Mining Agency of Japan and Sumitomo Metal Mining Co., Ltd., 1987) as follows:

Hishikari Lower Andesites. Lower part; andesitic pyroclastics with intertrappean andesite lava flows, overlaying the Shimanto Supergroup unconformably. Upper part; Two pyroxenes andesite. Ore veins of the mine are also embedded in this unit.

Kurozonsan Dacites. Hyperthene-augite bearing biotite-

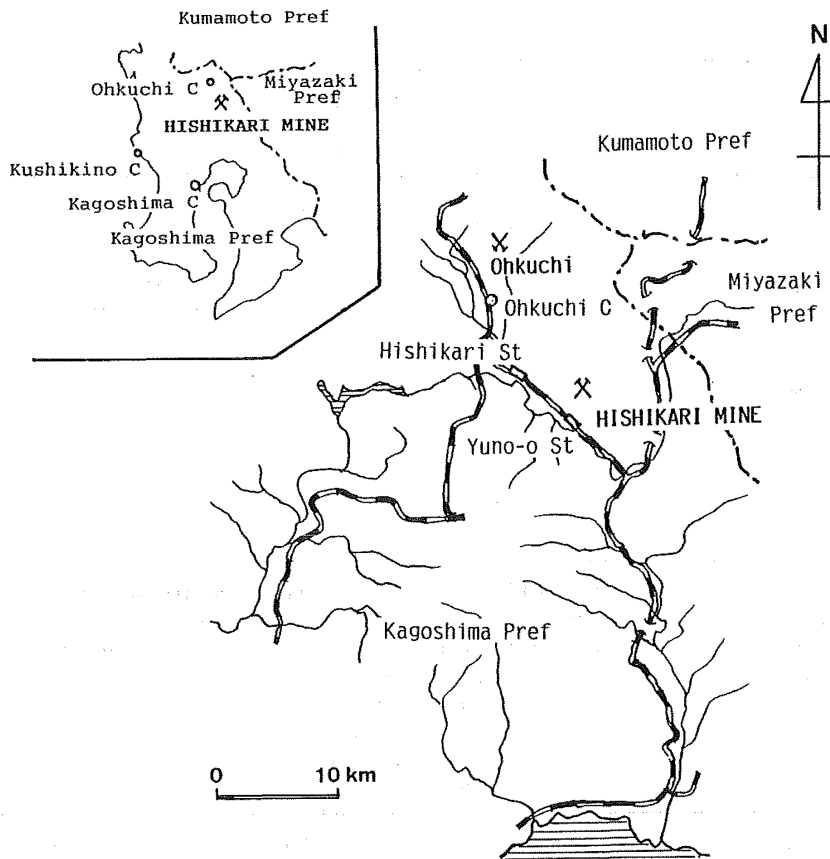


Fig. 1. Location map of the Hishikari mine.

hornblende dacite lava flows, with thin layer of dacitic pyroclastics in the lowest part.

Hishikari Middle Andesites. Olivine bearing two pyroxene andesite lava flows with andesitic pyroclastics in lower part.

Shishimano Dacites. Biotite-hornblende dacite lava flows and dacitic pyroclastics.

Hishikari Upper Andesites. Relatively lower part; andesitic pyroclastics. Relatively upper part; olivine bearing two pyroxene andesite lava flows.

The deposits are of epithermal gold-silver bearing quartz-adularia vein type. They are composed mainly of five major ore veins which strike $N50^{\circ}E$ and dip 70° to $90^{\circ}N$, and embedded in the Shimanto Supergroup and Hishikari Lower Andesites. Widths of the ore veins are 1 to 3 meters occasionally 8 meters and lengths along strike side are 400 meters. The main ore minerals are electrum, naumannite, chalcopyrite, pyrite and marcasite with small amounts of Ag-Au selenides, acanthite, sphalerite, galena and others (Urashima et al., 1987).

Magnetic Polarity and Absolute Age

Hishikari Lower Andesites.

Lava flows at the Kusumotogawa river have reversed polarity magnetizations (eight samples) and gives K-Ar ages of 1.18 ± 0.10 and 1.22 ± 0.10 .

Results from this place indicate the reversed period between the Jaramillo and Reunion subchrons within the Matuyama reversed chron.

At the Yamada dray road lava flows which gives K-Ar ages of 1.1 ± 0.5 , 1.31 ± 0.08 and 1.37 ± 0.07 Ma have normal polarity magnetizations (seven samples) and pyroclastics which are overlain by the lava flows have reversed polarity magnetizations (five samples).

Twenty five samples of pyroclastics and lava flows were collected in the mine. Those have normal polarity magnetizations. However, samples in the mine include hydrothermally altered rocks. During hydrothermal alteration processes, chemical remanent magnetizations may also be acquired (Ueno, 1987). It is necessary to consider hydrothermal effect on samples in the mine, but it is not yet done at present. K-Ar ages of the Hishikari Lower Andesites including described five ages from the Kusumotogawa river and Yamada dray road are 0.95 ± 0.09 to 1.78 ± 0.15 Ma (thirty-seven samples). Some of them may indicate younger ages by hydrothermal alteration. A fission track age of 2.8 ± 0.5 is reported.

Kurozonsan Dacites.

All nine samples from the lava flows of the Kurozonsan Dacites have reversed magnetizations. The pyroclastics which underlie the lava flows are reversely magnetized. The lava flows of this formation give K-Ar ages of 1.11 ± 0.06 to 1.25 ± 0.21 Ma (thirteen samples) and a fission track age of 1.59 ± 0.14 Ma.

Hishikari Middle Andesites.

Four samples from two separated rock bodies have normal polarity magnetizations. K-Ar ages of this formation are 0.78 ± 0.08 to 0.79 ± 0.12 Ma (three samples).

There is no normal chron or normal subchron during these ages. All K-Ar absolute ages, except for a mineral age from the Kurozonsan Dacite and mineral ages on adularia from ore veins, were obtained by whole rock measurement. The K-Ar whole rock ages reveal slightly young ages compared with fission track and K-Ar mineral ages. Then, the normal magnetization of the Hishikari Middle Andesites inferred to correspond to the Jaramillo normal subchron.

Shishimano Dacites.

Fresh samples of this formation have reversed polarity magnetization (fifteen samples). The K-Ar ages of the Shishimano Dacites are 0.66 ± 0.04 to 0.81 ± 0.04 Ma and the fission track age is 0.82 ± 0.17 Ma.

This reversed polarity falls in the Matuyama reversed polarity chron.

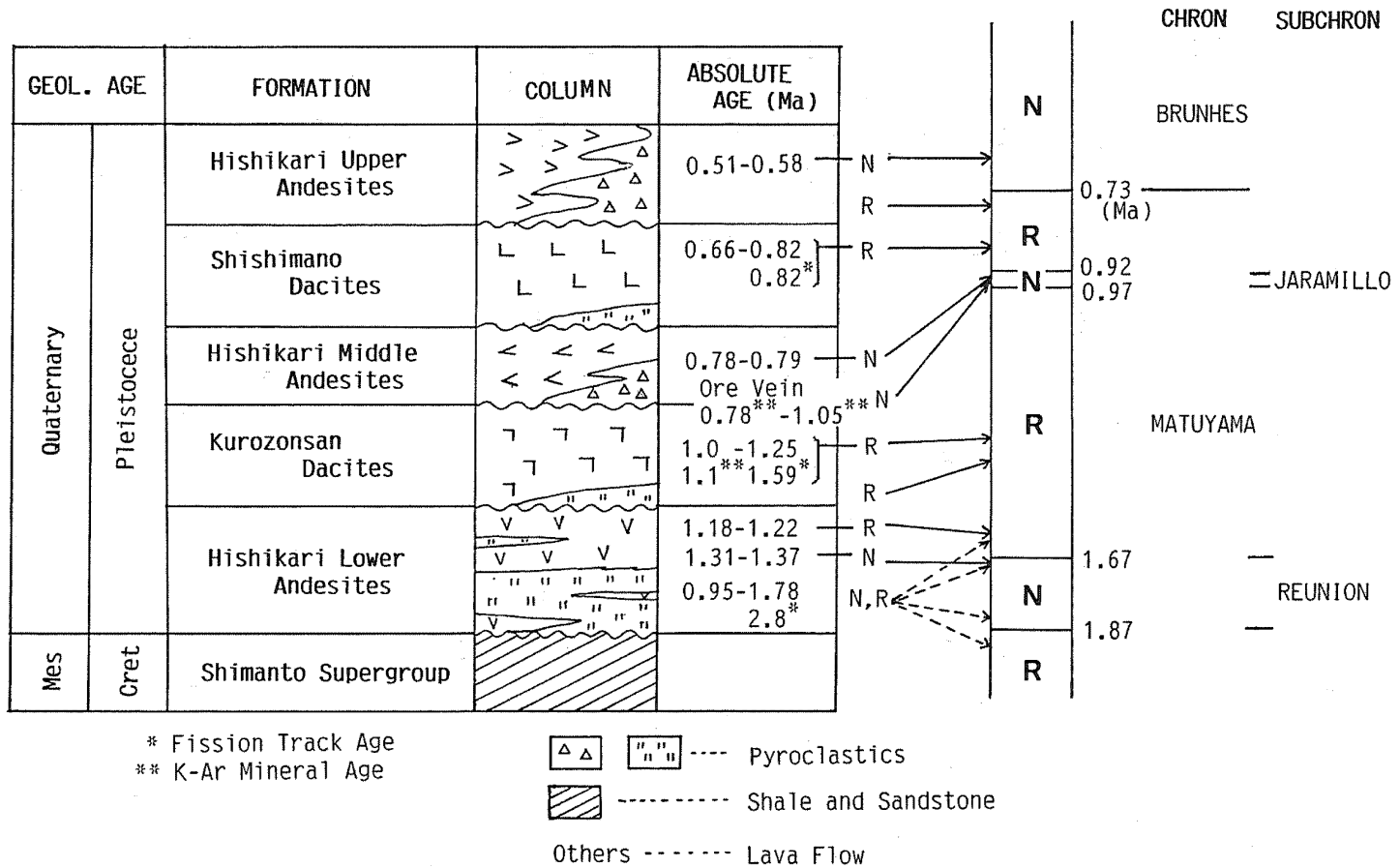


Fig. 2. Geological column and magnetic sequence in the Hishikari mining area. Unmarked ages are K-Ar whole rock ages.

Hishikari Upper Andestes.

The reported K-Ar ages of the Hishikari Upper Andesites are 0.51 ± 0.05 to 0.58 ± 0.10 (five samples). Lava flows of this formation have normal polarity magnetizations (four samples), meanwhile the pyroclastics which underlie the lava flows have reversed polarity magnetizations (two samples). The normal polarity magnetizations may correspond to the Brunhes normal polarity chron and the reversed ones to the later period of the Matuyama reversed chron.

Mineralization.

There are many mineral ages indicating the mineralization stage. K-Ar ages of adularia in ore veins are 0.78 ± 0.07 to 1.05 ± 0.07 Ma (fourteen samples) with one exception of 1.5 ± 0.3 Ma. Hematite bearing ores have normal polarity magnetizations (two samples). These mineral ages and normal polarity magnetizations may correspond to the Jaramillo normal subchron.

The possible polarity sequence are summarized in Figure 2. It is accounted that K-Ar whole rock ages indicate slightly young ages compared with K-Ar mineral ages and fission track ages as mentioned above.

References

- Abe, I., Suzuki, H., Isogami, A. and Goto, T. (1986) *Mining Geol.*, **36**, 117.
- Ishihara, S., Sakamaki, Y., Sakai, A., Teraoka, Y. and Terashima (1986) *Mining Geol.*, **36**, 495.
- Kondoh, K. (1986) *Mining Geol.*, **36**, 1.
- Metal Mining Agency of Japan and Sumitomo Metal Mining Co., Ltd. (1987) *Mining Geol.*, **37**, 227.
- Nishizawa, T. and Ibaragi, K. (1985) In: Urashima, Y. (ed.) *Gold-Silver Ore in Japan*, **3**, 1.
- Suzuki, R and Ibaragi, K. (1987) *Pacific Rim Congress 1987, Australia*.
- Ueno, H. (1987) *Econ. Geol.*, **82**, no.7 (in press).
- Urashima, Y., Ibaragi, K. and Suzuki, R. (1987) In: Urashima, Y. (ed.) *Gold Deposits and Geothermal Field in Kyushu*.
- Urashima, Y. and Ikeda, T. (1987) *Mining Geol.*, **37**, 205.

PROGRESS NOTE ON PALEO/ROCK MAGNETIC STUDY OF ANDESITES FROM
THE CENTRAL YAMAGUCHI PREFECTURE, WEST JAPAN

Haruo DOMEN

Institute of Physical Sciences, Faculty of Education
Yamaguchi University, Yamaguchi City, 753 Japan

Since the early 1970s, the present author has attacked on the outcrop (131.7°E, 34.3°N) of Quaternary andesites at the dam-site of the Lake Ohara (so called "Saba-gawa dam"); in the central Yamaguchi Prefecture, west Japan for the purpose of the paleo/rock magnetic study.

The outcrop of this Quaternary lava flow belongs to the Daisen-Aono yama volcanic zone which geological age is early or middle Pleistocene and the rock samples collected are pyroxene hornblend andesites. The outcrop attacked is well exposed freshly in about 150m wide along the trail at the lake side and the northern part of this outcrop contacts with the Cretaceous rock mass of Shunan Group; andesitic tuff. At the contact zone, the Quaternary andesite is metamorphosed and altered into redish brown in color and the Cretaceous tuff is also well altered into red.

In table 1, the natural remanent magnetization (NRM) of this Quaternary andesites are shown together with that of the Cretaceous rocks. Those data had been obtained on the rock samples collected before 1980.

The NRMs of samples from the contact zone of both Quaternary and Cretaceous rocks are rather widely scattered. The blacky Quaternary rock shows fairly strong intensity of NRM (10^{-4} emu/g). However, the redish Cretaceous one is slightly weak as compared with that of Quaternary one (10^{-5}).

The alternating field (AF) demagnetization on these NRMs could not so much improve the scattering directions.

Table 1. NRM data on Quaternary and Cretaceous rocks from the lake side of Ohara-Ko (Saba-gawa dam), the central Yamaguchi.

Polarity	No. of samples	D(E)	I(D)	K	$\alpha_{95\%}$
Quaternary andesite					
N	7	0.8°	66.2°	110	5.8°
(N)	17	22.8	70.8	23	7.6
O(N)	21	85.9	83.6	26	6.4
O(R)	2	166.1	59.9	10	92.2
Cretaceous tuff					
N	3	11.1	62.1	80	13.8
(N)	2	24.9	70.2	24	53.6
O(N)	5	-30.9	-7.4	2	74.4
(R)	1	155.3	3.1	-	-

Recently, some more samples have been obtained at the same sites mentioned above and also from the Cretaceous rocks at the vicinity. On these rock samples newly collected, the NRM measurements by means of an astatic and spinner magnetometers, AF demagnetization and thermomagnetic (Js-T) analysis are being undertaken and those data will be appeared in the very near future.

CLOCKWISE ROTATION OF THE SOUTH RYUKYU ARC INFERRED FROM PALEOMAGNETISM

Masako MIKI¹, Takaaki MATSUDA² and Yo-ichiro OTOFUJI³

1. The Graduate School of Science and Technology,
Kobe University, Kobe 657, Japan
2. Department of Geology, Himeji Institute of Technology,
Himeji 671-22, Japan
3. Department of Earth Sciences, Faculty of Science,
Kobe University, Kobe 657, Japan

The Okinawa Trough is a marginal basin which is now expanding. Paleomagnetic study was carried out on Tertiary rocks from southern part of the Ryukyu Arc in an attempt to discuss the aspect of opening of the Okinawa Trough.

More than 250 oriented hand samples were collected from Ishigaki-jima Island, Iriomote-jima Island and Yonaguni-jima Island. Samples for K-Ar dating were also obtained from several dikes. Magnetic stability was examined through alternating field and thermal progressive demagnetization experiments. Stable primary components of magnetization could be obtained from eighteen sites after thermal demagnetization at about 300°C.

The mean paleomagnetic direction for seventeen sites of Eocene volcanics (ryolites, tuffs and welded tuffs) is $D=29.5^\circ$, $I=42.6^\circ$ ($\alpha_{95}=10.6^\circ$). This value deflects clockwise by $18^\circ \pm 12^\circ$ from the expected field direction calculated from 40Ma pole of Eurasia of Irving (1977). Paleomagnetic direction of $D=-144.0^\circ$, $I=-32.1^\circ$ from a dike also shows clockwise deflection. The K-Ar age of this dike is 9.63 ± 0.80 Ma.

These results indicate that the South Ryukyu Arc has rotated clockwise $18^\circ \pm 12^\circ$ during the past 10Ma with respect to Eurasia. The area has undergone no significant north-south translation. This rotation can best be explained as follows; 1) the Okinawa Trough has been opened since 10Ma. 2) Rifting and crustal separation has occurred at the continental margin. 3) The Ryukyu Arc has been extruded seaward forming the arcuate shape. 4) This extrusion has caused the clockwise rotation of about 18° at the south end of the Ryukyu Arc. The amount of rotation of 18° matches so well with the geographical feature of this area.

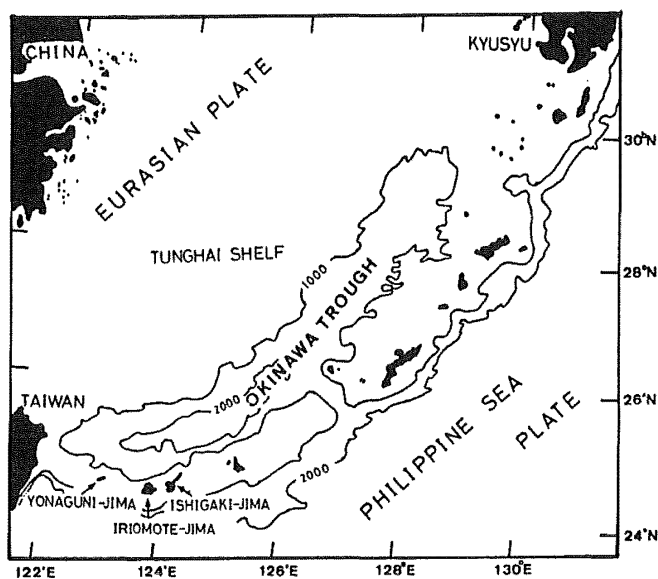


Fig.1
Index map of the studied area. Samples were collected from Ishigaki-jima Island, Iriomote-jima Island and Yonaguni-jima Island.

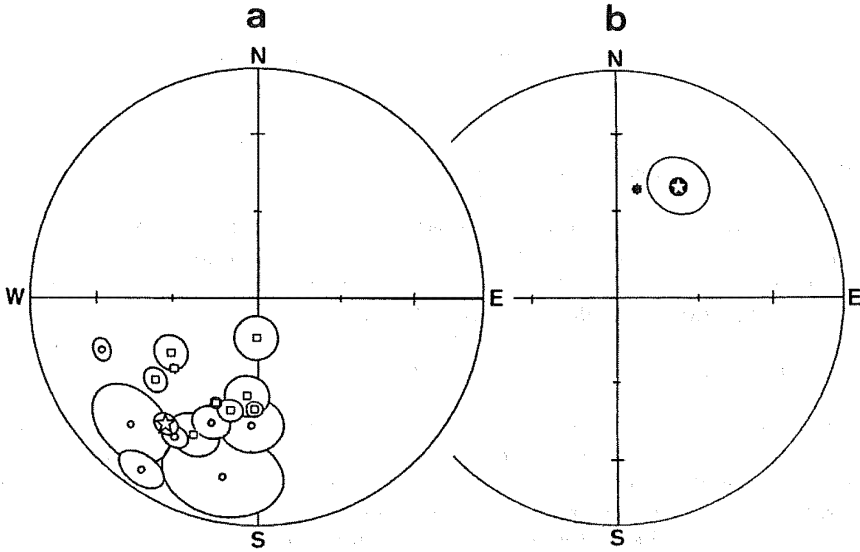


Fig.2

Characteristic paleomagnetic directions from South Ryukyu Arc.

a) The site mean magnetic directions with 95% confidence limits.

○, □: magnetic directions from Eocene volcanics (□: after tilting corrections). ☆: magnetic directions from the dike of 10Ma.

b) ⊙: the mean magnetic direction of Eocene volcanics with 95% confidence limits calculated from seventeen site means. * : expected geomagnetic field direction from 40Ma pole of Eurasia.

Projections are equal area, open (solid) symbols on the upper (lower) hemisphere.

Reference

Irving, E. (1977) Nature, 270, 304

(to be submitted to Tectonophysics)

THE PALEOMAGNETIC AGE-DETERMINATION OF THE KOBE SEDIMENTARY GROUP

Chizu ITOTA¹⁾, Hayao MORINAGA¹⁾, Hiroo INOKUCHI¹⁾,
Katsumi YASKAWA¹⁾ and Shiro ISHIDA²⁾

1) Faculty of Science, Kobe University, Nada, Kobe 657, Japan

2) Faculty of Science, Kyoto University, Sakyo, Kyoto 606, Japan

The Kobe Group, an age-unknown member of the Setouchi Miocene Series, is partly distributed in the Sanda Basin, Southwest Japan. A paleomagnetic attempt was made to determine the age of the Group by existence of the clear discrepancy in the magnetic declination due to the rotation of the Southwest Japan as was suggested by Otofujii and Matsuda (1987). Oriented samples were collected from twenty-one sites covering twelve tuff layers in the Sanda Basin.

Remanent magnetization of the samples was measured using a cryogenic magnetometer. The both optimum demagnetization method and level were chosen for each site through progressive thermal and AF demagnetization treatments for pilot samples. From the magnetic directions of all the samples obtained after each selected optimum demagnetization procedure, the mean direction with 95% confidence limit (α_{95}) was calculated at each site. The site means having the value of α_{95} larger than 20° were rejected.

There are three tuff layers having disputable directions; one (T9) shows different magnetic directions between two sites, i.e. the easterly and the almost parallel to the present field direction, and the other two (T10 and T4) have northerly directions which are almost the same as the present geomagnetic field direction. In order to know which is the original magnetic direction of T9 and to know if the northerly directions of T10 and

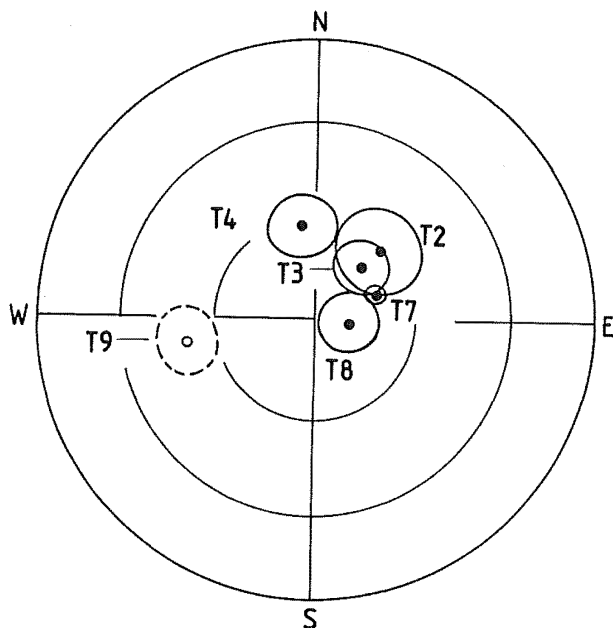


Fig.1 Site-mean directions with 95% confidence circles. The abbreviations adjacent to the circles denote tuff's name. Tuff with a lower number is older. Projection is equal area, solid (open) symbols and solid (dashed) lines on the lower (upper) hemisphere.

T4 can be regarded as those of the primary magnetization, the magnetic stability of the samples from these tuff layers was examined by anhysteretic remanent magnetization acquisition method. The direction parallel to the present field of T9 and that of T10 had to be abandoned through this examination.

After all, the reliable paleomagnetic directions (Fig.1) were obtained only for six tuff layers among twelve layers, including a reversed direction of T9 which was inverted to normal direction for statistical consideration. Easterly deflected declinations were obtained from the five layers, i.e. T2, T3, T7, T8, T9, the declination of which varied from 42.1°E to 95.6°E. The mean direction of these five layers is 64.4° in declination and 68.1° in inclination ($\alpha_{95}=12.6^\circ$). Only a layer (T4) has a northerly direction (Dec=-7.9° and Inc=62.0°). This direction is stratigraphically inconsistent with the other directions to regard the declinational discrepancy suggested by Otofujii and Matsuda, because T4 layer is intercalated between T3 and T7 layers. The paleogeomagnetic field at the sedimentation period of T4 layer might westward deflect for a while. This tuff is assumed to have been completely remagnetized at least near the sampling site, because the direction is similar to the secondary component of the remanence for T9 layer. An alternative interpretation is that the Southwest Japan suffered both clockwise and counter-clockwise rotations between the sedimentation periods of T3 to T7 layers.

The easterly direction value is concordant with the value of the paleomagnetic direction in the Southwest Japan before 15 Ma (Otofujii and Matsuda, 1987). The result of the present work indicates that the Kobe Group had already finished to form in the Sanda Basin before the clockwise rotation of the Southwest Japan about 15 Ma.

Reference

Otofujii, Y. and T. Matsuda (1987) Earth Planet. Sci. Lett., 85, 289

(To be submitted to J. Geomag. Geoelectr.)

MAGNETOSTRATIGRAPHY OF NEOGENE ROCKS AROUND THE YATSUO AREA IN TOYAMA PREFECTURE, JAPAN

Yasuto ITOH

Department of Geology and Mineralogy, Kyoto University,
Kyoto 606, Japan

Introduction

Neogene distributed around the Yatsuo area (Fig. 1), eastern part of Southwest Japan, is a well-exposed series of volcanic and marine sedimentary rocks. Recent geological study (Hayakawa and Takemura, 1987) showed that the sedimentary rocks around Yatsuo contained fruitful informations for drastic subsidence during late Early Miocene. Paleomagnetic studies have revealed that the Yatsuo area was subjected to a clockwise rotation at about 15 Ma (Itoh, 1986), and succeeding counter-clockwise rotation relative to the central part of Southwest Japan (Itoh, 1988). In order to clarify a history of such geological and tectonic events, a precise chronology of the Neogene rocks is required. Magnetostratigraphy is one of the strong tools for detailed chronology and world-wide correlation. This report presents results of magnetic polarity stratigraphy for the Neogene around the Yatsuo area. Sedimentation rates are estimated in some horizons on the basis of magnetostratigraphic correlation.

Sampling and measurements

Geologic map at 1:25,000 scale (Hayakawa, 1985) provided regional structural and stratigraphic control for the sampling sites. Samples were collected at 23 sites. Rock types of sampling sites were shale, siltstone, tuffaceous siltstone, tuff and andesite lava. Each site comprised 4 to 9 hand samples, which were independently oriented using a magnetic compass. Strike and dip of the strata were measured for tilt correction of the remanent magnetic direction.

Cylindrical specimens of 25 mm in diameter and 22 mm in length were cut from each hand sample. Brittle sediments were divided into 20 mm cubic specimens and mounted in plastic cases. Either a Schonstedt SSM-1A spinner magnetometer or a Sct C-112 cryogenic magnetometer was used to measure remanent magnetization.

Two specimens were selected from each site, and their magnetic stability was tested by means of progressive demagnetization with thermal and alternating field methods. Progressive alternating

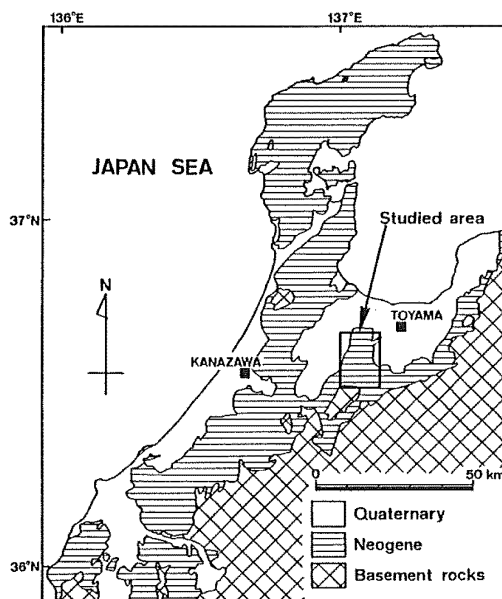


Fig. 1. Map showing the distribution of Neogene rocks around the Hokuriku Province. Studied area is bounded with thick lines.

field demagnetization was carried out stepwise up to 160 mT with a two-axis tumbler contained in a three-layered mu-metal shield. Progressive thermal demagnetization was carried out in more than 10 steps up to 700°C. Specimens were heated in air using a non-inductively wound electric furnace. The stray field inside the furnace was reduced to less than 5 nT

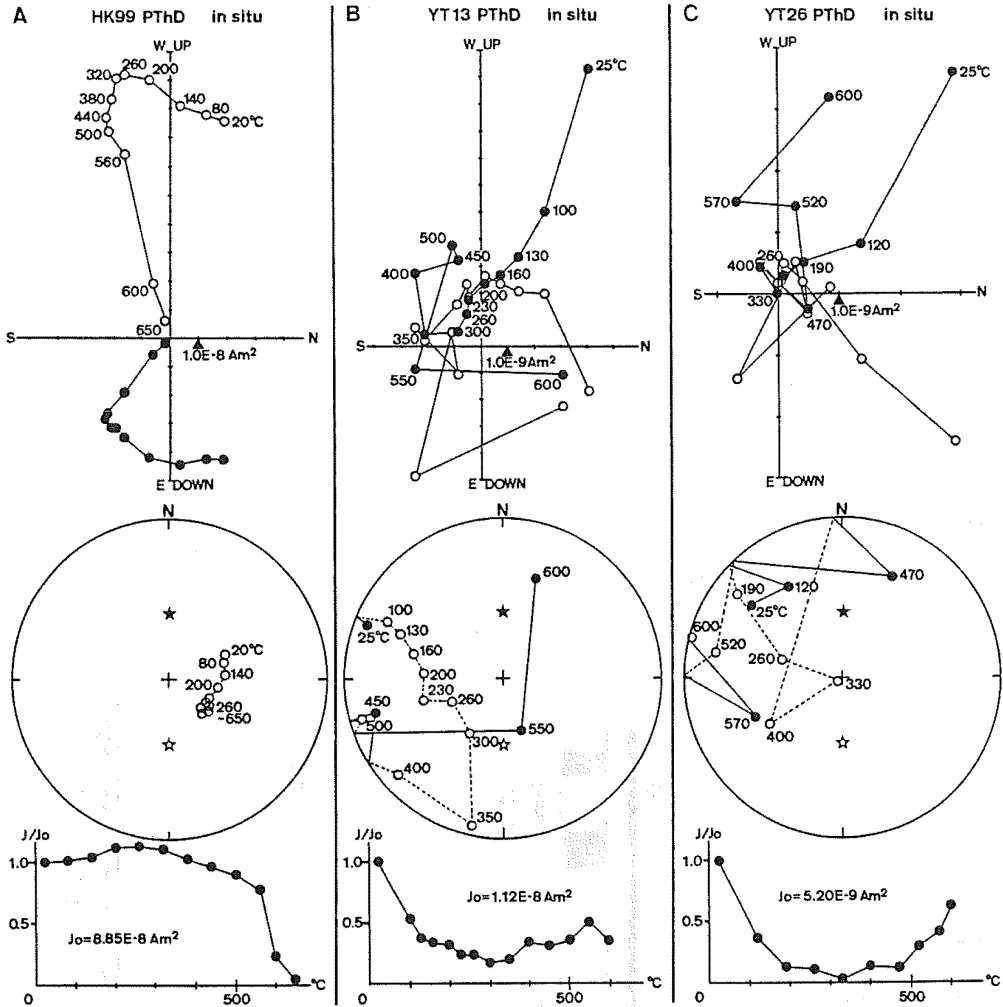


Fig. 2. Typical results of progressive thermal demagnetization of pilot specimens. Magnetic directions are plotted on both vector-demagnetization diagrams and equal-area nets in in-situ coordinates. Normalized intensity decay is also shown. As for the vector-demagnetization diagrams, solid (open) circles are projection of vector end-points on horizontal (N-S vertical) plane. Unit of coordinates is bulk remanent intensity. Numbers attached to symbols are temperature in °C. As for the equal-area nets, solid (open) circles are on the lower (upper) hemisphere. Solid and open stars represent normal and reversed axial dipole field directions, respectively. A: Successive magnetization vectors show a straight trend on the vector-demagnetization diagram and a definite end-point on the equal-area net indicating stable primary magnetization. B: Straight trend is not observed on the vector-demagnetization diagram. On the equal-area net, progressive change of magnetic directions shows an arciform trend approaching to the reversed axial dipole field, but no stable end-point. In this case, blocking temperature spectra of primary (reversed) and secondary (normal) magnetizations are overlapping each other. Acquisition of viscous remanence in the laboratory prevents us from determining high-temperature components. C: Primary magnetic direction or polarity cannot be determined because of serious magnetic unstableness.

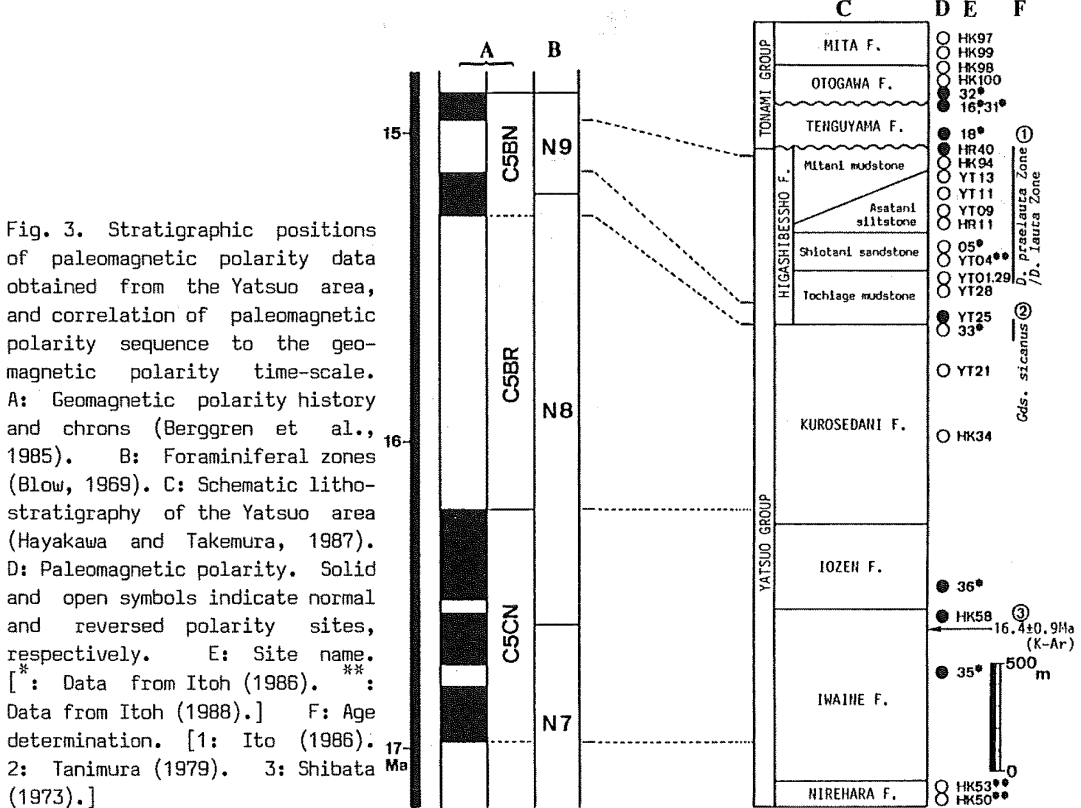
by a four-layered mu-metal envelope. Typical examples of progressive thermal demagnetization are shown in Fig. 2.

As a consequence, samples of 17 sites preserved reliable records of paleomagnetic polarity. The stratigraphic distribution of normal and reversed polarity sites is shown in Fig. 3 together with previous paleomagnetic data around the Yatsuo area.

Age assignments

Magnetobiostratigraphic data and K-Ar age obtained from the Yatsuo area enable us to correlate the obtained polarity sequence with the standard geomagnetic polarity time-scale. In the following discussion, geomagnetic reversal history presented by Berggren et al. (1985) is adopted as the standard time-scale.

Ito (1986) showed that the Higashibessho Formation, uppermost part of the Yatsuo Group, was assigned to the *Denticulopsis praelauta* Zone or *D. lauta* Zone of diatom biostratigraphy (Koizumi, 1985). The FOD (first occurrence datum) of *D. hyalina* which defines the top of the *D. lauta* Zone is associated with the upper part of Chron C5BN (Koizumi, 1985). On one hand, Tsuchi (1981) stated that the *Orbulina* Datum (i.e., planktonic foraminiferal N8/N9 boundary) corresponded with a level slightly above the base of the Higashibessho Formation in the Yatsuo area. Recent paleomagnetic studies, utilizing hydraulic piston corers, confirmed that the *Orbulina* datum level was in the lowest part of Chron C5BN (Hsu et al., 1984). On the basis of these magnetobiostratigraphic data, reversed polarity zone in the middle part of the Higashibessho Formation is correlative with the short reversed polarity interval in Chron C5BN, and the normally magnetized horizon in the basal part of the Higashibessho



Formation is assigned to the lowest normal polarity episode of Chron C5BN (Fig. 3).

As the Kurosedani Formation is assigned to the Blow's Zone N8 (Tsuchi, 1981), reversed polarity zone in the upper part of the Kurosedani Formation is correlative with Chron C5BR (Fig. 3).

The Iozen Formation is conformably overlain by the Kurosedani Formation (Hayakawa and Takemura, 1987), and K-Ar age of andesite lava in the Iwaine Formation is 16.4 Ma (Shibata, 1973). It seems, therefore, that the normal polarity zone in the Iozen and Iwaine Formations is assigned to Chron C5CN (Fig. 3).

Sedimentation rates

As the C5B/C5C chron boundary is assigned to the lower part of the Kurosedani Formation or the upper part of the Iozen Formation, average sedimentation rate of the fining-upward Kurosedani Formation ranges from 1.3 to 0.5 m per 1000 years.

Correlating the basal part of the Higashibessho Formation, maximum thickness of which is 100 m, with the lower part of Chron C5BN suggests that the lower part of massive mudstone in the Higashibessho Formation (Tochiage mudstone) deposited at rates of less than 0.7 m per 1000 years.

Sediments in the middle part of the Higashibessho Formation (upper part of Tochiage mudstone, Shiotani sandstone, Asatani siltstone, lower part of Mitani mudstone) accumulated during the short reversed polarity episode in Chron C5BN. Adopting this correlation, sedimentation rate ranges from 4.3 to 3.2 m per 1000 years.

Many magnetobiostratigraphic works associated with Deep Sea Drilling Project showed that the Neogene sedimentation rates in the Mediterranean, which had high biogenic productivity and large amount of influx of land-derived materials, had not exceeded 0.3 m per 1000 years (Cita et al., 1978). Therefore, it is suggested that the sedimentation rates calculated for the upper part of the Yatsuo Group are anomalously high for fine-grained marine sediments.

References

- Berggren, W. A., D. V. Kent and J. A. Van Couvering (1985) *Geol. Soc. London, Memoir 10*, 211-260.
- Blow, W. H. (1969) *Proc. 1st Int. Conf. Planktonic Fossils, Geneva*, pp. 199-422.
- Cita, M. B., W. B. F. Ryan and R. B. Kidd (1978) *Init. Repts. DSDP, 42* (U. S. Govt. Printing Office, Washington), 991-1002.
- Hayakawa, H. (1985) M.S. Thesis, Kyoto Univ.
- Hayakawa, H. and A. Takemura (1987) *J. Geol. Soc. Japan*, 93, 717-732.
- Hsu, K. J., J. La Brecque et al. (1984) *Geol. Soc. America Bull.*, 95, 863-876.
- Ito, Y. (1986) *NOM (News of Osaka Micropaleontol.)*, 14, 1-27.
- Itoh, Y. (1986) *J. Geomag. Geoelectr.*, 38, 325-334.
- Itoh, Y. (1988) *J. Geophys. Res.*, in press.
- Koizumi, I. (1985) *J. Geol. Soc. Japan*, 91, 195-211.
- Shibata, K. (1973) *Mem. Geol. Soc. Japan*, 8, 143-149.
- Tanimura, Y. (1979) *Fundamental data on Japanese Neogene bio- & chronostratigraphy*, 83-84.
- Tsuchi, R. (ed.) (1981) *Neogene of Japan (IGCP-114 Natl. W. G. Japan)*.

PALEOMAGNETIC INVESTIGATION FOR THE OGA PENINSULA
IN NORTHEAST JAPAN

Tadashi NISHITANI and Seiji TANOUE

Institute of Mining Geology, Mining College,
Akita University, Akita 010, Japan

1. Introduction

Paleomagnetic investigations associated with the position of Japan arc in the middle to late Miocene were presented. Paleomagnetic studies of Cretaceous rocks of Southwest Japan (Kawai et al., 1961, 1971) indicated that the directions of late Cretaceous sedimentary and volcanic rocks showed clockwise deviation from the Cretaceous field direction.

In recent years, Southwest Japan has been intensively studied. Late Tertiary rocks indicated that the rotation of Southwest Japan relative to the Eurasia continent started around 15 Ma. These movements caused the Japan arc rifting for the late Miocene (Otofujii and Matsuda, 1983, 1984; Hayashida and Ito, 1984).

Our main purpose in this study is to discover the paleomagnetic evidence for "late Miocene rotation" in Northeast Japan.

2. Sampling

More than 200 samples were collected by hand from 24 sites (Fig.1). Sampling points were within 30m for each sampling site. Ages were already determined using K-Ar dating or Fission track dating for above rocks (Nishimura and Ishida, 1972; Ohguchi et al., 1979; Suzuki, 1980; Kaneoka, 1983; Kimura, 1986). Stratigraphy in the Oga Peninsula (Huzioka and Takayasu, 1975) has been established. Pre-Tertiary basement rocks to alluvial deposits have made the successive formation. Samples were collected from Monzen, Daijima, Nishikurosawa, Onnagawa and Funakawa Formation. Kanpuzan volcanics were also sampled. We investigated basalts, tuff and igneous rocks within tuff in early Miocene to late Pleistocene. The samples for Monzen Formation were almost basalts except for three sites (MD2-01, MA4-01 and MT12-01), which were dacite, andesite and tuff, respectively. The sample (DB2-01) from Daijima Formation was basalt. Kanpuzan volcanics

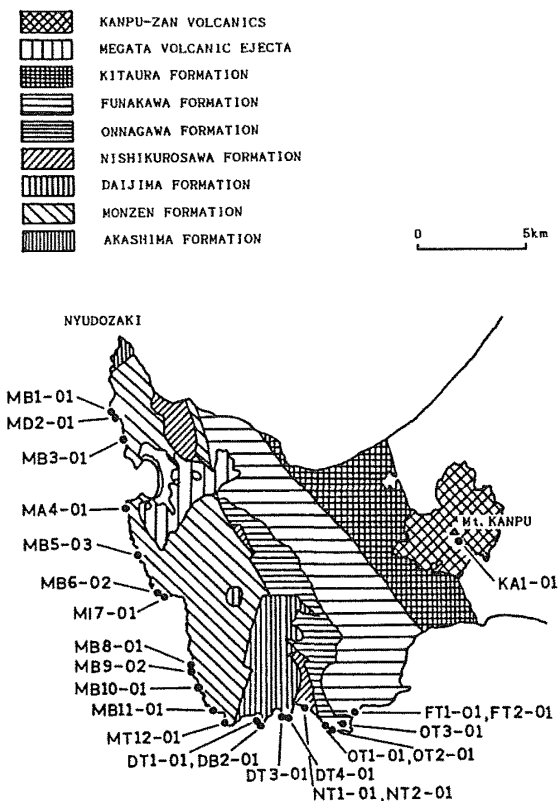


Fig.1 Geological map of the Oga Peninsula

was andesite and other samples were tuff and igneous rocks within tuff.

3. Measurement of magnetic component

Individual specimens were 25mm in diameter and 20-25mm long. Thermal demagnetization was used for all samples in order to erase the secondary magnetic components in basalts and tuff. Remanences were measured with Princeton SM-2 spinner magnetometer.

One or two pilot specimens for each site were progressively demagnetized thermally in 25-50°C step up to about 600°C. These results showed that more than 80 percent of all the specimens were magnetically stable. The optimum demagnetization temperature was 300°C to 500°C. At this temperature, the variation in directions was less than 10 degrees for all samples. In this investigation, the first temperature to stabilize direction was used for same locality. The characteristic direction after thermal demagnetization for each site was regarded reliable if the following criteria were satisfied;

- (1) one site has at least five specimens and
- (2) site mean direction has less than 10 degrees for 95% confidence circle.

3-1 Paleomagnetic directions

Reliable primary magnetic components were obtained through thermal demagnetization for 24 sites. The mean directions of declinations and inclinations were plotted by the equal area projection for Monzen, Daijima, Nishikurosawa, Onnagawa and Funakawa Formation, and Kanpuzan volcanics (Fig.2). Mean direction for each formations are listed in table I. The mean ages were calculated using the data of Kaneoka (1983). These ages were 31.5 Ma for Monzen, 22.5 Ma for Daijima, 16.5 Ma for Nishikurosawa, 14.0 Ma for Onnagawa and 12.4 Ma for Funakawa Formation, and 0.90 Ma for Kanpuzan volcanics.

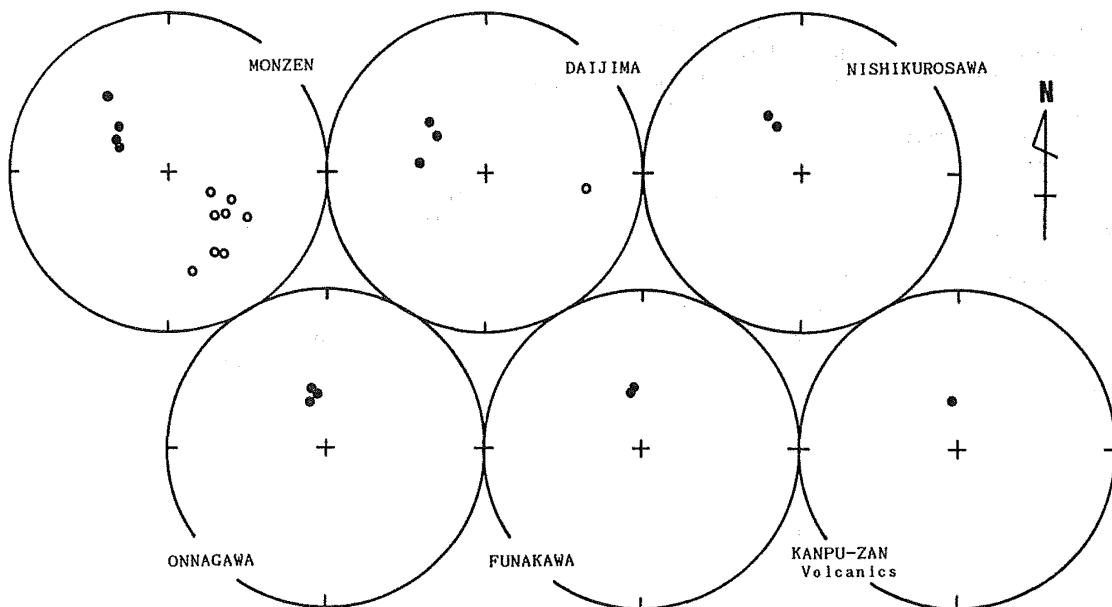


Fig.2 Site mean directions of the remanences obtained for each formation plotted by the equal area projection. Solid and open circles represented normal and reverse polarity.

Table I Summary of paleomagnetic poles for Northeast Japan.

Formation	Age (Ma)	B	Field direction			Pole position		p(°)	dp(°)	dm(°)
			Inc.(°)	Dec.(°)	A95	Lat.(°N)	Lon.(°E)			
Monzen	31.5	12	46.58	-44.65	8.67	51.46	45.51	62.11	7.18	11.16
Daijima	22.5	4	50.22	-68.84	18.77	36.07	62.57	59.02	16.85	25.15
Nishikurosawa	16.5	2	56.85	-21.17	5.67	73.33	48.18	52.53	5.98	8.23
Onnagawa	14.0	3	57.90	-6.73	4.36	84.62	37.77	51.49	4.72	6.42
Funakawa	12.4	2	56.95	-1.97	2.39	87.21	-6.17	52.57	2.53	3.48
Kanpuzan vol.	0.9	1	62.32	4.11	2.05	85.21	178.31	46.29	2.49	3.19

B is the number of the site. Inc. and Dec. denote the inclination and declination of the site mean direction for each formation after bedding correction, respectively. A95 is 95% confidence range of the formation. p is the ancient colatitude calculated from the inclination. dp and dm indicate error along the great circle passing through the sampling site and perpendicular to the circle from the paleomagnetic pole, respectively.

3-2 Monzen Formation (about 39.3-23.7 Ma)

This formation is a thick horizon in the Oga Peninsula and has a stratigraphic succession in early Miocene. Therefore, 12 sites were selected in order to cover the age of this formation and to investigate the directional change in detail. Inclinations and declinations after bedding correction for each site were denoted in Fig.3 and Fig.4. The vertical and horizontal bars in these figure indicate error ranges of inclination and declination, and that of geological time for each sampling site. Geologic time were calculated using geological map and column section in this region. The symbols in this figure cannot be exchanged for horizontal direction because these horizon for each site are clearly determined.

Declinations indicated the westward deviation for this formation, which consist of basalts, andesite and tuff in west coast part of the Oga Peninsula. This results are consistent with the declination value reported from Northeast Japan of the early Miocene period (Hamano and Tosha, 1987). The collected specimens in this region indicated that their declinations gradually deflected to the westward direction. The deviation angle from the present declination increased as the position in this formation approached to upper horizon. Inclinations for this formation can be summarized into 2 groups, around 35° and 50°.

Though the remanence direction below 200°C were dispersed it grouped above 300°C. Eight sites indicated reverse polarity and the other 4 sites showed normal polarity. They showed westward deviation. The formation mean direction was I=-46.6°, D=135.3° and α_{95} =8.7°.

3-3 Daijima and Nishikurosawa Formation (about 26.7-15.0 Ma)

These formations have been established middle Miocene. Samples were collected from 4 sites for Daijima and 2 sites for Nishikurosawa Formation.

Declinations of the Daijima basalt and tuff, which were collected from southmost shore in this area, denoted the tendency of westward deviations. One site showed reversal polarity and 3 sites showed normal polarity. The site mean direction of the Nishikurosawa Formation indicated normal polarity with westward declination, however, the deviation angle was small

compared with that of Monzen and Daijima Formation. Two sites in the middle part of Daijima Formation showed maximum deflection angle, about -80° , from the present geomagnetic pole.

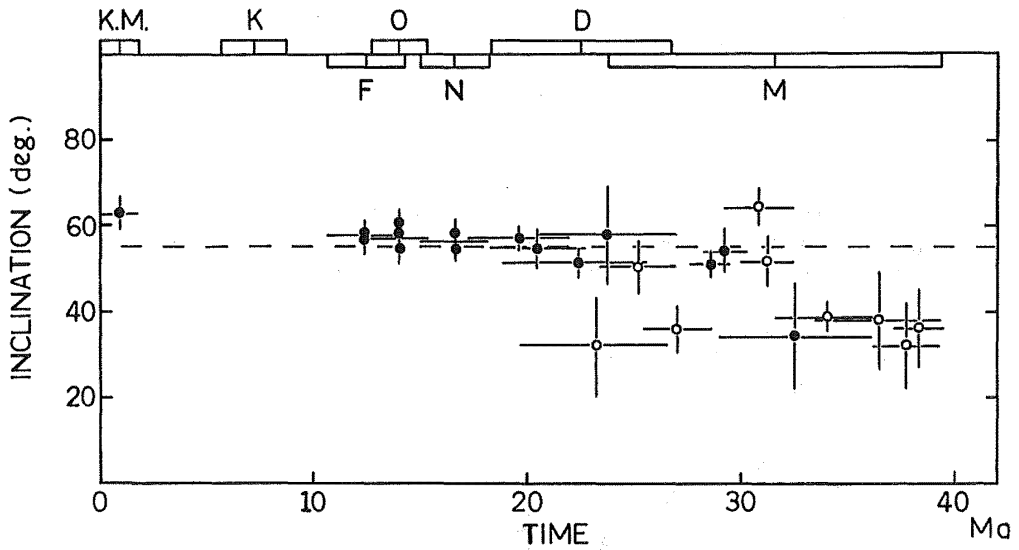


Fig.3 Relationship between inclination and time. Radiometric time range for each formation by Kaneoka (1983) is used. Broken line corresponds to the present inclination.

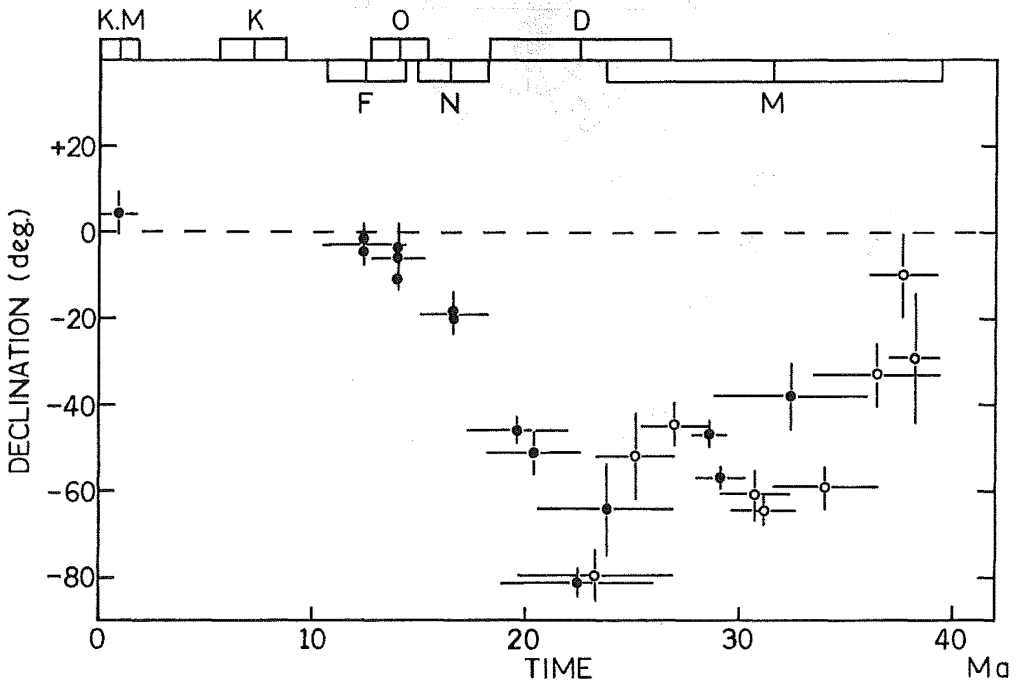


Fig.4 Relationship between declination and time. Radiometric time span for each formation by Kaneoka (1983) is used. Broken line corresponds to the present declination.

The Daijima and Nishikurosawa Formation showed almost the same inclinations except for 1 site. The mean direction for Daijima Formation was $I=50.2^\circ$, $D=-66.8^\circ$, $\alpha_{95}=8.7^\circ$ and for Nishikurosawa Formation was $I=56.9^\circ$, $D=-21.2^\circ$, $\alpha_{95}=5.7^\circ$, respectively.

3-4 Onnagawa and Funakawa Formation, and Kanpuzan volcanics
(about 15.3-0.90 Ma)

Samples were collected from 3 sites for Onnagawa, 2 sites for Funakawa Formation and 1 site for Kanpuzan volcanics. These formation assigned in late Miocene to Holocene.

Inclinations and declinations showed almost the same direction as the present value. The mean direction for Onnagawa Formation was $I=57.9^\circ$, $D=-6.7^\circ$, $\alpha_{95}=4.4^\circ$ and for Funakawa Formation was $I=57.0^\circ$, $D=-2.0^\circ$, $\alpha_{95}=2.4^\circ$ and for Kanpuzan volcanics was $I=62.3^\circ$, $D=4.1^\circ$, $\alpha_{95}=2.1^\circ$.

Based on these data obtained for each formation, paleomagnetic pole positions and 95% confidence level were calculated. VGP, inclination, declination and α_{95} were shown in Fig.5 and Table I.

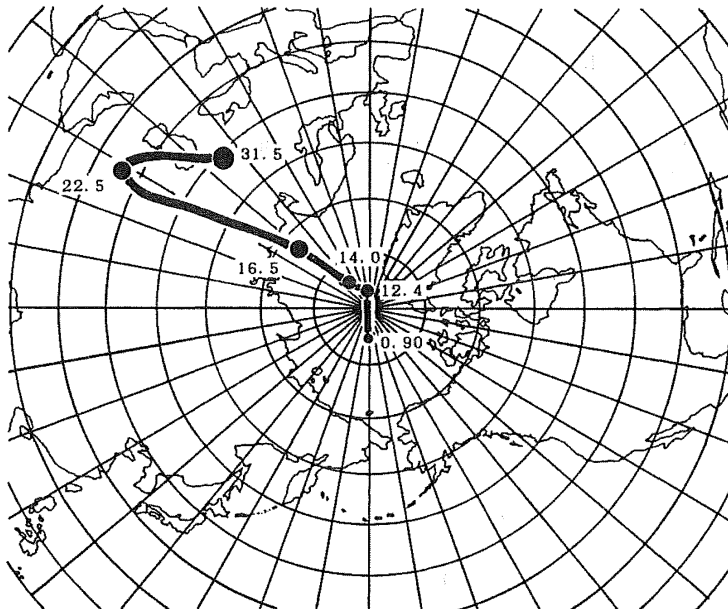


Fig.5 Apparent polar wander path for Northeast Japan from the paleomagnetic data in the Oga peninsula. Numericals shown in this figure are the mean radiometric ages (Ma) for each formation. The size of solid circles indicate relative errors.

4. Conclusion

Counter clockwise rotation and the time of rotation of Northeast Japan

Reliable data were obtained through thermal demagnetization and bedding correction. Paleomagnetic results of late Tertiary rocks in this study indicated that these early to middle Miocene rocks have had the westward directions after bedding correction. These results of the

westward direction suggests that the counter clockwise rotation occurred during late Miocene in Northeast Japan. We can estimate the time of counter clockwise rotation using above data and radiometric ages of Northeast Japan. The rotation began 23 Ma and lasted until 14 to 13 Ma referred to the data of Kaneoka (1983). The rotation in Southwest Japan occurred suddenly around 15 Ma (Otofujii, 1983, 1984). The present study, however, showed that the rotation continued for 10 Ma in Northeast Japan.

References

- Hamano, Y. and Tosha, T. (1987) Tectonics (in press).
Hayashida, A. and Y. Ito (1984) Earth Planet. Sci. Lett., 68, 335.
Huzioka, K. and Y. Takayasu (1975) Akita Univ., 49.
Kaneoka, I. (1983) Min. Geol. Spec. Issue, 11, 69.
Kawai, N., H. Ito and S. Kume (1961) Geophys. J. R. astr. Soc., 6, 124.
Kawai, N., T. Nakajima and K. Hirooka (1971) J. Geomag. Geoelectr., 23, 267.
Kimura, K. (1986) Earth 8, 370 (in Japanese).
Nishimura, S. and S. Ishida (1972) J. Japan. Assoc. Min. Petr. Econ. Geol., 67, 166.
Ohguchi, T., K. Yanai, Y. Ueda and S. Tamanyu (1979) J. Japan. Assoc. Min. Petr. Econ. Geol., 74, 217.
Otofujii, Y. and T. Matsuda (1983) Earth Planet. Sci. Lett., 62, 349.
Otofujii, Y. and T. Matsuda (1984) Earth Planet. Sci. Lett., 70, 373.
Suzuki, T. (1980) Jour. Geol. Soc. Japan, 86, 441.

A MAGNETOSTRATIGRAPHIC STUDY OF CRETACEOUS-PALEOGENE DEPOSITS IN AMAKUSA-SHIMOJIMA, KYUSHU, SOUTHWEST JAPAN

Kazuto KODAMA and Toshihiro BABA

Department of Geology, Faculty of Science, Kochi University,
Kochi 780, Japan

1. Introduction

Among the number of Cretaceous and Paleogene formations in Southwest Japan, the Upper Cretaceous-Tertiary system exposed on the Amakusa Islands in Western Kyushu, Southwest Japan has long been investigated as well as other intra-arc basin deposits in Kyushu; for example, the Goshonoura Group (Albian-Cenomanian), Mifune Group (Cenomanian-Turonian), and Ohnogawa Group (Turonian-Santonian) (e.g., Matsumoto, 1954). The age of each basin deposits has been estimated depending chiefly on the limited occurrence of molluscan fauna including ammonites and bivalves, and hence the complete biostratigraphy within an entire basin succession correlatable to the international geological time-scale has never been accomplished yet. However, it has been suggested by previous biostratigraphical and sedimentological investigations (Tashiro and Otsuka, 1978; Tashiro et al., 1980) that the formations exposed on the island of Amakusa-Shimojima in the Amakusa Islands include Cretaceous-Tertiary boundary strata which has been rarely found elsewhere in the world.

We began a line of magnetostratigraphic study of the continuous successions of the Amakusa Islands in order to establish, in combination with biostratigraphic studies, a time-stratigraphic classification, with special emphasis on the identification of the possible Cretaceous-Tertiary boundary. This brief article reports the results of a preliminary magnetostratigraphic study carried out on the Upper Cretaceous-Paleogene strata on the Amakusa-Shimojima.

2. Geological Setting

The Amakusa Islands, located some 100 km west of Kumamoto City in Western Kyushu, consist mainly of two large neighboring islands; Amakusa-Kamishima and Amakusa-Shimojima (Fig. 1). The Upper Cretaceous clastic sequence in Amakusa-Kamishima was named the Himenoura Group (Nagao, 1922), which is overlain unconformably by the Paleogene Akasaki Formation. The Himenoura Group yields an abundant mollusks including ammonites, inoceramids and trigoniids suggesting Coniacian to Upper Campanian in age (Ueda, 1962), which seem to be subdivided into three biostratigraphic zones (Tashiro and Noda, 1973). The Paleogene Akasaki Formation, which is

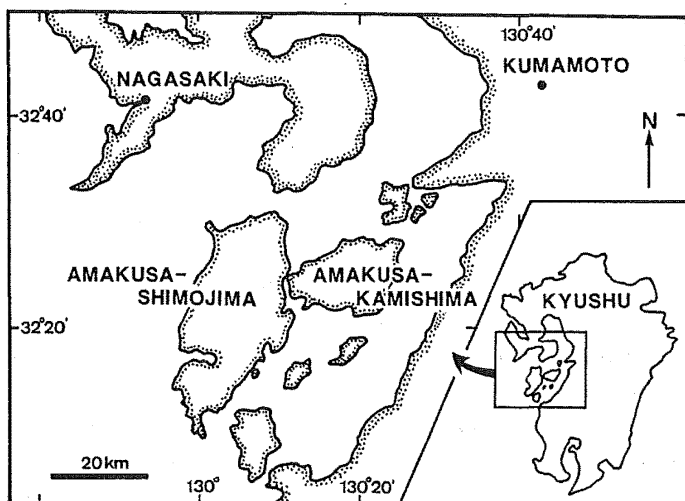


Fig. 1 Location of Amakusa-Shimajima, Amakusa-Kamishima and other islets of the Amakusa Islands in Western Kyushu, Southwest Japan.

characterized by the frequent intercalations of red beds, is overlain conformably by successive formations of clastic sediments as Shiratake, Kyoragi, Toishi, Ittyoda, and Sakasegawa in ascending order (Miki, 1975).

Similar Upper Cretaceous sequence more than three thousand meters in thickness is exposed also on Amakusa-Shimajima. Although the Cretaceous strata, which is overlain by the Paleogene Miroku Group, has long been correlated to the type Himenoura Group in Amakusa-Kamishima (Nagao, 1930), recent extensive sedimentological and biostratigraphical studies (Tashiro and Noda, 1973) revealed that the Himenoura Group is divisible into two subgroups; the Lower Himenoura and Upper Himenoura, each being assigned respectively to the Cretaceous strata in Amakusa-Kamishima and Amakusa-Shimajima. The Upper Himenoura Subgroup in Amakusa-Shimajima ranges in age from Middle Campanian to Maastrichtian by the occurrence of molluscan fauna (Tashiro and Otsuka, 1978) and preliminary fission-track age determinations (Yoshida et al., 1985). According to Tashiro and Otsuka (1978), the overlying Paleogene Miroku Group is divided into four formations as Co-Akasaki, Co-Shiratake, Kyoragi, and Toishi Formations in ascending order. The Co-Akasaki Formation, which is lithologically equivalent to Akasaki Formation in Amakusa-Kamishima, bears abundant larger foraminifera such as *Nummulites amakusensis* of the Lower Eocene (Hanzawa and Urata, 1964). It was reported recently (Tashiro et al., 1980) that the basal part of Co-Akasaki Formation yields nannofossils which is assigned to the lower Middle Eocene. Since the uppermost part of the Himenoura Subgroup may extend to Paleocene (Yoshida et al., 1985), it has been suggested that the possible Cretaceous-Tertiary chronological boundary lies within somewhere in the upper part of the Himenoura Subgroup (Tashiro and Otsuka, 1978), although the stratigraphic level of the boundary strata has never been identified by previous studies (e.g., Tashiro et al., 1980).

3. Sampling and laboratory procedures

According to the biostratigraphic classification of Tashiro and Otsuka (1978), the Upper Himenoura Subgroup is divided into four formations in ascending order from U-I, U-II, U-III, and U-IV (Fig. 2), which have been assigned in age to Middle Campanian, Upper Campanian, Uppermost Campanian or Maastrichtian, and Maastrichtian-Paleocene, respectively. Based on the difference in lithofacies, each formation is subdivisible further into two or three members; U-IIa, b, U-IIIa, b, and U-IVa, b, c. Apart from the lowest formation U-I exposed very locally on a few isolated islets south of Amakusa-Shimajima, most of the sequences are distributed widely in the eastern and western parts of the island, forming as a whole a pair of synclinal fold limbs with an axis striking NNE-SSW direction. The synclinal basin in the middle of the island is filled with the Paleogene and later clastic deposits. It has been also reported from the sedimentological viewpoints (Tashiro et al., 1980) that the Upper Himenoura Subgroup exhibits four major cyclic patterns of sedimentation, each showing upward coarsening sequence which consists of a basinal mud facies in the lower part and a shallow marine coarse clastic facies in the upper. This observation has been interpreted as a line of transgressive-regressive sequence probably of tectonic origin. However, we will use hereafter the conventional biostratigraphic classification of strata for the sake of convenience in discussing our results from the stratigraphical and geochronological points of view.

A total of 26 localities were visited for paleomagnetic sampling from the eastern and western parts of the island (Fig. 2), and one to three blocks oriented separately by a magnetic compass were collected at each locality. Rock types of the samples are fine-grained sandstone, shale, sandy mudstone, and mudstone. These oriented blocks were then drilled in the laboratory, and three or four cores 25.4 mm in diameter were cut out, which were sliced into 22 mm long cylindrical specimens for magnetic measurements. 120 specimens were thus prepared in total, and all of their remanent magnetizations were measured with a Schonstedt Model SSM-2A flux-gate spinner magnetometer facilitated with a personal computer. All of the samples were subjected to progressive alternating field demagnetization comprising seven steps from 10 mT to 40 mT with an interval of 5 mT. Results of the incremental a. f. demagnetization on each sample were plotted on Zijderveld diagram, and the directional data showing univectorial decay towards the origin without extremely erratic behaviors were selected and then analyzed using a line-fitting computer program to obtain optimum directions.

4. Results and discussion

Natural remanent magnetization from these samples ranged in intensity from 7.3×10^{-5} to 8.1×10^{-3} A/m with the majority of samples from 6×10^{-4} to 3×10^{-3} A/m. After all the measurements, 55 samples of 15 sites were selected from a total of 120 samples of 26 sites. The remaining samples were rejected because of their inconsistent and uninterpretable magnetic behaviors during a.f.

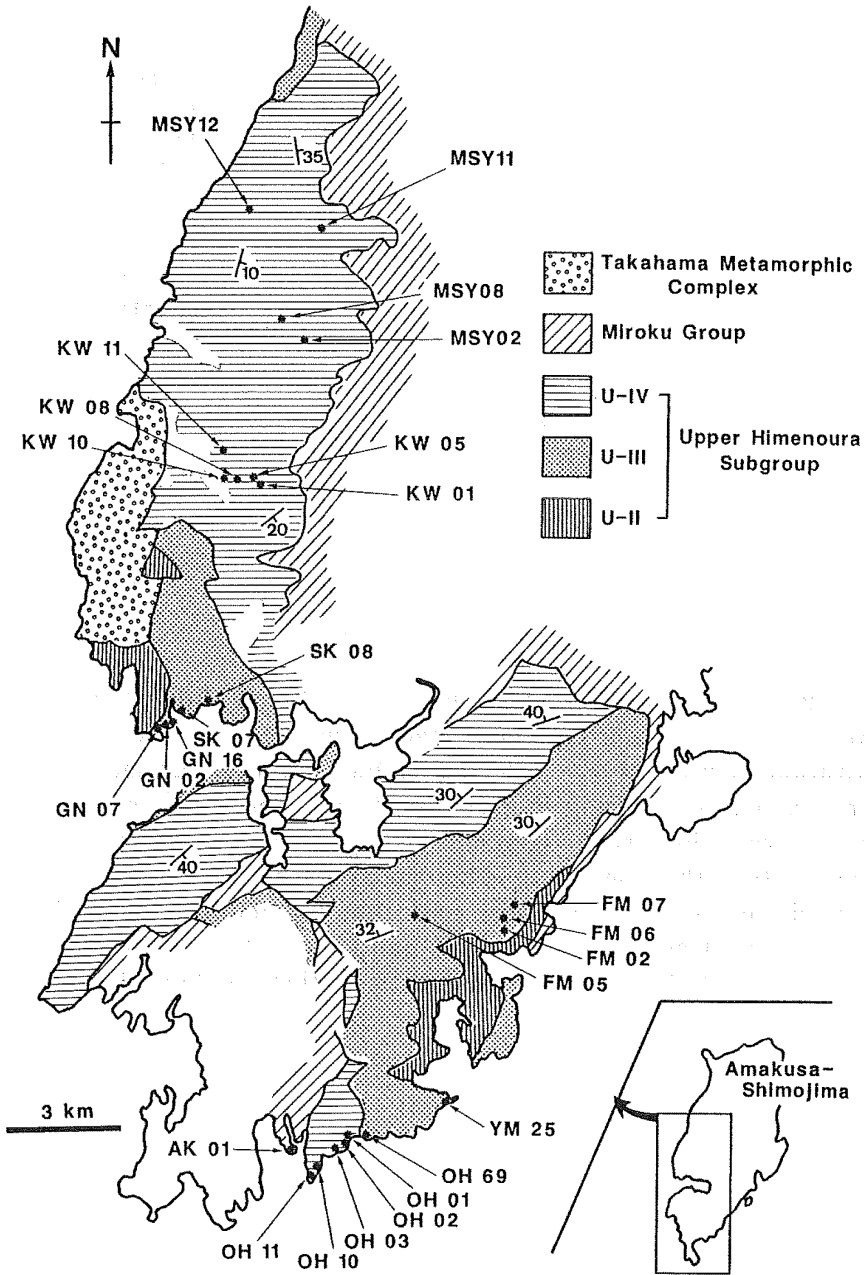


Fig. 2 Geological summary of the study area in Amakusa-Shimojima, after Tashiro and Otsuka (1978), and location of 26 sites for paleomagnetic sampling.

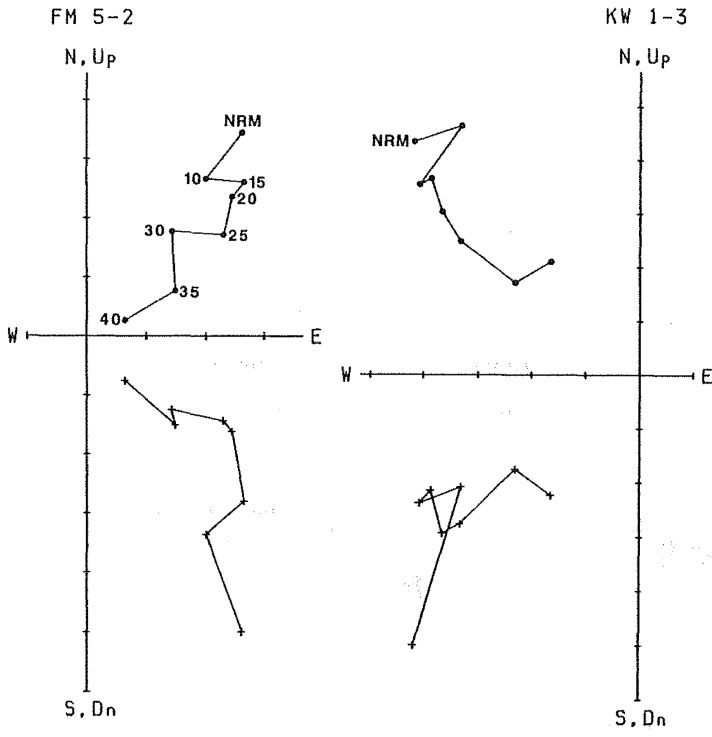
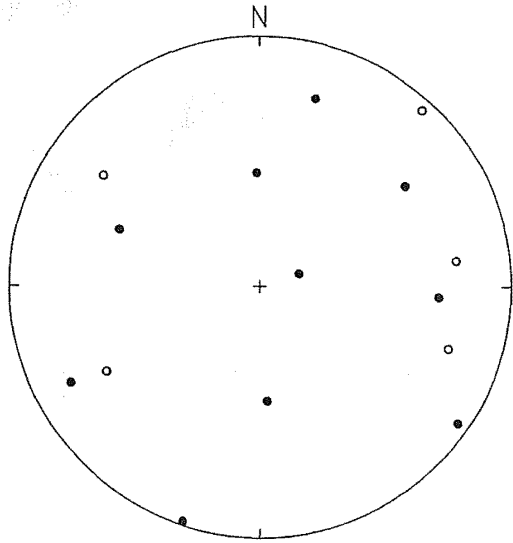


Fig. 3 Examples of orthogonal plots of vector endpoints during incremental alternating field demagnetization. Numbers are intensities of peak fields in mT. Solid circles are projections onto horizontal plane, and + are onto vertical.

demagnetization, and of too weak intensities below 10^{-5} A/m for reliable determinations with the spinner magnetometer. Although some of the magnetization vectors of the selected stable samples became erratic at the higher demagnetization levels in excess of 30 mT, the optimum directions were determined rejecting such unstable components. Typical examples of directional data of the samples thus determined are shown in Figure 3. Figure 4 shows the site mean directions after correction for bedding tilt which was done in a conventional way to rotate a tilted bed back to horizontal about a line of the strike. Figure 5 illustrates the schematic sections of Upper Himenoura

Fig. 4 Equal-area projection of 15 tilt-corrected site mean directions selected with a. f. demagnetization. Solid (open) circles are plots onto lower (upper) hemisphere.



Subgroup in western and eastern parts of Amakusa-Shimojima (Tashiro and Otsuka, 1978), location of sampling levels where stable magnetizations were found, and the stratigraphic variation of their mean inclinations. The stratigraphy-polarity relationship suggests that at least two reversed polarities were found; one is from the upper part of the formation U-IVc including four sites, and the other from the midst of U-IIIa although there is only one site with great uncertainty in direction. The seven sites between the two reversal groups and three sites from the lowest horizon seem to show normal polarities. The limited and uneven distribution of the present data set in the stratigraphic section makes it difficult to correlate these polarities to the standard geomagnetic polarity sequence. However, taking the reversal sequence contemporaneous with the age of the studied successions into consideration, these normal and reversed polarities may be correlated to some polarity chrons of the Upper Cretaceous and Paleogene, probably Maastrichtian to Danian, as indicated in Figure 6.

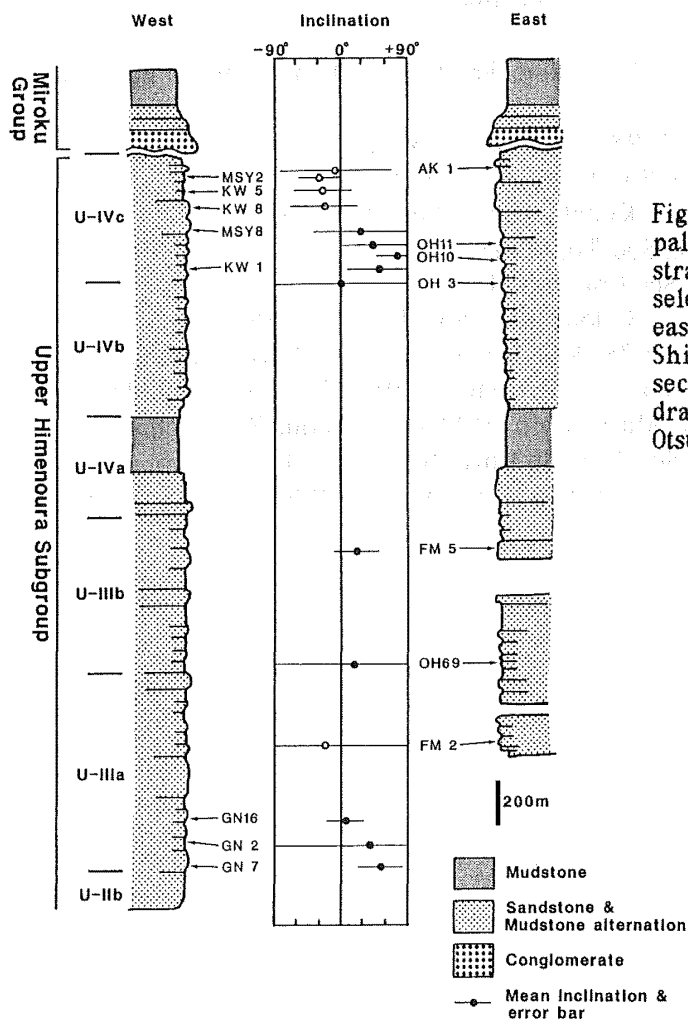


Fig. 5 Correlation of paleomagnetic inclinations and stratigraphic levels of 15 selected sites in the western and eastern parts of Amakusa-Shimojima. Stratigraphic sections are schematically drawn in part after Tashiro and Otsuka (1981).

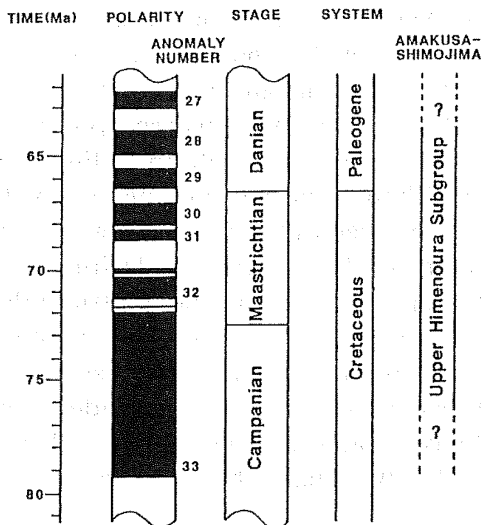


Fig. 6 Uppermost Cretaceous to Lowest Paleogene geomagnetic polarity sequence (black=normal, white=reversed), and possible time-stratigraphic correlation of the Upper Himenoura Subgroup in Amakusa-Shimajima. Polarity time scale is after Lowrie and Alvarez (1981).

References

- Hanzawa, S. and H. Urata (1964) Rep. Earth Sci., Dept. General Educ., Kyushu Univ., 11, 1.
- Lowrie, W. and W. Alvarez (1981) Geology, 9, 392.
- Matsumoto, T. (1954) Japan Soc. Prom. Sci., Tokyo, 313.
- Miki, T. (1975) Mem. Fac. Sci. Kyushu Univ., Ser. D., 9, 165.
- Nagao, T. (1922) Jour. Geol. Soc. Tokyo, 29, 90.
- Nagao, T. (1930) Jour. Fac. Sci. Hokkaido Univ., 1, 1.
- Tashiro, M. and M. Noda (1973) Jour. Geol. Soc. Jpn., 79, 465.
- Tashiro, M. and M. Otsuka (1978) Res. Rep. Kochi Univ., Natural Sci., 27, 113.
- Tashiro, M., H. Okada, A. Taira, and M. Otsuka (1980) Jour. Geol. Soc. Jpn., 86, 139.
- Tashiro, M., A. Taira, and T. Matsumoto (1980) Cretaceous Research, 1, 13.
- Ueda, Y. (1962) Mem. Fac. Sci., Kyushu Univ., Ser. D, 5, 14.
- Yoshida, S., M. Tashiro, M. Otsuka, and H. Nakazato (1985) FOSSILS, 38, 17.

PALEOMAGNETIC RESULTS FROM THE LATE CRETACEOUS KOTO RHYOLITES, SOUTHWEST JAPAN (II)

Masayuki TORII and Hisashi TSURUDOME

Department of Geology and Mineralogy, Kyoto University, Kyoto 606, Japan

1. Back ground and geologic setting

Paleomagnetic directions of the late Cretaceous rhyolitic welded tuffs and associated felsic intrusive rocks are obtained from the eastern coastal area of Lake Biwa (Fig. 1). The volcano-plutonic complex is collectively called the Koto Rhyolites [Mimura and Kawata, 1970]. The rhyolites is a part of regional extent of the felsic rocks emplaced on the pre-Cretaceous accretionary terranes throughout the southwestern half of the Japanese island arc [e.g., Taira, 1985]. The Mesozoic felsic magmatism, as an overview, took place widely along the eastern edge of the Asian continent, and played an important rôle to amalgamate allochthons with the past continental margin to form a crustal backbone such as of the present Japanese island arc [e.g., Takahashi, 1983]. Paleomagnetic directions of the Koto Rhyolite, hence, will give us a piece of evidence for a paleo-reconstruction of the Japanese island arc.

The Koto Rhyolites are exposed mainly on the western flank of the Suzuka mountain range forming a hilly backyard of Lake Biwa, while more than ten small-size masses of the Koto Rhyolites are sporadically distributed on the coastal alluvial plain and also in the lake bottom standing as three islets [Nishikawa *et al.*, 1979]. Those small rocky masses comprise welded tuff and/or felsic intrusions which are lithologically identical with that of the main mass on the hilly area, but a stratigraphic relationship between the hilly backyard and the coastal plain is not so clear due to their isolated distribution [Nishikawa *et al.*, 1983]. It is also difficult to make clear about the stratigraphic relationship among a number of small masses on the coastal plain. The proposed stratigraphy by Nishikawa *et al.* [1979], shown in Fig. 2, is only based on the observation at one outcrop where four different rock units are exposed (site 16-18 in Fig. 1). Two Rb-Sr whole rock isochron dates [Seki, 1978] and ten fission-track dates [Ito, 1986] were reported, which suggest that the igneous activity of the Koto Rhyolites took place at about $70 \text{ Ma} \pm 10 \text{ Ma}$.

Fukuma and Torii [1986] reported paleomagnetic results from the main mass of the Koto Rhyolites. They found that the felsic rocks, both the welded tuff and intrusive rocks, bore a fairly well-documented magnetostratigraphy and a paleomagnetic pole. Thus we intended to make a paleomagnetic study of the isolated small masses on the coastal plain to give an idea about the stratigraphic relationship with the main mass. And we planned to estimate a paleomagnetic pole position of the late Cretaceous from Southwest Japan.

2. Paleomagnetic analysis

We collected samples at 19 sites as illustrated in Fig. 1. Stratigraphic positions of those sites are indicated in Fig. 2; each one site from the lower Azuchi and Koshigoe welded tuffs, 12 sites from the wide-spread Kamewari welded tuff, and five sites from the latest felsic intrusive rocks. A

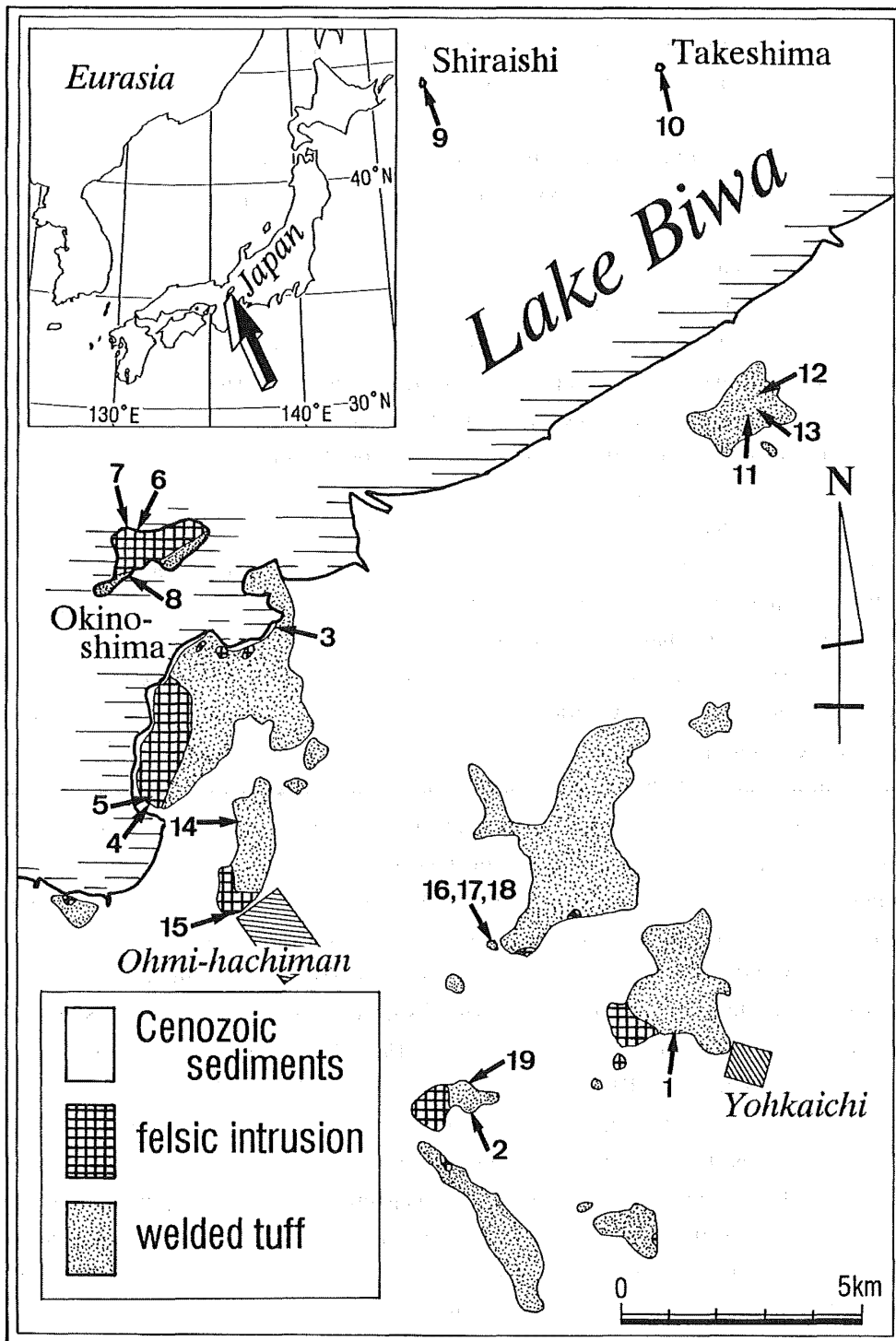


Fig. 1 Index map and sampling location for the paleomagnetic study. Geologic map is simplified after Matsuoka, [1979].

<i>Rock unit</i>	<i>Site</i>
<i>felsic intrusive rocks</i>	5,6,7,9(?),10
<i>Kamewari welded tuff</i>	1,2,3,4,8,11,12,13 14,15,17,19
<i>Koshigoe welded tuff</i>	18
<i>conglomerate</i>	
<i>Azuchi welded tuff</i>	16

Fig. 2 Stratigraphic positions of the samples with simplified stratigraphy of the Koto Rhyolites on the coastal plain area [after *Nishikawa et al.*, 1979].

tilt angle of the welded tuff was determined through a cutaxitic arrangement of glassy lenses at site 2, 11, 13, 14, 15, 16, and 17, and the maximum tilt angle does not exceed 20°. Judging from a gentle attitude of the welded tuff so far observed in this area, we think that the post-blocking tilting are not so large for the associated intrusive rocks where we could not make a direct measurement.

NRM intensity of the welded tuff range from 10⁻¹ to 10⁻⁴ A/m, and that of the intrusive rocks is from 10⁻⁴ to 10⁻⁵ A/m. We carried out magnetic measurement by using ScT cryogenic magnetometer of which noise level is 1×10⁻⁸ mAm². Two or more samples were selected as pilot samples on the basis of the NRM direction and intensity. Then those samples were demagnetized stepwise by a thermal method (11 to 13 steps to 670°C) or an alternating field method (max. 100 mT). We analyzed demagnetization behavior by plotting an end point of each demagnetized vector on the vector-demagnetization diagram. Thereby we determined remanent components by principal components analysis method [*Kirschvink*, 1980]. One of the notable aspect of the demagnetization behavior is the presence of stable components at the moderate temperature range which do not converge to the origin of vector-demagnetization diagram (Fig. 3).

As a typical example, several remanent components are displayed on Fig. 3, which are derived from the samples of site 2 and site 18. We decided multi-components of the remanence mainly by the stepwise heating and by results of the partial demagnetization at some particular temperatures. Three components of the moderate to high temperature range are thereby recognized for site 2; A, 220°C to 400°C; B, 400°C to 520°C; and C, 550°C to 610°C (Fig. 3 a). Site 2 is a good exposure of the Kamewari welded tuff, whereas nearby site 19 comprise fairly weathered rocks and does not yield a significant remanent direction. The component of the highest temperature (C) is the most plausible candidate of a primary remanent component for the case of TRM. If so, a possible heat source of secondary components (A and B) could be the nearest intrusive rock as shown in the geologic map of Fig. 1. Virtually antipodal relationship among the A, B, and C components and their significantly clockwise deflection may imply that the timing of secondary overprintings were not so later than the time of primary acquisition.

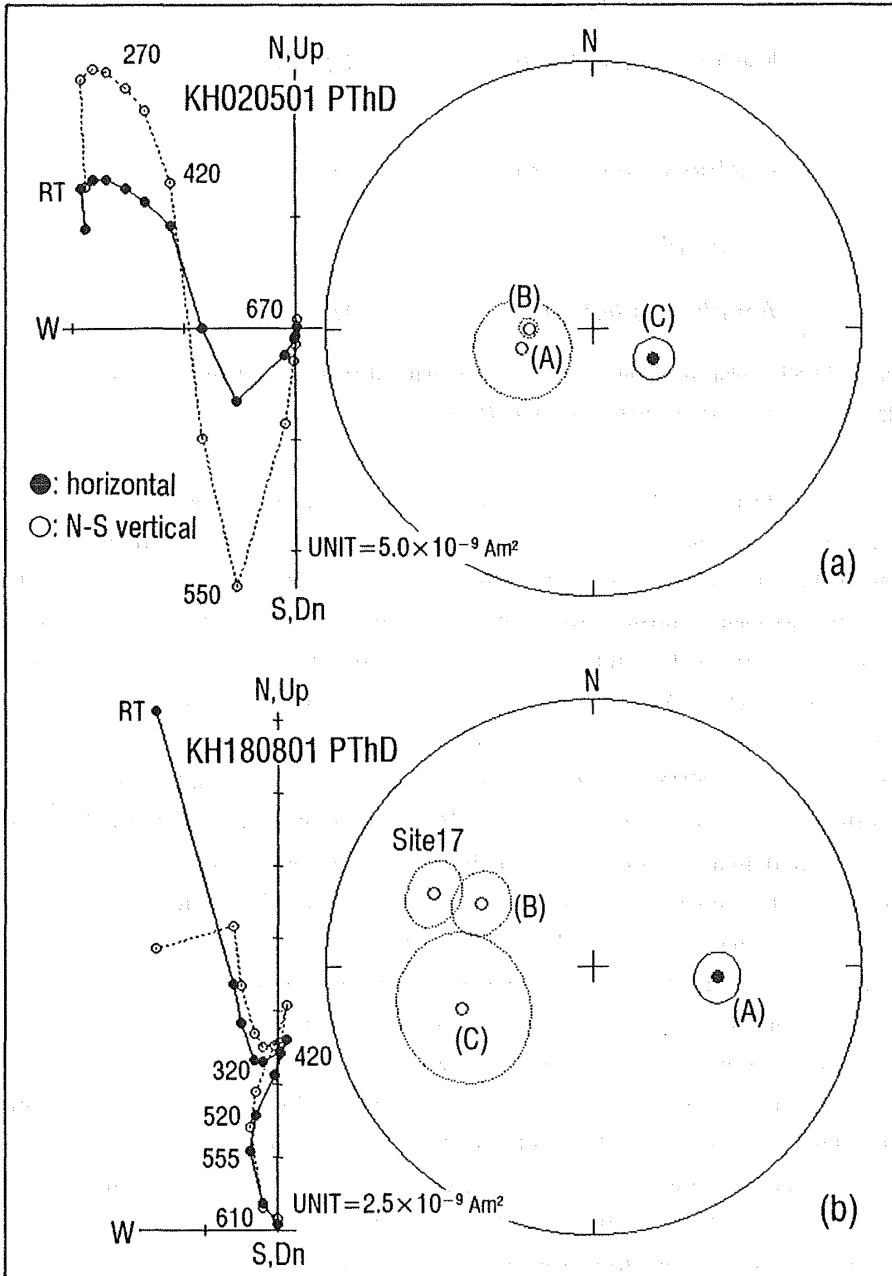


Fig. 3 Components of remanent vector revealed by the thermal demagnetization. (a) vector-demagnetization diagram of the pilot sample and possible multi-components of remanent vector plotted on equal-area projection from Site 2 (Kamewari welded tuff). (b) site 18 (Koshigoe welded tuff).

We disclosed three remanent components by the thermal treatment of site 18 (Koshigoe welded tuff) where the only place we can observe the directly overlying Kamewari welded tuff (site 17) on the Koshigoe welded tuff (Fig. 2). The Koshigoe welded tuff is found to be suffered by a thermal alteration to some extent. The component A is unblocked between 320°C to 420°C and having positive inclination. The component B appears from 520°C to 550°C, and C from 550°C to 580° (Fig. 3 b). Both the B and C show negative inclination with an antipodal direction to the component A. The overlying Kamewari welded tuff (site 17), the only possible heat source for overprinting, has similar direction with the component B of negative inclination. We think that the component of the highest temperature (C) could be the primary and component B might be a secondary one heated up by the overlying Kamewari welded tuff. Although the A component of positive inclination showing virtually antiparallel to the B or C, we can not give a full understanding for the secondary heat source, if A was TRM.

The polarity of the primary remanence of the Kamewari welded tuff at site 2 is positive as discussed above. The polarity of site 17 is, however, reversed. This apparent inconsistency may goes to ambiguity of the stratigraphic correlation or improper nomination of the primary component. If the secondary remanence of this igneous pile is not produced by a simple TRM process, it is possible to exclude the component of the highest temperature from the candidate of the primary remanence. But it is evident that the remanent directions of A, B, and C components of both site 2 and 17 are showing fairly well clustered vectors of antiparallelism. Thus we regard the direction of A, B, and/or C would be a paleomagnetic direction at late Cretaceous time.

3. Paleopole from the Koto Rhyolites

Nine sites yielded stable remanent directions which are characterized by the convergence of the vector-end points of the stepwise thermal demagnetization toward the origin of the vector-demagnetization diagram: the Azuchi welded tuff (site 16), the Kamewari welded tuff (site 2, 3, 4, 8, 11, 13, 17), and the intrusive rocks (site 7). We regard these directions as of primary remanence. These site-mean directions deflect clockwise as shown in Fig. 4(a). At some sites, remanent vectors treated at the moderate temperature make a tight cluster, which do not converge to the origin as a primary component. These directions point virtually parallel or antiparallel direction with the above-mentioned primary one (Fig. 4 b). This fact suggest that the both the high and moderate temperature components were blocked under an influence of the past geomagnetic field which is unlike to the direction of the present dipole field. We think that further examination of the "secondary" components will be very helpful to asses remanent directions of the source rock which had given the overprinting magnetization. The stratigraphic correlation among the rock units comprising the Koto Rhyolites is still somewhat controversial, and we have to make a further data collection to fix the inconsistency.

An overall-mean direction is calculated by combining nine site-mean directions (after inclination conversion into positive); $D=95.1^\circ$, and $I=51.4^\circ$ ($\alpha_{95}=9.9^\circ$). *Fukuma and Torii* (1986) reported paleomagnetic direction from the maine mass of the Koto Rhyolites as $D=77.9^\circ$, $I=61.1^\circ$, and $\alpha_{95}=6.5^\circ$, which is calculated by combining 18 site-means. The two overall-mean directions are statistically identical, and thus we combined all site-means into one to give a new

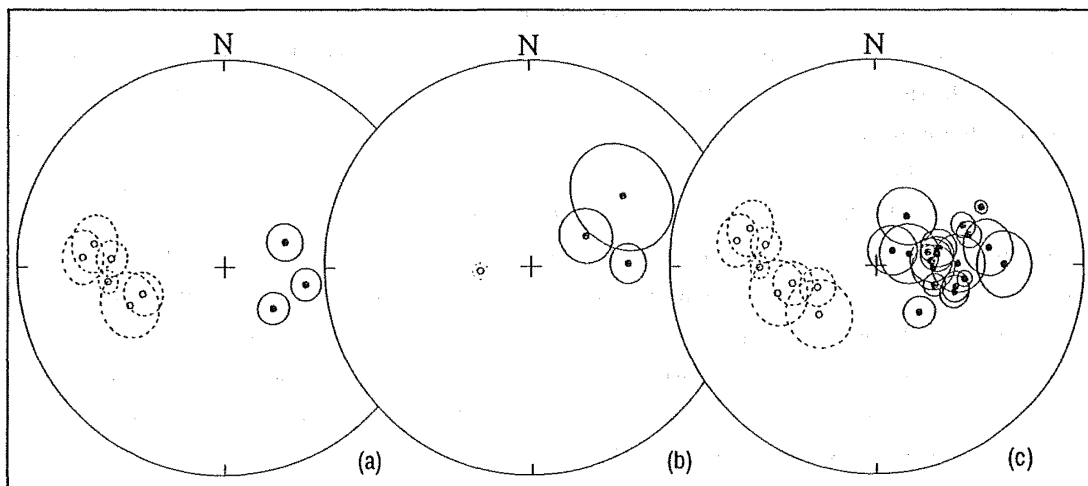


Fig. 4 Site-mean direction of the Koto Rhyolites after demagnetization and tilt correction. (a) site-mean directions from the coastal plain area, (b) direction of "secondary" components, (c) site-mean directions of the present study and those of the main mass [Fukuma and Torii, 1986].

overall-mean (Fig. 4 c). The calculated mean direction is $D=84.6^\circ$, $I=58.2^\circ$, and $\alpha_{95}=5.6^\circ$ ($N=27$). Virtual geomagnetic pole (VGP) is then calculated; the latitude and longitude of the VGP are 26.0°N and 166.8°W , respectively. The pole position coincides with that of 60 Ma and 80 Ma poles obtained from Yamaguchi and Go river areas, the western part of Southwest Japan [Otofujii and Matsuda, 1987]. This result supports that the two area, Koto area and Yamaguchi-Go river area, shared common late Cretaceous paleopole, that is they were united in a single ridged block at the time of late Cretaceous. In this context, the paleopole from the Koto Rhyolites gives further evidence to the clockwise rotation of Southwest Japan [e.g., Otofujii et al., 1985].

Reference

- Fukuma, K and M. Torii, *Rock Magnetism and Paleogeophys.*, 13, 26-29, 1986.
 Ito, H and S. Nishimura, *Rock Magnetism and Paleogeophys.*, 13, 30-31, 1986.
 Kirschvink, J. L., *Geophys. J. R. astr. Soc.*, 62, 699-718, 1980.
 Mimura, K. and K. Kawata, *J. Geol. Soc. Japan*, 76, 110, 1970.
 Matsuoka, C., (ed.) *Land and Life in Shiga*, Foundation of Nature Conservation in Shiga Prefecture, pp. 541.
 Nishikawa, K., T. Nishibori, T. Kohayakawa, T. Tajima, K. Tsuji, and Y. Sato, in *Land and Life in Shiga*, Foundation of Nature Conservation in Shiga Prefecture, 229-244, 1979.
 Nishikawa, K., T. Nishibori, T. Kohayakawa, T. Tajima, M. Joshima, K. Mimura, and M. Katada, *J. Japan Assoc. Min. Petr. Eco. Geol.*, 77, 51-64, 1983.
 Otofujii, Y. and T. Matsuda, *Earth Planet. Sci. Lett.*, 85, 289-301, 1987.

- Otofujii, Y., A. Hayashida, and M. Torii, in *Formation of Active Ocean Margins*, eds. N. Nasu, K. Kobayashi, S. Uyeda, I. Kushiro, and H. Kagami, TERRAPUB, Tokyo, 551-566, 1985.
- Seki, T., *Mem. Fac. Sci., Kyoto Univ.*, 16, 71-110, 1978.
- Taira, A., in *Formation of Active Ocean Margins*, eds. N. Nasu, K. Kobayashi, S. Uyeda, I. Kushiro, and H. Kagami, TERRAPUB, Tokyo, 835-851, 1985.
- Takahashi, M., in *Accretion Tectonics in the Circum-pacific Region*, edited by M. Hashimoto and S. Uyeda, TERRAPUB, Tokyo, 69-88.

PALEOMAGNETISM OF HOLE 504B, COSTA RICA RIDGE
 ROCKMAGNETISM AND FORMATION MAGNETISM

Hajimu KINOSHITA, Department of Earth Sciences, Chiba University, Chiba 260
 and
 Toshio FURUTA, Ocean Research Institute, University of Tokyo, Tokyo 164

Rockmagnetic and paleomagnetic properties of Hole 504B, drilled on the southern flank of Costa Rica Rift zone by Ocean Drilling Program (as well as Deep Sea Drilling Project) are presented based upon measurements of basement formations from several legs (CRRUST 1982, Cann et al 1983, Anderson et al 1982, Anderson et al 1985, Becker et al 1988). Intensity of NRM, magnetic susceptibility, saturation magnetization, Curie temperature of rocks recovered from the hole showed that the basement formation drilled so far can be divided into several magnetic zones in a parallel fashion with that of rock alteration petrographic characteristics.

Downhole magnetic field measurements revealed that there are mainly three magnetic layers significantly different in formation magnetization from each other. Statistical results of downhole magnetization indicate that the fluctuation of formation magnetization can only be explained by some blocky motion of basement layers as the lithospheric plate moves away from the Costa Rica Rift zone. This motion may have been induced by listric faulting which has formed a network of conduits of hydrothermal circulation as inferred from geothermal and geochemical analyses of Hole 504B.

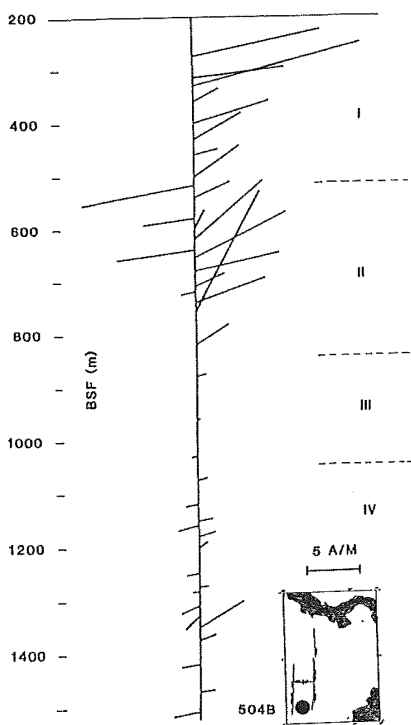


Fig. 1(left) Downhole distribution of inclination values of recovered core samples. Length of each bars give NRM intensity and upward and downward pointing NRM vectors are plotted on separate half space to avoid complication.

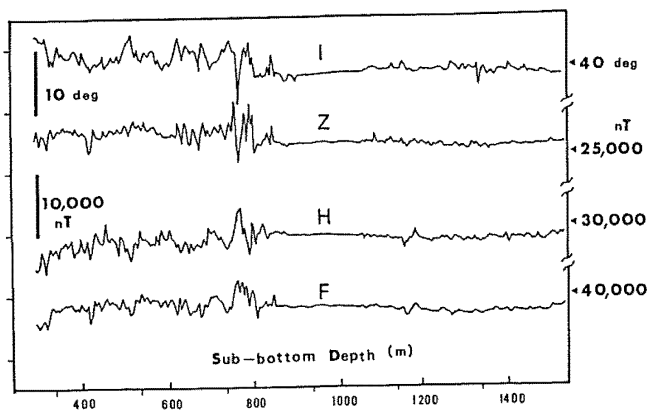


Fig. 2(bottom left) Distribution of downhole magnetic field parameters as indicated by thick symbol characters. Strengths and angles are shown along ordinate separately.

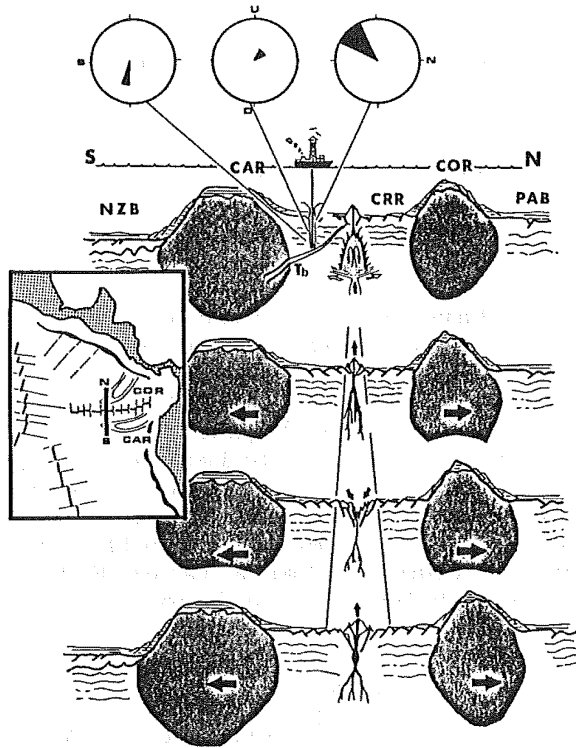


Fig. 3 Cross section of lithosphere of this area and its drift. The section is projected along N-S line, a thick bar in the insert. Nazca Plate, Carnegie Ridge, Costa Rica Rift, Cocos Ridge and Pacific Plate are shown by symbol letters. Thick arrows are direction of opening and thin arrows show motion of crustal volcanic blocks. Black fans in circles show approximate inclination and their standard deviation for individual upper, middle and lower sections of the basement layers reached by DSDP as well as ODP (Leg 69 - 111).

References

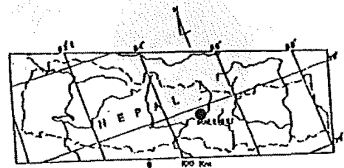
- Anderson, R. and cruise participants (1982) *Nature*, 300, 589-594
 Anderson, R. and cruise participants (1985) *Init. Rept.* 83, 443-478
 Becker, K. and cruise participants (in print) *Init. Rept.* 111
 Cann, J. and cruise participants (1983) *Init. Rept.* 69
 CRRUSI' (1982) *Geol. Soc. Am. Bull.*, 93, 862-875

ON THE SECONDARY MAGNETIZATIONS OBSERVED IN NAWAKOT
COMPLEX ROCKS, MALEKHU AREA, CENTRAL NEPAL

Pitambar GAUTAM and Mitsuo YOSHIDA

Department of Geology and Mineralogy, Faculty of Science,
Hokkaido University, Sapporo 060, Japan

Paleomagnetic measurements have been carried out on some Late Pre-Cambrian to Paleozoic rocks of Nawakot Complex, Lesser Himalaya, Nepal. Samples were collected from an approximately 5 Km NE-SW route running parallel to Thaple and Malekhu Kholas in the vicinity of the town of Malekhu (27.8°N, 84.8°E) situated on the left bank of the Trishuli river. A brief geological description following Stocklin (1980) and the sampling details are presented in Fig. 1 and Table 1. The Nawakot Complex, which consists exclusively of low-grade metasediments, together with the overlying Kathmandu Complex constitutes a large WNW-ESE trending structure known as the Mahabharat Synclinorium.



LEGEND

-  RADUWA FM.
Garnetiferous Schists, Quartzites
-  ROBANG FM:
Phyllites, Mica Schists with Amphibolites
-  MALEKHU LIMESTONE
-  BENIGHAT SLATES
with Phyllites and Quartzites
-  DHADING DOLOMITE
-  NOURPUL FM.
Quartzites, Metasandstones, Phyllites
- MBhT Mahabharat Thrust
- ML Sampling sites
-  River, Khola, Stream

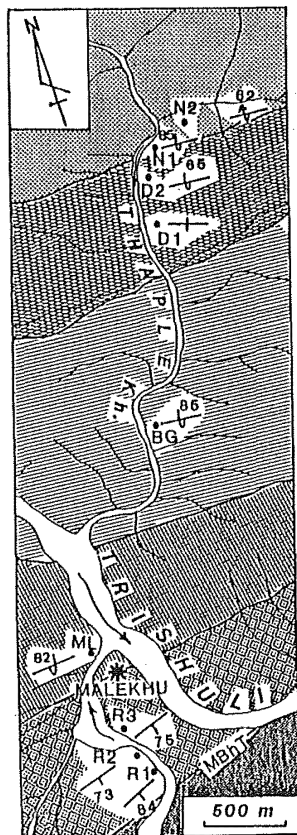


Fig. 1
Geological sketch map of the Malekhu area showing sampling sites. Index map shows the location of Malekhu.

Table 1 Sampling details of Nawakot Complex rocks, Malekhu

Formation	Site Index	Rock type (Sampled)	Bedding Strike/Dip of strata *
Robang	R1	Hematite schist	N 68 E/84 SE
	R2	Phyllite, amphibolite	N 73 E/73 SE
	R3	Chloritic phyllite	N 70 E/75 SE
Malekhu	ML	Fine-crystalline limestone	N 85 E/82 NW (OVT)
Benighat	BG	Quartzose slate	N 86 W/85 NE (OVT)
Dhading	D1	Sparry dolomite	N 72 W/90 SW
	D2	Bluish-grey dolomite	N 88 W/65 NE
Nourpul	N1	Semi-pelitic phyllite	N 88 W/85 NE (OVT)
	N2	Quartz phyllite	N 86 W/62 NE (OVT)

* OVT - overturned

Reliable data could be obtained only from limited number of sites (Table 2). Samples from other sites were found either to be too weakly magnetized (NRM intensities less than 0.01 mA/m) or highly inhomogeneous. The stability of the directions was assessed through stepwise alternating field followed by thermal demagnetization experiments. Typical demagnetization results are shown in Fig. 2.

Table 2 Results of magnetic measurements

Site	n(N)	NRM Intensity (mA/m)	Demag. status (mT)	Mean direction (uncorr.)				Mean direction (corr.)			component and polarity
				D	I	k	a_{95}	D_c	I_c		
R1	3(7)	235-762	30	234	34	64	10	212	-9	S2 (R)	
BG	3(7)	0.64-1.47	53	327	70	116	7	196	10	S2 (R)	
D1	3(3)	0.19-0.42	20	000	43	81	8	-	-	S1 (N)	
N1	3(7)	25.5-47.9	30	096	-50	123	7	41	1	S2 (N)	
N2	3(7)	4.1-16.8	0-20*	007	51	17	19	-	-	S1 (N)	
	3(6)		50	134	-61	44	12	26	7	S2 (N)	

Mean of S2 component (after bedding correction):
(Normal & Reverse combined)

$$D = 028, I = 1, k = 36, a_{95} = 11$$

n and N are the number of samples and specimens, respectively; D, I and D_c , I_c are the declinations and inclinations in degrees before (uncorr.) and after (corr.) bedding correction. k is the estimate of Fisher's precision parameter and a_{95} is the semi-angle of cone of 95 % confidence, in degrees. Parameters calculated giving unit weight to samples. (N) and (R) in the last column denote normal and reverse polarities, respectively.

* Direction calculated from NRM to 20 mT demagnetization data.

Mean direction from site D1 and the softer component from site N2 are very close to the dipole field direction at present for Malekhu ($I=47^\circ$) and are interpreted to represent the recent field component of secondary origin (S1). Such a component could be identified in some of the specimens from other sites as well (e.g. specimen BG-3C, Fig. 2). Tilt correction of the remaining directions showed that they form two groups which are

almost antipodal to each other. These two groups are assumed to represent roughly a pair of normal and reverse polarities. The mean direction, then, was calculated by reversing the directions from sites R1 and BG and combining with the other two. This resulted in a mean direction with NNE declination and almost horizontal inclination ($I=1^\circ$).

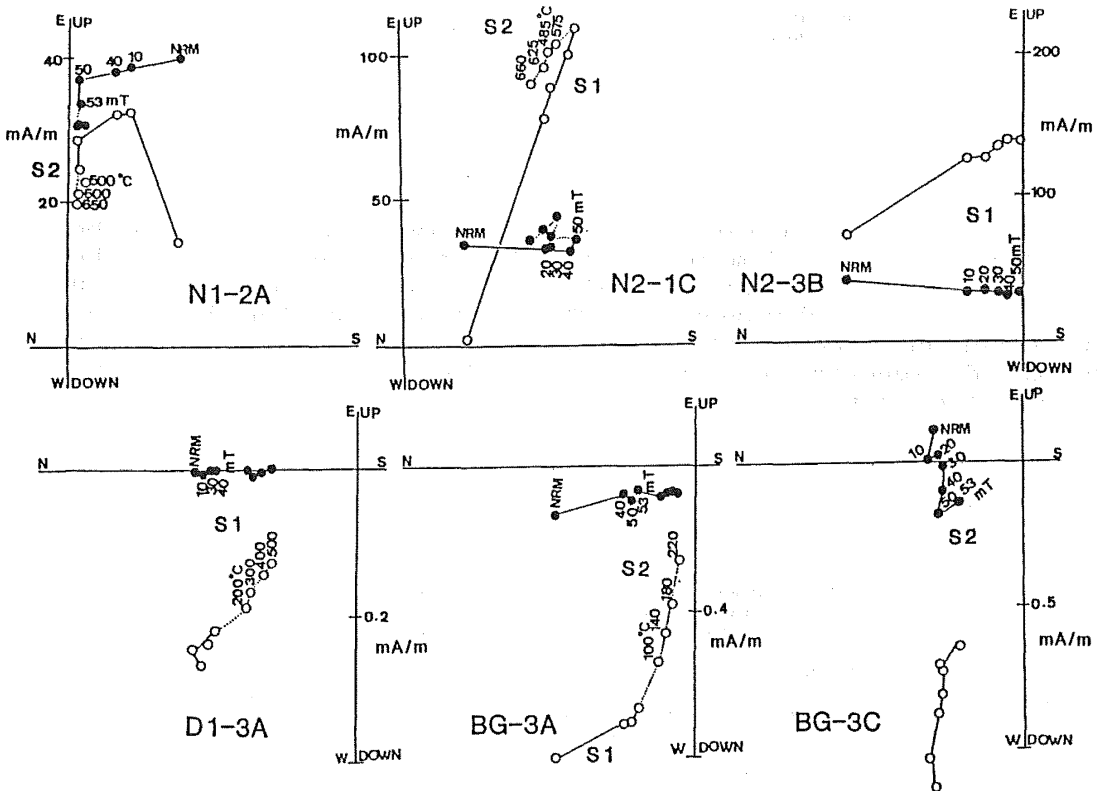


Fig.2 Zijderveld diagrams of some representative specimens. Solid and open circles are projections of the tip of the vector at successive alternating field demagnetization (AFD) and thermal demagnetization (THD) levels on the horizontal and N-S vertical planes, respectively. For clarity, the path during AFD is shown by solid lines with peak field values (in mT) placed besides the solid circles whereas the path during THD is shown by dotted lines with temperature (in $^\circ\text{C}$) besides open circles. S1 and S2 placed against the linear segments denote the components.

An attempt is made to interpret the later direction by comparing it with those to be expected in the area from the Indian APWP. The expected directions for the town of Malekhu were calculated from the Indian APWP data, simulated from India-Africa relative movement data with Africa fixed to a hotspot frame (Klootwijk et. al., 1985, Table 2C) under the hypothetical assumption that no relative latitudinal movement of the Malekhu area has occurred relative to the Indian Shield.

Comparison of inclinations (Fig. 3) suggests the most probable acquisition period somewhere during 45-55 Ma. The mismatch in declination suggests further that the Malekhu area might have experienced approximately 45° clockwise rotation relative to the shield. The possible age range of the acquisition suggests the secondary nature of the observed direction (hence designated as S2).

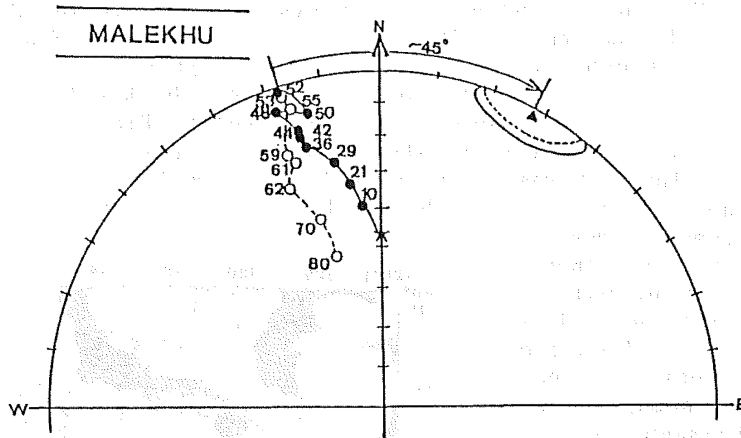


Fig. 3 Comparison of the mean direction S2 (triangle) with the directions (circles) expected in Malekhu for the period 10 to 80 Ma according to Indian APWP (Klootwijk et. al; 1985, Table 2C). Solid and open symbols denote positive and negative inclinations, respectively.

Macroscopic and microscopic examination of the samples and thermomagnetic data suggest the carrier of the remanence to be hematite. A probable origin of hematite in the Nawakot Complex rocks during regional metamorphism in Eocene time or recrystallization of the existing hematite with complete remagnetization is suspected. The magnetization S2 is correlatable to the secondary magnetizations dated around 50 Ma which are attributed to the probable thermo-chemical effects associated with the initial India-Asia collision (Klootwijk et. al., 1985, 1986, Gautam, 1987).

References

- Gautam, P. (1987) J. Fac. Sci. Hokkaido Univ., Ser. IV, 2, 259-324.
 Klootwijk, C. T., P. J. Conaghan and C. McA. Powell (1985) Earth Planet. Sci. Lett., 75, 167-183.
 Klootwijk, C. T., R. Nazirullah and K. A. de Jong (1986) Earth Planet. Sci. Lett., 80, 394-414.
 Stocklin, J. (1980) J. Geol. Soc. London, 137, 1-34.

(Submitted to J. Nepal Geol. Soc.)

ROTATION OF THE PHILIPPINE SEA PLATE INFERRED FROM PALEOMAGNETISM OF THE PALAU AND THE YAP ISLANDS

Yasuhisa ADACHI, Hiroo INOKUCHI, Yo-ichiro OTOFUJI,
Nobuhiro ISEZAKI and Katsumi YASKAWA

Department of Earth Sciences, Faculty of Science, Kobe University,
1-1, Rokkodai-cho, Nada-ku, Kobe 657

The Philippine Sea is a marginal basin bounded on the east side by the Izu-Ogasawara-Mariana island arc-trench system. The Kyushu-Palau Ridge ranges nearly north and south on the center of the Philippine Sea Basin from the southeast of Kyushu to the Palau Islands (Figure 1). Paleomagnetic study for the Palau Islands on the southern end of the Kyushu-Palau Ridge and the Yap Islands on the western of the Caroline Ridge across the Yap Trench, was carried out to discuss the tectonic history of the Philippine Sea Plate. More than 170 samples were collected from 31 sites; 16 sites in the Palau Islands and 15 sites in the Yap Islands.

Natural remanent magnetization (NRM) of most specimens was stable and each primary component was obtained through thermal demagnetization treatment rather than alternating magnetic field demagnetization method. Paleomagnetic results from the Palau Islands reveal that the stable remanent magnetization of Eocene and Oligocene samples has an easterly declination of about 60° (Figure 2). On the other hand, the stable remanent magnetization of the samples from the Yap Islands has a northerly declination or a westerly declination of about 40° before bedding correction but seems to have an easterly declination after bedding correction (Figure 3).

Paleomagnetic results from the Palau Islands indicate that this Islands had undergone clockwise rotation of about 60° since the Oligocene. The large easterly declination is not only found in paleomagnetic results from the Palau Islands but also in those from the Ogasawara (Kodama et al., 1983), Saipan (McCabe and Uyeda, 1983) and Guam (Kobayashi, 1972 and Larson, 1975) islands. Therefore, the rotation of the Palau Islands is not due to tectonics of the only Palau but the tectonics of the West Philippine Sea: the easterly declination observed between the Palau and the Ogasawara Islands suggests that the whole Philippine Sea Plate was rotated. Clockwise rotation of the Philippine Sea Plate is

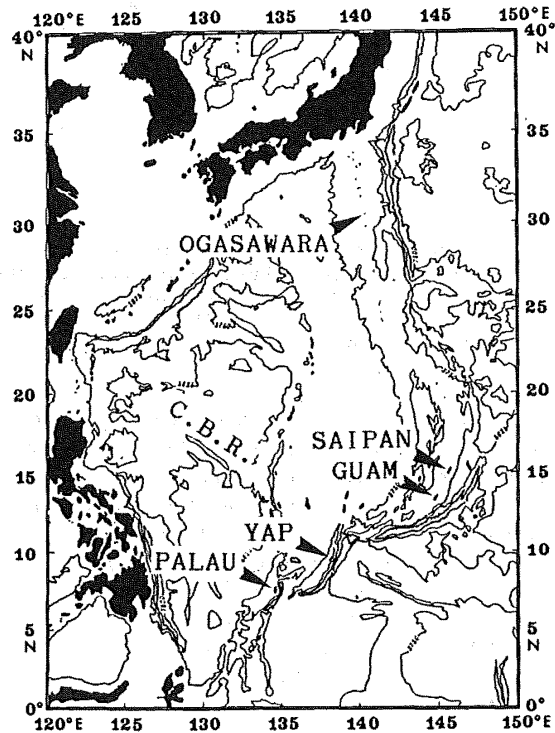


Fig.1 Outline map of the West Philippine Sea, showing major geomorphological features and location of the Ogasawara, Saipan, Guam, Yap and Palau islands.

supported by the evidence of the magnetic anomalies of the West Philippine Sea (Shih, 1980).

We propose the following process to account for the clockwise deflection in declination of the Palau Islands.

(1) The Philippine Sea Plate was produced from the Pacific Plate by the development of a transform fault.

(2) This transform fault changed to the subduction zone in the Eocene because of the change of the Pacific Plate motion from NNW to NW. The volcanic activity associated with the subduction of the Pacific Plate formed the proto Kyushu-Palau Ridge which bounded the Philippine Sea Plate on the east side.

(3) The volcanic rocks on the proto Kyushu-Palau Ridge recorded the northerly remanent direction (Figure 4a).

(4) The remanent magnetization of the proto Kyushu-Palau Ridge had been turned to about 60° associated with the clockwise rotation through about 60° of the

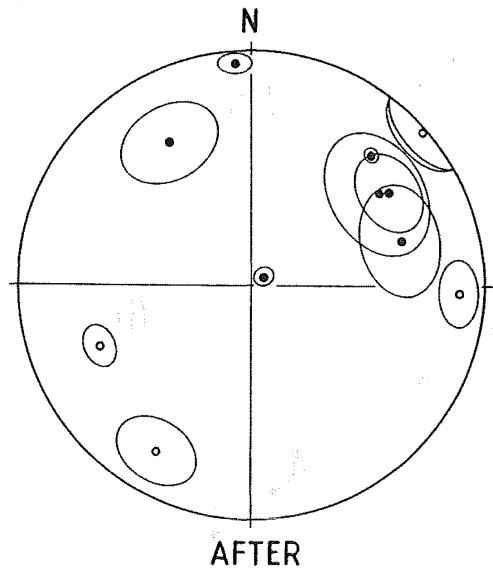


Fig.2 Paleomagnetic field directions and 95% confidence circles of sites are shown for the Palau Islands. Solid symbols are on the lower hemisphere and open symbols are on the upper hemisphere of equal-area projection.

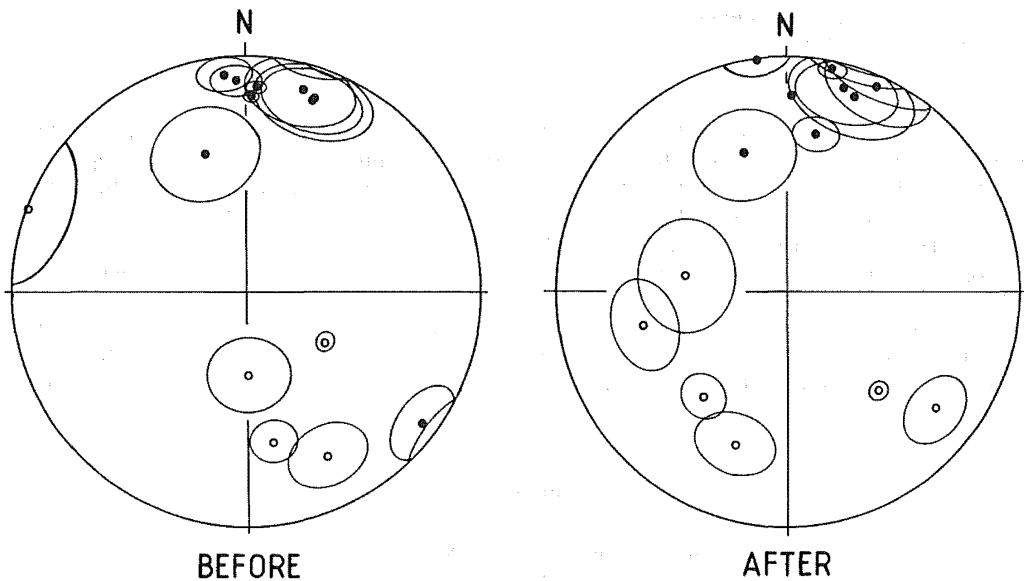


Fig.3 Paleomagnetic field direction and 95% confidence circles of sites are shown for the Yap Islands before and after bedding correction. Solid symbols are on the lower hemisphere and open symbols are on the upper hemisphere of equal-area projection.

Philippine Sea Plate since the Oligocene (Figure 4b).

(5) Parallel opening of the Shikoku and the Parece Vela Basin during 30-15 Ma separated the proto Kyushu-Palau Ridge into the present Kyushu-Palau Ridge and its eastern arc, while one of the northern part of the eastern arc formed the Ogasawara, and southern part of it moved farther eastward due to opening of the Mariana Basin and formed the Guam and Saipan islands. The islands from Palau to Ogasawara have been kept the easterly declination values (Figure 4c).

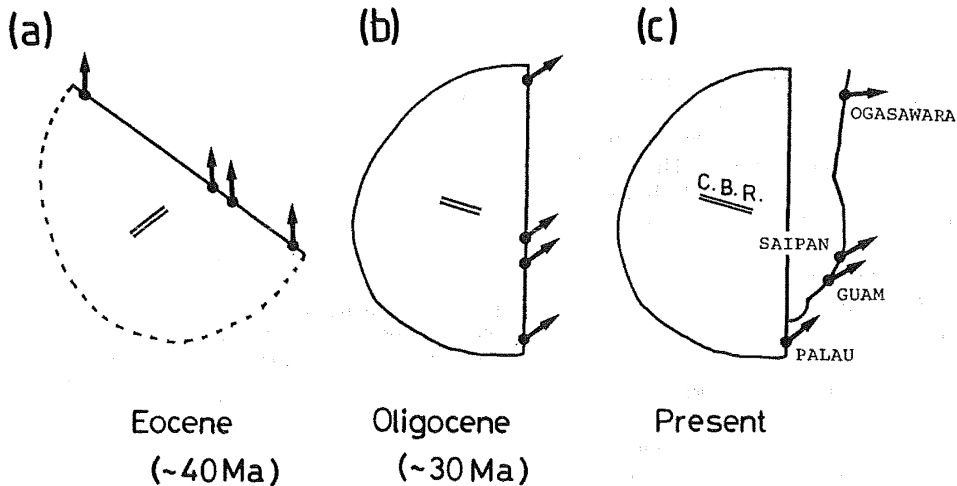


Fig.4 The model of the Philippine Sea Plate is shown in order of age. Pointing arrows are paleomagnetic declinations on each island. C.B.R. is the Central Basin Ridge.

An alternative explanation for the easterly declination of the Palau Islands is the rotation of the Palau Islands Arc due to the back arc spreading of the West Philippine Sea Basin. This explanation requires that the magnetic lineation of this basin should be aligned parallel to the Palau Islands. The lineation direction of the west of the Palau Islands, however, is about $N70^{\circ}W$ at present, which is nearly right direction to the Palau Islands.

Paleomagnetic direction of the Yap Islands indicates that NRM of the rocks had been acquired after the rotation of the plate ceased or that the Islands was further rotated counterclockwise by a collision of the Caroline Ridge.

REFERENCES

- Kobayashi, K. (1972) Izu Peninsula. Tokai Univ.Press, Tokyo, 385.
 Kodama, K., B.H.Keating, and C.E.Helsley (1983) Tectonophys., 95, 25.
 Larson, E.E., et al. (1975) Geol.Soc.Am.Bull., 86, 346.
 McCabe, R. and S.Uyeda (1983) Geophys.Monogr., Am.Geophys.Union, 27, 281.
 Shih, T.-C. (1980) Geophys.Monogr., Am.Geophys.Union, 23, 49.

(To be submitted to Nature.)

PALEOMAGNETISM AND K-Ar AGES IN HIVA-OA ISLAND, MARQUESAS,
FRENCH POLYNESIA

Hiroshi KATAO¹⁾, Hayao MORINAGA²⁾, Masayuki HYODO²⁾,
Hiroo INOKUCHI²⁾, Jun-ichi MATSUDA²⁾, and Katsumi YASKAWA²⁾

- 1) Earthquake Research Institute, University of Tokyo,
Bunkyo, Tokyo 113, Japan
- 2) Department of Earth Sciences, Faculty of Science,
Kobe University, Nada, Kobe 657, Japan

The angular dispersion of the ancient geomagnetic field at given locality and/or their corresponding virtual geomagnetic poles (VGPs) are useful to provide valuable information on paleosecular variation (PSV) of the geomagnetic field. PSV data of the world indicate a strong latitude dependence; angular dispersion of VGP increases with latitude (McElhinny and Merrill, 1975). Various models are proposed to describe secular variation and its latitude dependence.

Geomagnetic secular variation observed in the Pacific region is lower than those observed in other regions (Fisk, 1931; Fleming, 1939; Vestine et al., 1947; Vestine and Kahle, 1966). The non-dipole field intensity in the Pacific region is very low at present. This notable feature has been recognized since 1829, when the oldest reliable spherical harmonic analysis was performed. Doell and Cox (1971 and 1972) showed anomalously low secular variation based on both observatory data and paleomagnetic data during the Brunhes polarity chron in Hawaii, and explained that this phenomenon is caused by a lateral inhomogeneity of lower mantle which is coupled to the core in such way as to partially prevent the generation of non-dipole field beneath the central Pacific Ocean. This phenomenon is named the Pacific non-dipole low or the Pacific dipole window. It is profoundly interesting how far this non-dipole low region extends to. Unfortunately, there are few informations on the dimension of the Pacific dipole window, except for the Hawaiian Islands.

Hiva-Oa Island (9.75°S and 139.0°W) is one of volcanos composing the Marquesas Islands. Marquesas chain exhibits volcanic migration from northwest to southeast, and is explained to have been formed through the volcanic activity generated at a hotspot which is situated at 112 km southeast of Fatu-Hiva Island (10.5°S and 138.35°W) in the same way as Hawaii-Emperor chain (Duncan and McDougall, 1974; Jarrard and Clague, 1977).

In 1979, we collected 211 oriented rock samples from 36 sites of lava flows and dykes in Hiva-Oa Island. Samples were oriented by a magnetic compass. One to five core subsamples, 25 mm long and 25 mm in diameter, were prepared from each sample in the laboratory.

Remanent magnetization of subsamples was measured using spinner magnetometer. Stepwise demagnetization in alternating-field (AF) up to 50 mT was performed on three or more pilot subsamples from each site. Median destructive field (MDF) ranged from 5 mT to over 50 mT; generally between 20 mT and 30 mT. Most of pilot subsamples did not significantly change their remanent direction during stepwise AF demagnetization. Other pilot subsamples lost the secondary component at the AF levels up to 30 mT. The optimum demagnetization levels (ODF) were determined to give characteristic field direction every site. All subsamples were demagnetized in ODF determined every site.

Stepwise thermal demagnetization was also performed on pilot subsamples from four sites. Directions of magnetization did not significantly change under thermal demagnetizing process. Consequently no behavior, which is different from that during AF demagnetization treatments,

was observed during thermal one.

The paleomagnetic results show that both normal and reversed polarities are present; 13 sites are normal and 23 sites are reversed. Mean field directions every site are shown using equal-area projection (Fig.1). VGPs for the sites having reversed polarity are inverted to give a distribution confined to the northern hemisphere. Mean pole for all VGPs is located on 88.0°N and 126.3°W. These VGP positions were calculated using the present location of Hiva-Oa Island. No correction of VGP positions for plate motion is needed. Because, when Hiva-Oa is brought back to the position of 2 m.y. ago using the rotation pole of Pacific plate, the angular distance corresponding to the distance is a few degrees.

Eleven samples from 5 sites of reversed polarity and from 6 sites of normal one were dated by K-Ar method. The K-Ar age and its error were calculated in accordance with Cox and Dalrymple (1967) using the refined constants: $\lambda_e = 0.581 \times 10^{-10} \text{yr}$, $\lambda_\beta = 4.962 \times 10^{-10} \text{yr}$, $^{40}\text{K}/\text{K}_{\text{total}} = 1.167 \times 10^{-2}$ at percent (Steiger and Jager, 1977).

Our ages lie in a range 2.74-1.77 m.y., which are in good agreement with the ages reported by Duncan and McDougall (1974). Two pairs of samples; N1 and M2, BH4 and BH8, show the ages consistent with stratigraphic sequence. For example, the age of the dyke sample N1 which intruded into the lava sample M2 is younger than that of the sample M2.

The obtained K-Ar ages and the paleomagnetic polarity data are in good accordance with the geomagnetic reversal time scale constructed by Mankinen and Dalrymple (1979) except for the samples of BF5 and BH4 (Fig.2). The

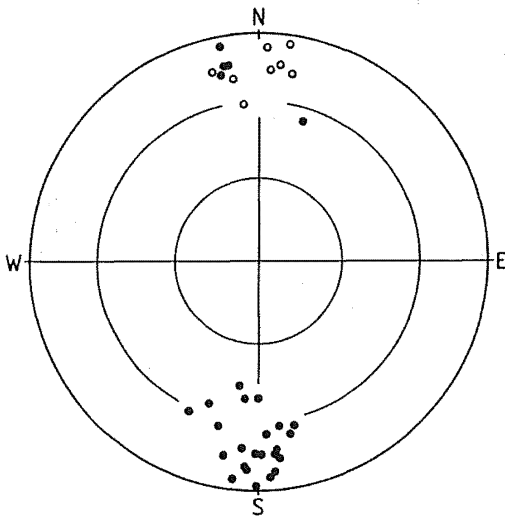


Fig.1 Mean directions of remanent magnetization after AF demagnetization for 36 sites.

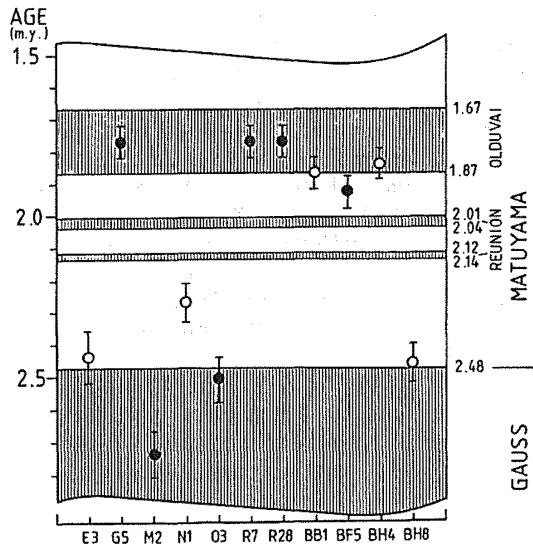


Fig.2 Diagram of the geomagnetic polarity vs. K-Ar ages for volcanic rock samples. Solid (Open) circles indicate samples of normal (reversed) polarity. Shaded pattern represents periods of normal polarity (Mankinen and Dalrymple, 1979).

ages show that the volcanic activity of Hiva-Oa continued on about 1 m.y. without a distinct hiatus.

Reliability of paleomagnetic data of Hiva-Oa is ascertained through both AF and thermal demagnetizations, presence of normal and reversed polarity and their consistency with geomagnetic time scale. These data are suitable to investigate PSV in Pacific region.

It is difficult to determine a minimum age range of paleomagnetic data which is needed to obtain meaningful PSV value. Since most of the paleomagnetic studies that have been made for investigations of PSV generally cover only a part of the Brunhes polarity chron, it is likely that no more than one tranquil or noisy period which are 0.2-0.6 m.y. long should be represented. In order to estimate PSV value fully and effectively, it appears to be necessary to use paleomagnetic data distributed over a very long period, such as several millions of years (McElhinny and Merrill, 1975). Recently Heki (1983) pointed out that meaningful estimates of PSV can be obtained at least over the time interval of more than a few times 10^4 years. Since the interval of paleomagnetic data from Hiva-Oa is longer by two orders than 10^4 years, our estimate of PSV is obviously meaningful.

Paleomagnetic data used to estimate PSV value are required to be random in time. If lava flows were produced during a short period, angular dispersion should not represent a value of complete secular variation, and should be biased toward the lower value. It appears based on geochronological data that lava eruption and dyke intrusion did not occur during some short periods.

Angular dispersion was calculated from paleomagnetic results of 32 in 36 sites. In order to maintain statistical uniformity, four sites with the greater α_{95} than 9° were excluded from dispersion analysis (Isaacson and Heinrichs, 1976). Mean VGP position was 88.1°N and 117.9°W with the α_{95} of about 4.2° for 32 poles. The geographic pole is contained within the 95% confidence limit circle. The dispersion due to secular variation for Hiva-Oa was estimated to be 13.6° with respect to mean VGP, and its upper and lower limits were 16.4° and 11.6° , respectively. Since it is generally recognized that the averaged geomagnetic field can be represented by a geocentric axial dipole field, dispersion analysis was also made with respect to the geographic pole on the assumption that true mean VGP is located on the geographic pole. The dispersion due to secular variation was 13.8° with respect to geographic pole, and its upper and lower limits were 16.6° and 11.8° , respectively.

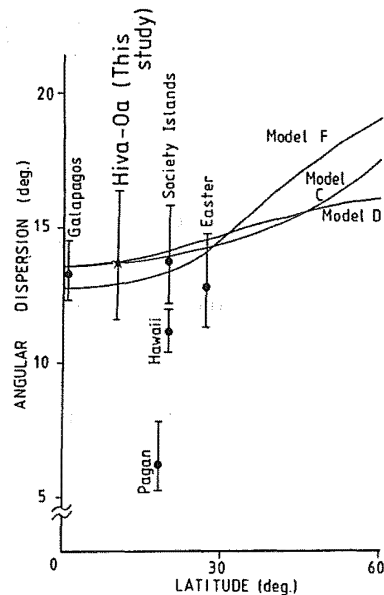


Fig.3 Virtual geomagnetic pole angular dispersions covering the past 5 m.y. in the Pacific Ocean: Galapagos (Doell and Cox, 1972), Society (Duncan, 1975), Easter (Isaacson and Heinrichs, 1976), Pagan (U.S.-Japan P. C. P. M., 1975), Hawaii (McWilliams et al., 1982), Model C (Cox, 1962), Model D (Cox, 1970), and Model F (McFadden and McElhinny, 1984).

The angular dispersion value of Hiva-0a (13.8°) is consistent with the values predicted by secular variation models (Fig.3); e.g., Model C (Cox,1962), Model D (Cox,1970) and Model F for the past 5 m.y. (McFadden and McElhinny, 1984). It is concluded that low secular variation as reported on the Hawaiian Islands did not exist in the Marquesas Islands region at least during the period from 2.74 to 1.62 m.y.

References

- Cox, A. (1962) *J. Geomag. Geoelectr.*, 13, 101.
Cox, A. (1970) *Geophys. J. R. Astr. Soc.*, 20, 253.
Cox, A. and G. B. Dalrymple (1967) *J. Geophys. Res.*, 72, 2603.
Doell, R. R. and A. Cox (1971) *Science*, 171, 248.
Doell, R. R. and A. Cox (1972) *The Nature of the Solid Earth* (edited by E. C. Robertson, McGraw-Hill, New York), 245.
Duncan, R. A. (1975) *Geophys. J. R. Astr. Soc.*, 41, 245.
Duncan, R. A. and I. McDougall (1974) *Earth Planet. Sci. Lett.*, 21, 414.
Fisk, H. W. (1931) *Bull. Int. Geod. Geophys. Union*, No.8, 280.
Fleming, J. A. (1939) *Physics of the Earth*, 8, Terrestrial Magnetism and Electricity (McGraw-Hill, New York).
Heki, K. (1983) *J. Geomag. Geoelectr.*, 35, 383.
Isaacson, L. B. and D. F. Heinrichs (1976) *J. Geophys. Res.*, 81, 1476.
Jarrard, R. D. and D. A. Clague (1977) *Rev. Geophys. Space Phys.*, 15, 57.
Mankinen, E. A. and G. B. Dalrymple (1979) *J. Geophys. Res.*, 84, 615.
McElhinny, M. W. and R. T. Merrill (1975) *Rev. Geophys. Space Phys.*, 13, 687.
McFadden, P. L. and M. W. McElhinny (1984) *Geophys. J. R. Astr. Soc.*, 78, 809.
McWilliams, M. O., R. T. Holcomb, and D. E. Champion (1982) *Phil. Trans. R. Soc. Lond. A*, 306, 211.
Steiger, R. H. and E. Jager (1977) *Earth Planet. Sci. Lett.*, 36, 259.
U.S.-Japan Paleomagnetic Cooperation Program in Micronesia (1975) *J. Geomag. Geoelectr.*, 28, 57.
Vestine, E. H., L. Laporte, C. Cooper, I. Lange, and W. C. Hendrix (1947) *Carnegie Inst. Wash. Publ.*, 578.
Vestine, E. H. and A. B. Kahle (1966) *J. Geophys. Res.*, 71, 527.

(Submitted to *J. Geomag. Geoelectr.*)

PALEOMAGNETIC EVIDENCE FOR TECTONIC DEFORMATION OF THE NARROW ZONE ALONG THE INDUS-ZANGBO SUTURE BETWEEN INDIA AND EURASIA

Yo-ichiro OTOFUJI*, Shoubu FUNAHARA*, Jun MATSUO*,
Fumiyuki MURATA*, Takashi NISHIYAMA**, Xilan ZHENG***
and Katsumi YASKAWA*

* Department of Earth Sciences, Faculty of Science,
Kobe University, Kobe 657, Japan

** Department of Mineral Science and Technology,
Faculty of Engineering, Kyoto University, Kyoto 606, Japan

*** Institute of Geology, Academia Sinica, Beijing, China

The northward movement of the Indian continent and its subsequent indentation toward the Eurasian continent have given rise to internal deformation in the southern part of Eurasia (Tapponnier et al., 1982). Because the Tibetan region has behaved as a buckler against the frontal attack of northward movement of the India since 50 Ma (Gansser, 1964; Dewey & Bird, 1970; Burg & Chen, 1984), an abundant geological evidence on the tectonic deformation is probably preserved in this region. To determine the deformed aspect of the Tibetan region, we studied paleomagnetism in the western part of the Tibetan plateau.

In 1985, during an expedition to western Tibetan Plateau which followed the 3000 Km long Kaxigal-Lhasa road, seventy three oriented samples were collected from 16 separate sites of the post-Jurassic sequence for paleomagnetic investigation (Fig. 1).

The counterclockwise deflection about 60° of declination was revealed in the narrow zone along the Indus-Zangbo suture zone, while the north to northeast direction in remanent magnetization ($D=-9^{\circ}\sim 32^{\circ}$) was observed in the Tibetan region far

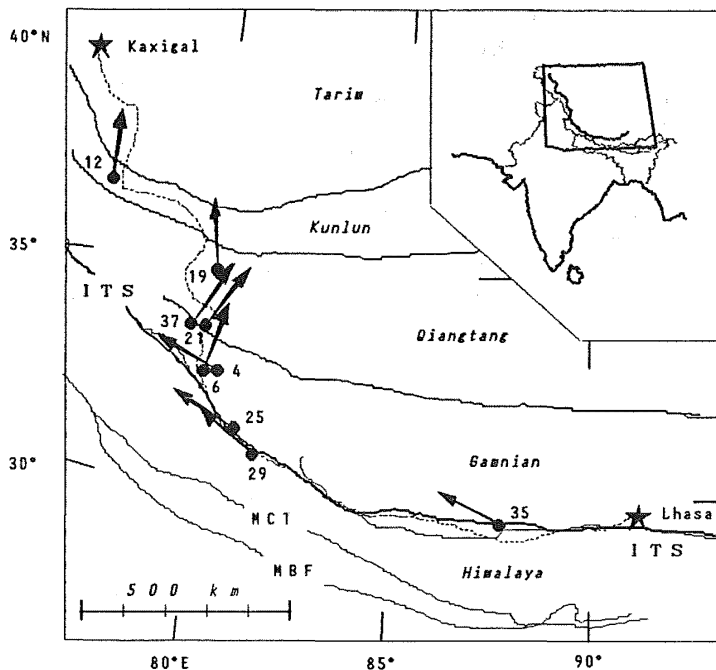


Fig. 1. Sketch map of the sampling route (dashed line) from Kaxigal to Lhasa in western Tibet together with the major tectonic units and the stratigraphical regions. Heavy line is Indus-Zangbo suture zone (ITS). MCT, Main Central Thrust; MBF, Main Boundary Fault. Arrows indicate the mean paleomagnetic direction at the sampling sites.

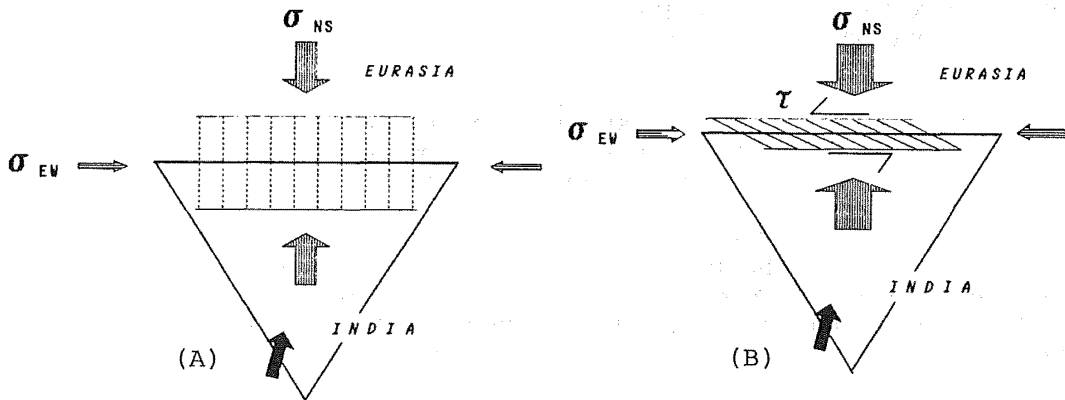


Fig. 2.

Simplified geometric model for deformation of the narrow zone between India and Eurasian continents. (A) When the normal stress on the suture zone (σ_{NS}) became larger than west-east normal stress (σ_{EW}) during the collision of the India toward Eurasia, the north-south direction (dotted lines) was the orientation of potential slip planes. (B) As the north-south normal stress (σ_{NS}) increased up to the critical state, the slip began along these planes (solid lines). The left lateral shear stress (τ) caused the counter-clockwise rotation to the crustal blocks in the narrow zone between India and Eurasia continents. Black arrows: direction of motion of the India relative to Eurasia.

apart from the suture zone (Fig. 1). A constant orientation of the westward declination characterizes the remanent magnetization for a narrow zone along the Indus-Zangbo suture with width of about 40 Km over a large range of about 900 Km. These paleomagnetic data indicate that significant tectonic deformation have occurred exclusively in the narrow zone along the suture zone.

The crustal blocks in the narrow zone is rotated in the compressive regime accompanied with left lateral shear stress due to the collision of the continents (Fig. 2). The large north-south normal stress σ_{NS} on the Indus-Zangbo suture zone produced the slip line with north-south direction during the collision of India. India has progressed northeastward with respect to Eurasia since the India-Eurasia collision up to present (Patriat & Achache, 1984), so that the left lateral shear τ prevailed in the Indus-Zangbo suture zone. A deformation of domino style with lateral displacement to the left could begin in the narrow zone along the suture under the conditions of further increase in the north-south normal stress σ_{NS} and left lateral shear τ . The narrow zone along the Indus-Zangbo suture consumed tangential stress acting on the plate boundary between India and Eurasia.

REFERENCES

- Burg, J.P. & Chen, G.H. (1984) *Nature* 311, 219.
 Dewey, J.F. & Bird, J. M. (1970) *J. geophys. Res.* 75, 2625.
 Gansser, A. (1964) *Geology of Himalaya* (Wiley, London)
 Patriat, P & Achache, J. (1984) *Nature* 311, 615.
 Tapponnier, P., Peltzer, G., Le Dain, A.Y., Armijo, R. and Cobbold, P. (1982) *Geology* 10, 611.

(Submitted to Nature)

LARGE NORTHWARD TRANSLATION OF EAST ASIA DURING LAST 20 My INFERRED FROM POLAR WANDERING PATH FOR EAST ASIA

Yo-ichiro OTOFUJI

Department of Earth Sciences, Faculty of Science,
Kobe University, Kobe 657, Japan

The Eurasian continent is a mosaic of continental blocks. They have moved relative to each other. Continental blocks of East Asia have undergone rotation and translation with respect to the main part of Eurasia during the Cenozoic (Molnar and Tapponnier, 1975; Tapponnier and Molnar, 1979; Tapponnier et al., 1982). Although the paleomagnetism offers a quantitative method for elucidating the deformation aspect, the East Asian apparent polar wandering (APW) path has been too poorly defined to use as a constraint to establish the timing and degree of block motion of East Asia.

In East Asia, Southwest Japan is fairly unique to have the APW path which can be traced back to 100 Ma. Since Southwest Japan has been situated along the plate boundary between Eurasia and Pacific plates, the continuous geologic activity has been kept producing igneous rocks in this area since 100 Ma ago. Paleomagnetic works for the igneous rocks of Southwest Japan provided the APW path over the last 100 My (Otofujii and Matsuda, 1987) (Fig. 1a). We construct the APW path of East Asia for last 100 My on the basis of that of Southwest Japan, and present the northward translation of the East Asia with respect to northern Eurasia.

THE EAST ASIAN APW PATH DURING LAST 100 My

Southwest Japan and East Asia have been united until Middle Miocene. The Japan Sea was opened between them at about 15 Ma following the studies of the marine magnetic anomalies (Isezaki, 1986), radiometric dating of the Japan Sea floor (Kaneoka, 1986) and the marine paleobiogeography of the Japan Sea coast (Chinzei, 1986). As Southwest Japan was rifted from East Asia and rotated clockwise at about 15 Ma associated with the opening of the Japan Sea (Otofujii et al., 1985), the original paleomagnetic poles before 20 Ma for Southwest Japan were transferred to the positions of the observed APW path of Southwest Japan (Fig. 1a). The abrupt change of the APW path between 20 Ma and 10 Ma for Southwest Japan is probably due to this clockwise rotation. The original paleomagnetic poles prior to the opening of the Japan Sea represents the APW path of East Asia.

The APW path for East Asia between 100 Ma and 20 Ma is constructed from paleomagnetic poles recalculated from a paleoposition of Southwest Japan (Fig. 1b): The paleoposition of Southwest Japan before 20 Ma is obtained by the counter-clockwise rotation about an Euler pole of 129°E, 34°N through 42°. The pivot point of 129°E, 34°N was proposed as an Euler pole for the rotation of Southwest Japan from the geometrical viewpoint (Otofujii and Matsuda, 1983). This Euler pole is concordant with the geoscientific view that the rotation of Southwest Japan is associated with a fan shape opening of the Japan Sea, which widens northeastward (Faure and Lelevee, 1987;

Otofujii et al., 1985; Otofujii and Matsuda, 1987).

Reliability of the paleoposition of Southwest Japan is ascertained through the comparison between the paleomagnetic pole position for East Asia and that recalculated from paleoposition of Southwest Japan (Fig. 2). The Cretaceous poles of East Asia have been recently obtained from Korea (Otofujii et al., 1986; Lee et al., 1987), North China (Lin et al., 1985) and South China (Lin et al., 1985; Kent et al., 1986): the mean pole positions is (162°W, 72°N, $\alpha_{95}=6^\circ$). The corresponding paleomagnetic pole for Southwest Japan is calculated from the data of 100Ma: This pole represents the Cretaceous pole for Southwest Japan, because these data record the paleomagnetic direction during Cretaceous normal polarity chron (Otofujii and Matsuda, 1987). As Southwest Japan is rotated back through 42° about the Euler pole of 129°E, 34°N, the observed paleomagnetic pole of 100 Ma for Southwest Japan is transferred to the position of 170.9°W, 72.2°N. This pole position agrees with the Cretaceous pole of East Asia. Even if the Euler pole is shifted by 3 degrees around 129°E, 34°N, the angular distance between pole positions obtained from East Asia and paleoposition of Southwest Japan does not exceed 5 degrees. This good

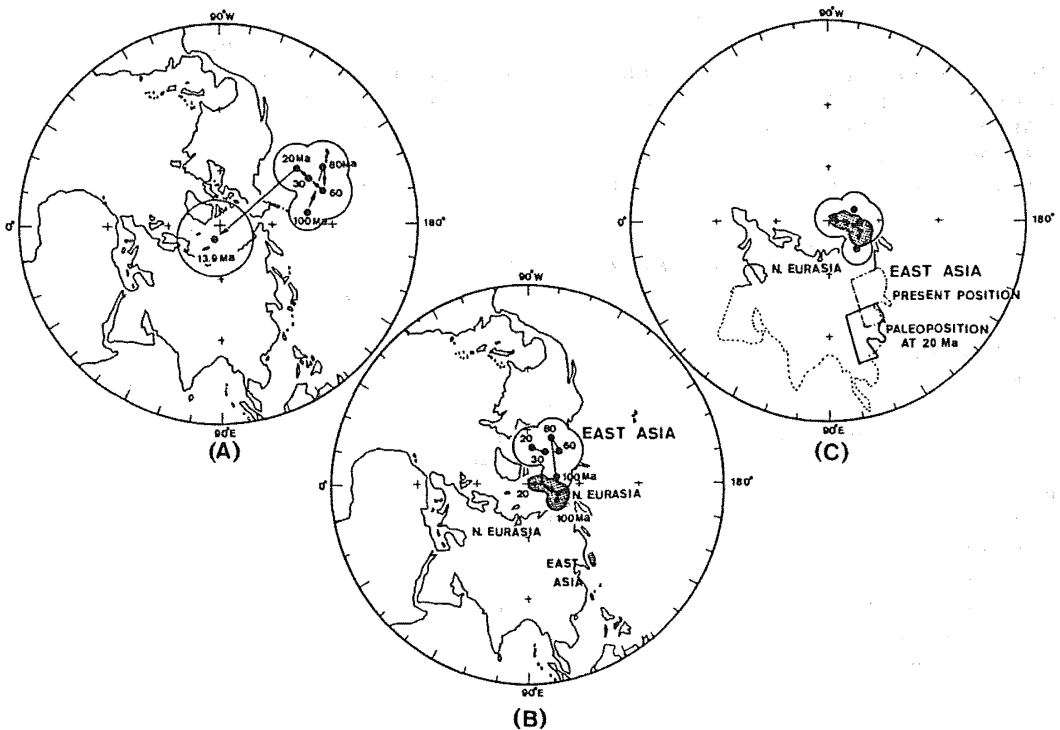


Fig. 1. (a) An apparent polar wandering (APW) path with 95% confidence for Southwest Japan since 100 Ma. (b) The APW path for East Asia between 100 Ma and 20 Ma, which is constructed by transference of the observed APW path of Southwest Japan to the original one prior to the opening of the Japan Sea. The APW path for East Asia is compared with that for northern Eurasia (shaded). (c) The APW path between 100 Ma and 20 Ma for East Asia is in good agreement with that of northern Eurasia (shaded) when East Asia is displaced southward by 1700 Km (the characteristic position of 120°E, 40°N of East Asia is shifted to a position at 110°E, 25°N.) and rotated counterclockwise through 10° with respect to the present meridian.

coincidence of the poles strongly demonstrates that the counterclockwise rotation of Southwest Japan about the Euler pole of 129°E, 34°N through 42° is an appropriate mode for transference of the present position of Southwest Japan to its paleoposition. The paleomagnetic poles from this paleoposition of Southwest Japan provides a reasonably reliable APW path for East Asia between 100 Ma and 20 Ma.

LARGE NORTHWARD TRANSLATION OF EAST ASIA

The APW path of East Asia is compared in Fig. 1b with that of northern Eurasia (Irving, 1977) which is constructed on the basis of the data from Europe, Russian platform and Siberia. The APW path for East Asia deviates significantly from that of northern Eurasia. The pole path for East Asia lies on the far sided position by about 18° of the pole path for northern Eurasia from East Asia position. The observed deviation is, however, unlikely to be ascribed to the effect of a northward offset of axial dipole as the amount of the deviation is more than four times larger than the value expected from the dipole off-set theory (Wilson, 1971).

The APW paths of East Asia and northern Eurasia are similar in form, although the deviation between the two paths is observed. Both paths reveal convex arcs. The amount of displacement of the path between 100 Ma and 20 Ma for East Asia is 21°, in comparable to 16° which is the results from the northern Eurasia. The similarity in pole paths suggests that the northern Eurasia and East Asia had been placed on a single tectonic unit until 20Ma.

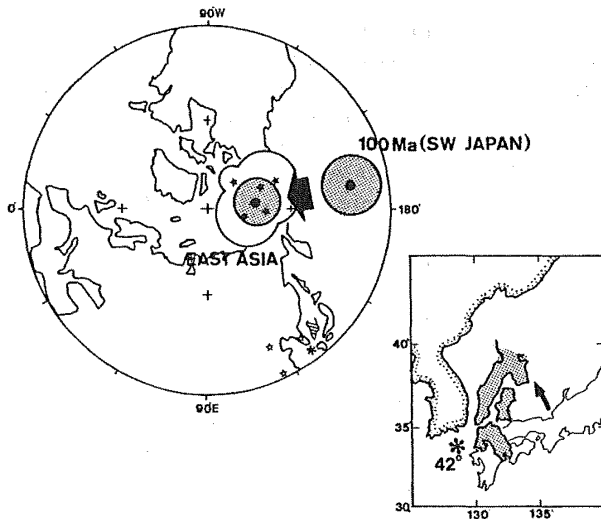


Fig. 2. Paleomagnetic poles (shaded) of 100 Ma for Southwest Japan with their 95% confidence calculated from the present position and the paleoposition of Southwest Japan, respectively. Pole position of 170.6°W, 41.5°N is transferred to a position of 170.8°W, 72.2°N, when Southwest Japan is rotated counterclockwise about the pivot of 129°E, 34°N (shown by asterisk) through 42°. For comparisons are shown the Cretaceous paleomagnetic poles (shown by stars) and their 95% confidence for East Asia: Korea, North China Block (NCB), South China Block (SCB). Open stars show the studied areas of paleomagnetism in East Asia.

The deviation between the two paths is explained by the relative motion of East Asia with respect to northern Eurasia. The inclination values ($I(EA)$ and $I(NE)$) at the characteristic position of East Asia of 120°E, 40°N are calculated for five periods of last 100 My from the APWs of East Asian and northern Eurasia. The mean inclination difference ($I(EA) - I(NE)$) for the five periods is $-16.7 \pm 7.6^\circ$. This indicates that East Asia should

have situated at lower latitude by about 15° (1700 Km in distance) from the present position. The APW path of East Asia is in good agreement with that of northern Eurasia (Fig. 1c), when the characteristic position of 120°E, 40°N of East Asia is shifted back to a position at 110°E, 25°N and rotated counter-clockwise through 10° with respect to the present geographic coordinate system.

The East Asian APW path presents a new view of tectonic aspects for East Asia: East Asia and northern Eurasia occupied the same rigid plate between 100 Ma and 20 Ma, and East Asia then moved about 1700 Km northward accompanied with the clockwise rotational motion. This northward motion mainly occurred between 20 Ma and 10 Ma.

DISCUSSION

The northward motion has been suggested for East Asia. The Cretaceous paleomagnetic data of the eastern part of the North China Block (NCB), the South China Block (SCB) and Korea significantly deviates from that of northern Eurasia (Lin et al., 1985; Courtillot and Besse, 1986; Lee et al., 1987). This discrepancy requires the northward translation of East Asia. Kent et al. (1986) indicates a 1500 Km northward translation of

Sichuan province, western part of the SCB, based on the upper Cretaceous paleomagnetic data. The northward motion has been expected to have occurred in some time since Cretaceous.

The construction of the East Asian APW path rejuvenates the estimation for the timing of the northward motion. The northward motion of the Amuria plate (Fig. 3), north of the NCB, is a geological evidence for this timing. The sinistral strike-slip movement has been documented along the Baikal rift zone, and the compression features are observed in the Stanovoy range stretching between Lake Baikal and Okhotsk Sea (Zonenshain and Savostin, 1981; Kimura

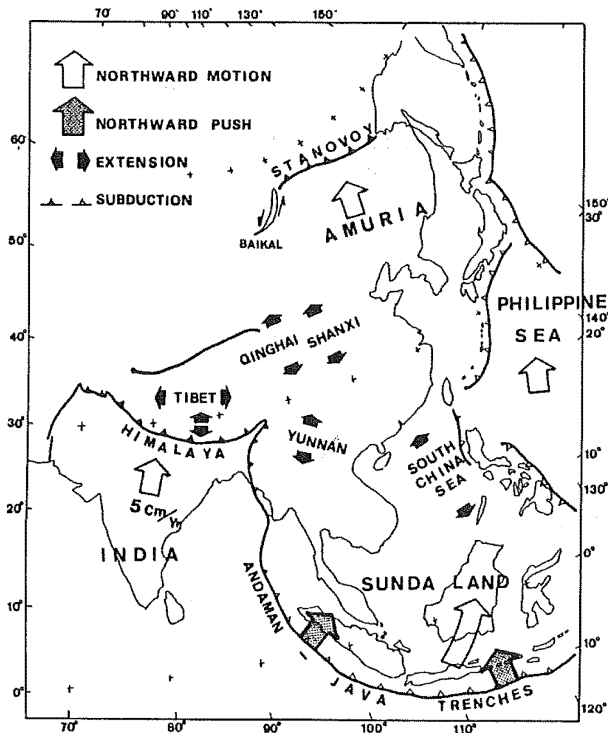


Fig. 3. Simplified Oligo-Miocene tectonic map of eastern Asia. Northward motion is observed in the neighboring regions of East Asia; India, Sunda land, Philippine Sea and Amuria. The northward motion of Sunda land and Philippine sea is ascribable to northward push by the Andaman and Java trenches to the southern margin of the Eurasia plate. Extensional regime develops at the southern part of Asian continent in the Neogene.

and Tamaki, 1986). The Oligocene to Miocene age is assigned to these tectonic events. A great amount of latitudinal convergence between Amuria and Siberia (part of northern Eurasia) took place at the Stanovoy range, so that East Asia, comprising the eastern part of NCB, the SCB and the Amuria plate experienced large northward translation in the late Tertiary, possibly between 20 Ma and 10 Ma.

Although penetration of India toward Eurasia is qualitatively responsible for the northward translation and clockwise rotation of East Asia (Tapponnier et al., 1982), all the amount of the northward translation of 1700 Km for East Asia between 20 Ma and 10 Ma is hardly explained solely by the convergence between India and Eurasia. The Indian subcontinent collided with the southern part of Eurasia at about 50 Ma (Patriat and Achache, 1984; Besse et al., 1984), whereas East Asia began to move later than 20 Ma. The convergence rate between the India and the Eurasia plates has been kept at about 5 cm/year since the collision of India, on the basis of marine magnetic anomalies in the Central Indian Ocean (Patriat and Achache, 1984). While the India has penetrated about 2500 Km in horizontal distance into Asia during last 50 My, India has advanced only about 500 Km toward Eurasia between 20 Ma and 10 Ma. The penetration of India only gives rise to one third of the significant northward translation of East Asia.

Another mechanism is the northward migration of the Andaman and Java trenches which are a plate boundary between the Indo-Australia and Eurasia plates (Fig. 3). Northward moving continents of India and Australia is catenated by a chain of these trenches. The chain also probably migrated northward and pushed the southern part of Eurasia plate northward in the Miocene associated with the northward advance of the India and Australia continents. The northward movement of the southern part of the Eurasia plate is expected from the geological evidences of the Miocene counterclockwise rotation of the Sunda land consisting of Malay Peninsula, Kalimantan and western arm of Sulawesi (Jarrard and Sasajima, 1980), and the northward motion of the Philippine Sea plate since the Oligo-Miocene (Lauden, 1977; Shih, 1980; Seno and Maruyama, 1984). The northward push by the trenches to the Eurasia plate may be responsible for the northward motion of East Asia since 20 Ma.

An alternative explanation for the mechanism is intracontinental north-south extension within the Asian continent (Fig. 3). The extensional regime later than the Oligo-Miocene has been observed in the convergent Himalaya region (Burchfiel, 1985), Tibet (Klootwijk et al., 1985; Armijo et al., 1986; Powell, 1986) and Qinghai Plateaus (Ma and Wu, 1987), the Shanxi and the Western Yunnan graben systems (Ma and Wu, 1987), and the South China Sea (Pautot et al., 1986). Neogene intracontinental activity could have facilitated a further northward translation of East Asia.

REFERENCES

- Armijo, R., Tapponnier, P., Mercier, J.L. and Han, T. (1986) *J. Geophys. Res.*, 91, 13,803.
Besse, J., Courtillot, V., Pozzi, J.P., Westphal, M. and Zhou, Y.X. (1984) *Nature*, 621.
Burchfiel, B.C. and Royden, L.H. (1985) *Geology*, 13, 679.
Chinzei, K. (1986), *J. Geomag. Geoelectr.* 38, 487.

- Courtillet, V. and Besse, J. (1986) *Nature*, 320, 86.
- Faure, M. and Lalevee, F. (1987) *Geology*, 15, 49.
- Irving, E. (1977) *Nature*, 270, 304.
- Isezaki, N. (1986) *J. Geomag. Geoelectr.*, 38, 403.
- Jarrard, R.D. and Sasajima, S. (1980) : in Hayes, D. H., ed., *The tectonic and geologic evolution of Southeast Asian Seas and Islands: American Geophysical Union Monograph 23*, 293.
- Kaneoka, I. (1986) *J. Geomag. Geoelectr.*, 38, 475.
- Kent, D.V., Xu, G., Huang, K., Zhang, W.Y. and Opdyke, N.D. (1986) *Earth Planet. Sci. Lett.*, 79, 179.
- Kimura, G. and Tamaki, K. (1986) *Tectonics*, 5, 389.
- Klootwijk, C.T., Conaghan, P.J. and Powell, C. McA. (1985) *Earth Planet. Sci. Lett.*, 75, 167.
- Lee, G., Besse, J., Courtillet, V. and Montigny, R. (1987) *J. Geophys. Res.*, 92, 3580.
- Lin, J.L., Fuller, M. & Zhang, W.Y. (1985) *Nature*, 313, 444.
- Louden, K.E. (1977) *J. Geophys. Res.*, 82, 2989.
- Ma, X. and Wu, D. (1987) *Tectonophysics*, 133, 243.
- Molnar, P. and Tapponnier, P. (1975) *Science*, 189, 419.
- Otofujii, Y., Hayashida, A. and Torii, M. (1985) in Nasu, N., et al., ed., *Formation of Active Ocean Margins*, p.551-566, (TERRAPUB, Tokyo)
- Otofujii, Y., Kim, K.H., Inokuchi, H., Morinaga, H., Murata, F., Katao, H. and Yaskawa, K. (1986) *J. Geomag. Geoelectr.* 38, 387.
- Otofujii, Y. and Matsuda, T. (1983) *Earth Planet. Sci. Lett.*, 62, 349.
- Otofujii, Y. and Matsuda, T. (1987) *Earth Planet. Sci. Lett.*, 85, 289.
- Patriat, P. and Achache, J. (1984) *Nature*, 311, 615.
- Pautot, G. et al. (1986) *Nature*, 321, 150.
- Powell, C. McA. (1986), *Earth Planet. Sci. Lett.*, 81, 79.
- Seno, T. and Maruyama, S. (1984) *Tectonophysics*, 102, 53.
- Shih, T.C. (1980): in Hayes, D. H., ed., *The tectonic and geologic evolution of Southeast Asian Seas and Islands: American Geophysical Union Monograph 23*, 49.
- Tapponnier, P. and Molnar, P. (1979) *J. Geophys. Res.*, 84, 3425
- Tapponnier, P., Peltzer, G., Le Dain, A.Y., Armijo, R. and Cobbold, P. (1982) *Geology*, 10, 611.
- Wilson, R.L. (1971) *Geophys. J. R. astr. Soc.*, 22, 491.
- Zonenshain, L.P. and Savostin, L.A. (1981) *Tectonophysics*, 76, 1.

(submitted to *Geology*)

**PALEOMAGNETIC STUDY OF PRECAMBRIAN ROCKS OF SRI LANKA IN VIEW OF
GONDWANA RECONSTRUCTION WITH ANTARCTICA**

M. FUNAKI¹, M. YOSHIDA² and P.W. VITANAGE³

- 1: National Institute of Polar Research, 9-10, Kaga 1-chome, Itabashi-ku, Tokyo 173, Japan
- 2: Department of Geosciences, Osaka City University, 3-138, Sugimoto 3-chome, Sumiyoshi-ku, Osaka 558, Japan
- 3: Department of Geology, Peradeniya University, Peradeniya, Sri Lanka

1. Introduction

Although Sri Lanka has been considered a Gondwana fragments connected Antarctica when the Gondwanaland was reconstructed, the situation is fairly vague among the reconstruction models due to lack of its geological and geophysical data. However, following two kinds of representative reconstruction model were proposed for Sri Lanka with respect to East Antarctica based on the 2000m bathometric: (1) Sri Lanka plate is a part of Indian plate having no deformation between both plates up to present placed in the offing Lützow-Holm Bay connected the east Gunnerus Bank in Enderby land, East Antarctica (i.e., Barron et al., 1978). (2) Sri Lanka was situated between Madagascar and Queen Maud Land in East Antarctica isolated from Indian plate in Gondwanaland (i.e., Smith and Hallam, 1970). Recently (1) model has been supported by the geological and geochronological evidences (i.e., Grew and Manton, 1979; Collerson and Sheraton, 1986).

More than 200 rock samples were collected from the south part of Sri Lanka for the structural and petrological studies. In these rocks samples, a total of 136 samples with orientation were supplied with paleomagnetic study for understanding of the relationships between Sri Lanka and Queen Maud Land. The rock types of these samples are gneiss, quartzite, gneissose granite and dolerite dike rocks. Although one or a few samples were collected from one site or one outcrop, the sampling sites (more than 75 sites) covered wide area of the south half of Sri Lanka. Probably no paleomagnetic study has been reported for Sri Lanka up to present. This study may give fundamental paleomagnetic futures for Sri Lanka in view of Gondwana reconstruction with East Antarctica.

2. AF and thermal demagnetizations

Every sample was AF demagnetized up to 15mT in step of 5mT for removing of secondary magnetization as viscous remanent magnetization (VRM) and isothermal remanent magnetization (IRM). Based on the AF demagnetization curves, the natural remanent magnetization (NRMs) of the samples were judged roughly stable or unstable; if angular deviations of NRM among 5, 10 and 15mT AF demagnetization do not exceed 20°, the NRM is stable, otherwise it is unstable. The stable NRM component was recognized from 102 samples and the optimum AF demagnetization field intensity was decided to 10mT.

The samples having stable NRM component obtained by the AF demagnetization to 15mT were demagnetized thermally in the atmosphere up to 580°C in step of 50°C for detecting of NRM stability against heating and the NRM blocking (T_B) temperature. The samples having the stable NRM component against both of AF and thermal demagnetizations were used in this study. Almost all Vijayan samples, except a few samples, have relatively low main T_B temperature less than 430°C. In general, their directions are stable in lower temperature than that T_B temperature, but they become shift widely over those temperatures. Many samples from Highland group have relatively high main NRM T_B temperature more than 530°C and the directions are very stable at least 480°C.

2. NRM distributions

The samples having stable NRM components against AF demagnetization were classified to 3 groups based on their T_B temperatures and the NRM directions demagnetized to 10mT were shown in Fig. 1. In this figure, each NRM distributions of $T_B < 330^\circ\text{C}$, Fig. 1(a), diffused widely through the both hemispheres, although the NRM directions of relatively low inclination (Inc) and $280\text{--}350^\circ$ declination (Dec) are dominant. The distribution $T_B \geq 530^\circ\text{C}$, Fig. 1(c), denotes clearly defined two clusters A and B which mean directions and α_{95} values are $\text{Inc}=61.2^\circ$, $\text{Dec}=260.4^\circ$, $\alpha_{95}=5.8^\circ$ and $\text{Inc}=68.7^\circ$, $\text{Dec}=349.0^\circ$, $\alpha_{95}=6.9^\circ$ respectively. Their samples consist of Highland Series and magnetize toward the normal polarity (upward direction). The distribution Fig. 1(b), $330 \leq T_B < 530^\circ\text{C}$, has mixed characteristics with Fig. 1(a) and (c). The NRM directions of 2 dolerite dyke samples magnetized toward normal polarity are almost parallel each other having a cluster C in Fig. 1(c) which mean NRM direction is $\text{Inc}=24.6^\circ$, $\text{Dec}=67.5^\circ$ with $\alpha_{95}=21.7^\circ$. These mean NRM directions of clusters are listed in Table 1. In this table, precision parameter, K, and confidence of 95% probability of declination, Δ_{95} are also listed.

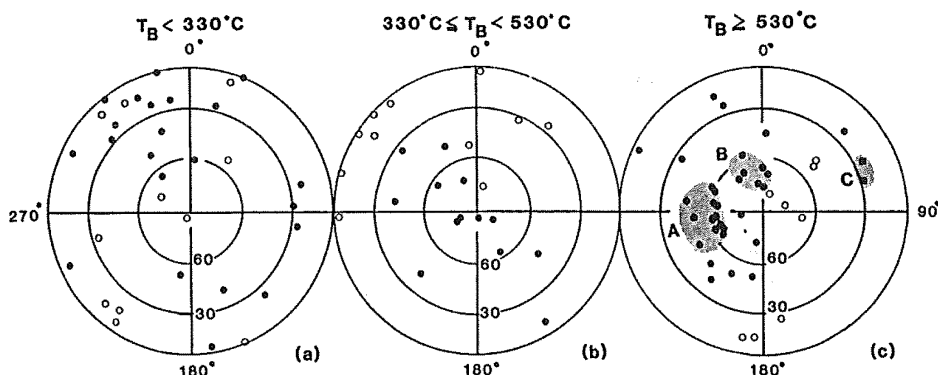


Fig. 1

Distributions of the stable NRM direction classified by the NRM blocking (T_B) temperature. Cluster A and B (circle) are the samples from Highland Series and C is that of dolerite dykes (square). Equal-area projection.

Table 1.
Paleomagnetic results of Sri Lanka and East Antarctica.

	Sri Lanka			East Antarctica			
	A	B	C	D	E	F	G
N	16	7	2	35	16	26	32
Inc	61.2	68.7	24.6	55.2	-80.6	-69.4	-52.0
Dec	260.4	349.0	67.5	347.2	314.8	237.6	50.9
K	41	78	135	40	24	136	46.6
α_{95}	12.1	19.3	24.0	6.8	55.1	6.8	6.2
Δ_{95}	5.8	6.9	21.7	3.9	7.7	2.4	3.8
Lat	2.3°S	44.0°N	24.0°N	15.1°S	75.3°S	45.3°S	41.8°S
Lon	34.1°E	71.7°E	59.5°E	28.7°E	90.9°E	152.0°W	133.5°W
after rotation to Antarctica							
pLat	19.1°S	45.0°S	35.4°S				
pLon	33.0°E	95.4°E	164.4°W				

A-C: Sri Lanka. The rotated pole position and the angle of Sri Lanka with respect to Antarctica: (10°S , 26.5°E , -101.2°). D: Cambro-Ordovician VGP from Ongul Island (Funaki and Wasilewski, 1986). E: Proterozoic VGP from Austhove (Funaki, 1987), F: Jurassic VGP from McMurdo Sound (Funaki, 1984), G: Jurassic VGP from Queen Maud Land (Løvlie, 1979).

3. Discussions

Since the soft magnetic components are usually demagnetized almost completely by AF demagnetization to 15mT, essentially stable NRM components were demagnetized thermally and the T_B temperatures were obtained resulting

from the hard NRM components. These hard NRM may be originated from thermal remanent magnetization (TRM) or thermochemical remanent magnetization (TCRM), because the samples are metamorphic or intrusive rocks. However, ferrimagnetic pyrrhotite is a magnetic carrier of stable NRM components frequently for the granulite of Ongul Island in Lützow-Holm Bay (Funaki and Wasilewski, 1986). Usually the NRM of pyrrhotite can not believe for the paleomagnetism due to its crystal anisotropy. As the ferrimagnetic pyrrhotite changes to paramagnetics by heat treatment over 330°C, the reliable NRM may be obtained by thermal demagnetization over 330°C. Therefore, cluster A, B and C plotted in Fig. 1(c) have high reliability without any effects of IRM, VRM and pyrrhotite.

Recently the geological evidences have been accumulated for Sri Lanka and Enderby Land. Main formations of Precambrian shield in Sri Lanka are Highland and Vijayan Series (i.e., Cooray, 1978). The Highland Series, which occupied wide area of central Sri Lanka, consist of the granulite facies considering high P-T conditions and the Vijayan one consist of amphibolite facies. They are contrasted with Lützow-Holm Complex and Yamato-Bergica Complex respectively. Grew and Manton (1979) elucidated the geochronological similarity between Sri Lanka and Lützow-Holm Bay region. Yoshida and Funaki (1978) inferred the similarity of structural trends and rock types between Sri Lanka and Lützow-Holm Bay regions which supported strongly to above reconstruction models. From these viewpoints, this fit in Fig.3 agrees well with the geology and geochronology between juxtaposed areas of Precambrian shield.

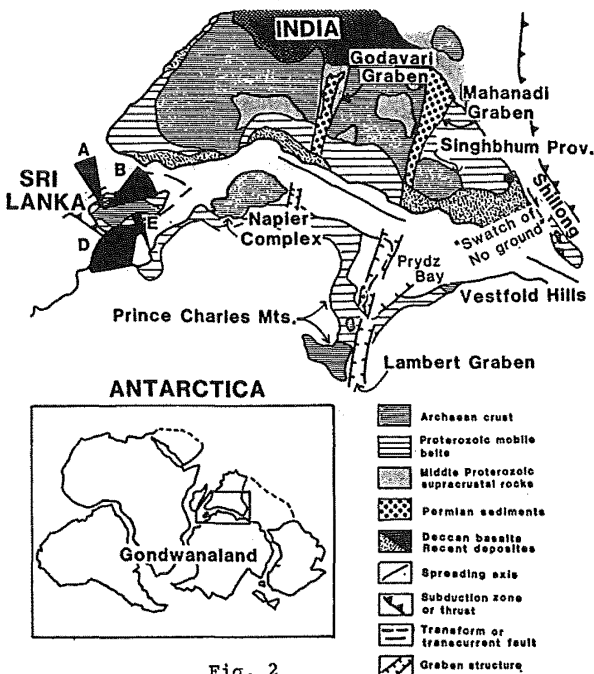


Fig. 2

Fig. 2
Reconstruction model of Sri Lanka, India and Antarctica and showing NRM declinations with α_{95} values for Sri Lanka and Lützow-Holm Bay region. Source: Collerson and Sheraton (1986).

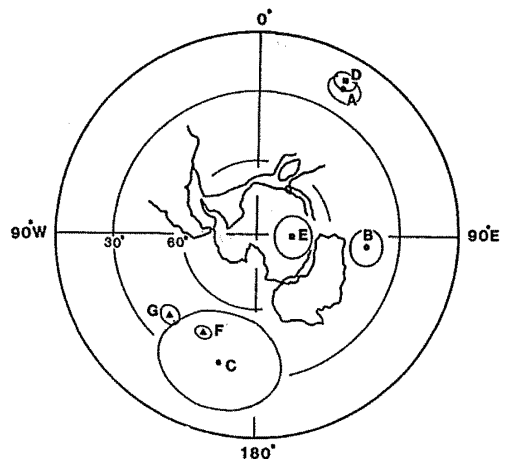


Fig. 3

Fig. 3
After rotated VGP positions and their α_{95} values obtained from Sri Lanka (A, B, C) with respect to East Antarctica (D, E, F, G). A, and D for Cambrian-Ordovician (Ca 480-500ma), B and E for Proterozoic (700ma ?), C, F and G for Mesozoic VGPs.

The NRM direction and calculated VGP position from the samples of Ongul Island in Lützw-Holm Bay were clarified by Funaki and Wasilewski (1986) as shown in Table 1. They considered that every gneiss rocks having stable NRM components of Ongul Island remagnetized completely under reversed GMF direction at Ca 480ma of the final metamorphism in this region, then granite and pegmatite dyke intrusions occurred under the normal GMF one after short term from that metamorphism. Funaki and Wasilewski (1987) obtained a steep NRM direction, as shown in Table 1, from gneiss of Austhovde in the west coast of Lützw-Holm Bay. Probably the NRM was acquired at Ca 700ma, which may be a peak metamorphism in this region (i.e., Shiraishi et al., 1987).

Jurassic rocks of Ferrar dolerite in the Antarctic Mountains have been investigated paleomagnetically as listed in Table 1. According to the Gondwana polar wander path, the Gondwanaland did not shift largely from Permo-Triassic to Jurassic Periods (McElhinny, 1973). Actually the VGP positions of Jurassic Ferrar dolerite and Permo-triassic Beacon Supergroup from McMurdo Sound in Antarctica do not differ largely. It may be therefore that the Jurassic VGP positions from Antarctica in Table 1 are representative ones from Permo-Triassic to Jurassic periods.

Figure 2 explains the relationships between Sri Lanka and Lützw-Holm Bay adjusted their NRM declination of cluster A and D referring their similar inclinations (61.2° , 55.2° respectively), which figure was modified to the reconstruction model proposed by Barron et al., 1978 and summarized by Collerson and Sheraton, 1986. Where, Sri Lanka was rotated with respect to East Antarctica taking the Euler's pole position Lat= 10° S, Lon= 26.5° E and the rotation angle -101.2° which was decided by adjustment of NRM directions of cluster A and C. In this model, the declination of cluster B does not fit to that of E (Austhovde) taking consideration of their α_{95} values, although their inclinations are relatively steep.

The VGP positions after rotation referred to above Euler's pole for Sri Lanka with respect to East Antarctica are listed in Table 1 and plotted in Fig. 3. The VGP positions of A and D and C, F and G fit each other taking consideration of their α_{95} values, although those of E and B do not fit. Probably the agreement of these VGP positions supports following aspects of Sri Lanka; (1) Sri Lanka situated in the offing Lützw-Holm Bay connected the west side of the Gunnerus Bank as reconstruction model (i.e., Barron et al., 1978; Collerson and Sheraton, 1986 for Sri Lanka and East Antarctica); (2) the NRM of the samples including cluster A acquired at the same time of Ross Orogeny and that of cluster C acquired at Mesozoic Era; (3) Sri Lanka was separated after Jurassic Period. However the disagreement of the VGP B and E gives the uncertainty of paleomagnetic data, age determination and reconstruction model for Sri Lanka and Lützw-Holm Bay region. So that it needs in detailed adjustment of Sri Lanka in view of the reliable paleomagnetic results with East Antarctica.

The Gondwana reconstruction model in Fig. 3, except the position of Sri Lanka, is essentially same model with Smith and Halam (1970), which the rotation pole position for India is Lat= 1° N, Lon= 7.7° W and the angle -88.9° with respect to East Antarctica. The model of Barron et al. (1978) resembles that of Smith and Hallam for India and East Antarctica. It suggests that the Sri Lanka rotated clockwise with respect to India referred to their models. However, there is a possibility that the rotation of Sri Lanka is to be neglected taking consideration of the α_{95} values.

4. Conclusions

The NRM directions of Highland Series of Sri Lanka made two clusters at inclination and declination and α_{95} values as 61.2° , 260.4° , 5.8° (cluster A) and 68.7° and 349.0° , 6.9° (cluster B) respectively and that of the Mesozoic dolerite dyke rocks clustered at incli. 24.6° , decli. 67.5° with α_{95} value 21.7° (cluster C) respectively. Although the samples from Vijayan Series have relative low inclinations, no cluster was decided due to worse precision.

Among the Gondwana reconstruction models of Sri Lanka with respect to East Antarctica, the model proposed by Barron et al., (1978) and summarized by Collerson and Sheraton (1986) is agreement with paleomagnetic reconstruction model. Namely Sri Lanka situated in the offing Lutzow-Holm Bay connected Gunnerus Bank in Enderby Land. Reasonable Euler's pole position and the rotation angle from Sri Lanka to Antarctica is (Lat=10.0°S, Lon=26.5°E) and -101.2° respectively. After the rotation of Sri Lanka, the VGP positions of Highland Series and dolerite dyke were consistent with that of the samples related to Ross Orogeny and Jurassic Ferrar dolerite in East Antarctica. After dolerite dyke intrusions, probably after Jurassic Period, Sri Lanka separated from East Antarctica.

References

- Barron, E.J., Harrison, C.G.A. and Hay, W.W. (1978), *Ame. Geophys. Union, Trans.* 59, (5), 436-449.
- Collerson, K.D. and Sheraton, J.W. (1986): *Antarctic oasis*, Academic Press Australia, 21-62.
- Cooray P.G. (1978), *Third regional conference on geology and mineral resources of Southeast Asia*, Bangkok, Thailand, 701-710.
- Funaki, M. (1983), *Antarct. Rec.*, 77, 20-32.
- Funaki, M. and Wasilewski, P. (1986), *Mem. Natl. Inst. Polar Res., Spec. Issue*, 43, 37-47.
- Funaki, M. and Wasilewski, P. (1987): *8th Symp. Antarc. Geoscience.* (abstract), 46.
- Grew, E.S. and Manton, W.I. (1979), *Science*, 206, 443-444.
- Løvlie, R. (1979), *Geophys. J. R. Astron. Soc.*, 59, 529-537.
- McElhinny, M.W. (1973), *Paleomagnetism and plate tectonics*. Cambridge Univ. Press, Cambridge, 260.
- Smith, A.G. and Hallam, A. (1970), *Nature*, 225, 139-144.
- Shiraishi, K., Hiroi, Y., Motoyoshi, Y. and Yanai, K. (1987): *Gondwana Six: Structure, Tectonics and Geophysics*. Geophysical Monograph, 40, 309-318.
- Yoshida, K., Yanai, K., Yoshikura, S., Ishikawa, T. and Kanisawa, S. (1982), *Antarctic Geosciences*, ed. C. Craddock, The Univ. Wisconsin Press, Madison, Wisconsin, 511-519.
- Yoshida, M. and Funaki, M. (1987), unpublished.

MAGNETIZATION OF ERIMO SEAMOUNT

Toshitsugu YAMAZAKI

Geological Survey of Japan, Tsukuba, Ibaraki, 305, Japan

The average magnetization vector of Erimo Seamount is obtained by a linear least square inversion using the topographic and magnetic anomaly data acquired during the KAIKO project. As the dipole anomaly of the seamount is superimposed on the magnetic lineations of the oceanic crust, the contribution of the lineations was estimated using a two-dimensional block model, and was subtracted from the observed data before the inversion. The VGP (Virtual Geomagnetic Pole) position, 69°N, -39°E, is here proposed as the revision of the widespread value of Uyeda and Richards (1966). Combined with the recently proposed ages of the seamount, 100 to 120 Ma, the VGP position provides an important clue in establishing the early Cretaceous pole position of the Pacific Plate.

The inversion assuming a planar regional field, which is the conventional way of removing the anomalies caused by bodies other than the seamount, was performed for comparison. The results differ considerably from those by the former procedure. The derived structure of the seamount (a thick non-magnetic cap) and the VGP position did not agree with the submersible observation and the age of the seamount, respectively. A planar regional field is not an adequate approximation of magnetic lineations.

Table 1. Results of the inversion of magnetic anomalies of Erimo Seamount.

Model	Dec. (+east)	Inc. (+down)	Intensity (A/m)	Regional field(1)			G ⁽²⁾	VGP	
				Co (nT)	Cn (nT/km)	Ce		Lat. (N)	Lon. (E)
Magnetic lineations subtracted	1	36	5.8	57.3	0 ⁽³⁾	0 ⁽³⁾	5.7	69	39
Planar regional field approximation									
(1) Uniform magnetization	-25	30	8.9	189.4	-0.68	-5.23	4.0	57	12
(2) Top 800m non-magnetic	-26	29	10.2	179.4	0.42	-6.04	4.4	56	14
Uyeda and Richards (1966)	-19	22	10.4	*	*	*	2.0	56	0

(1) $Co+Cn \cdot x+Ce \cdot y$; x in the north direction, y in the east direction.

(2) Goodness of fit ratio (Vacquier and Uyeda, 1967).

(3) Fixed to zero.

* A planar regional field was assumed but these coefficients were not given in the paper.

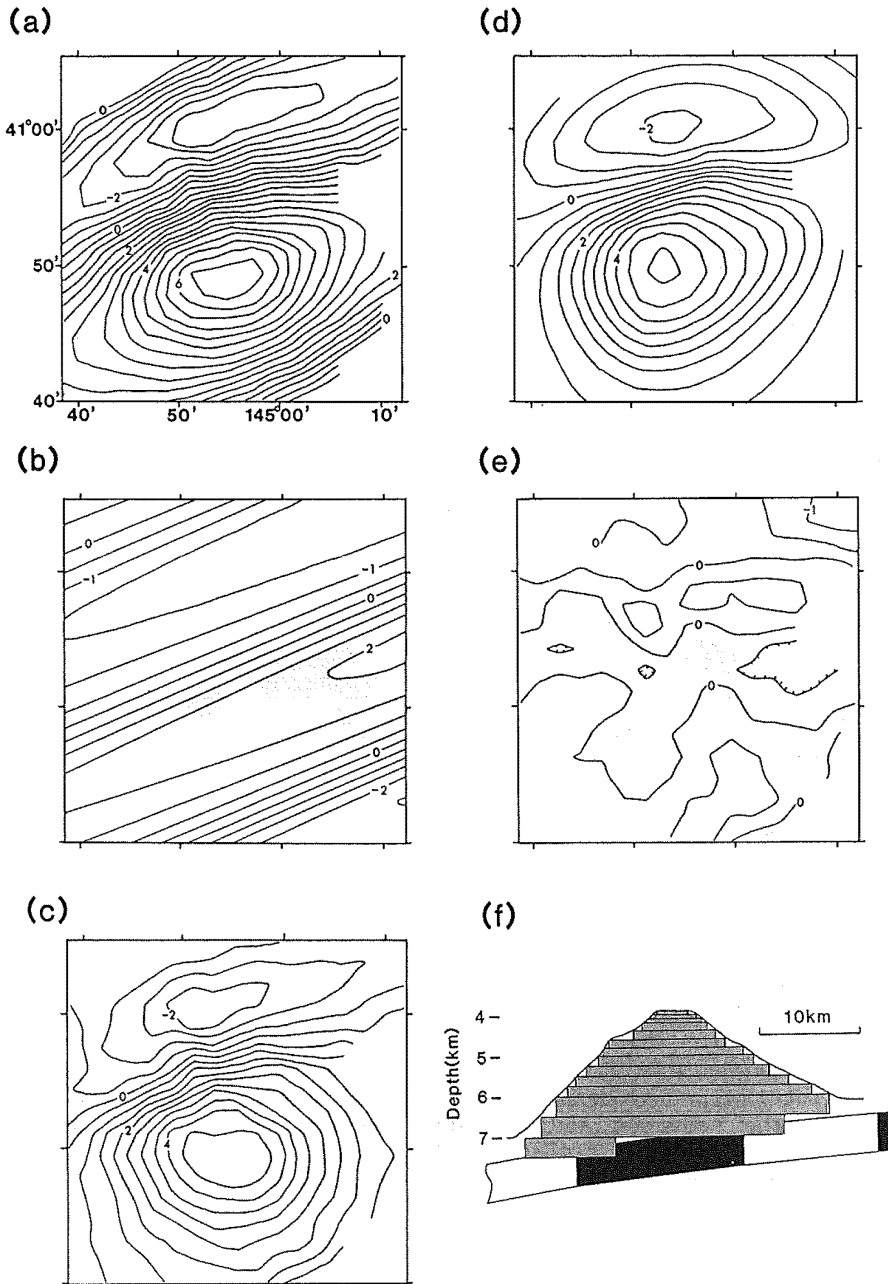


Fig. 1 Observed magnetic anomalies and results of calculation by the procedure in which the contribution of magnetic lineations was estimated independently and was subtracted from the observed anomalies before the inversion. (a) Observed magnetic anomalies. Contours are at 50 nT intervals. (b) Contribution of the magnetic lineations. (c) Magnetic anomalies after the contribution of the lineations was subtracted. (d) Calculated magnetic anomalies. The sum of the anomalies from the seamount and a constant field. (e) Residual anomalies ((a)-(b)-(d)). (f) A cross section of the magnetic model. The seamount approximated by a stack of polygons rests on the oceanic crust of the two-dimensional blocks.

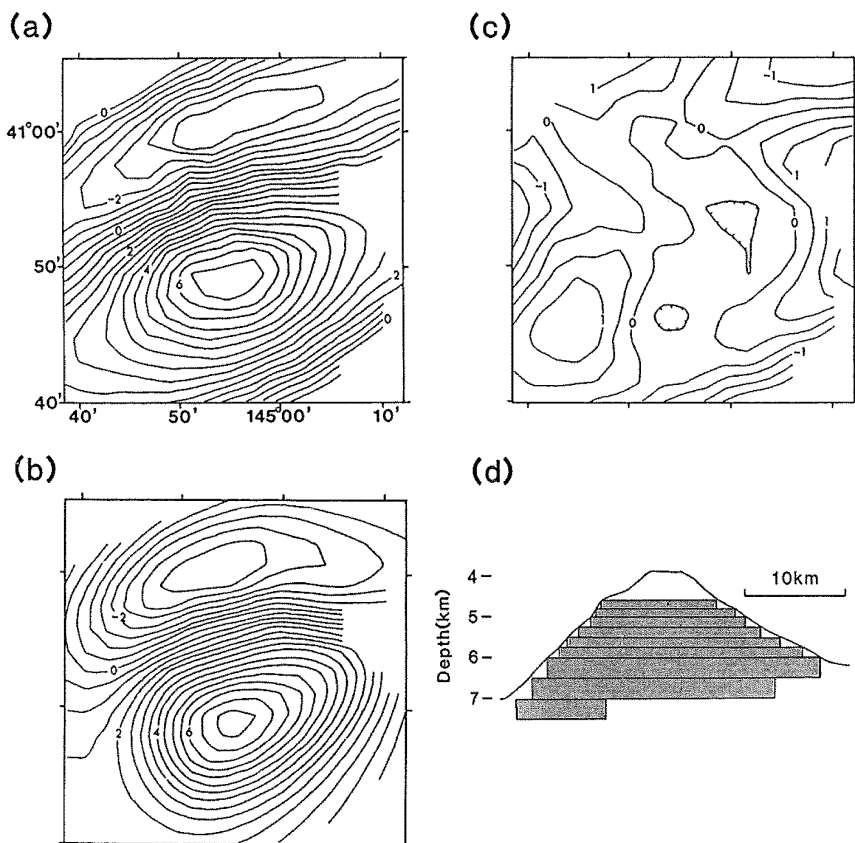


Fig. 2 Observed magnetic anomalies and results of calculation by the conventional procedure in which the inversion was performed assuming a planar regional field. That is, the magnetic lineations were approximated by the planar regional field. (a) Observed magnetic anomalies. Contours are at 50 nT interval. (b) Calculated magnetic anomalies. The sum of the anomalies from the seamount and a planar regional field. (c) Residual anomalies. (d) A cross section of the magnetic model. To fit the observation, a non-magnetic cap of 800m in thickness is required.

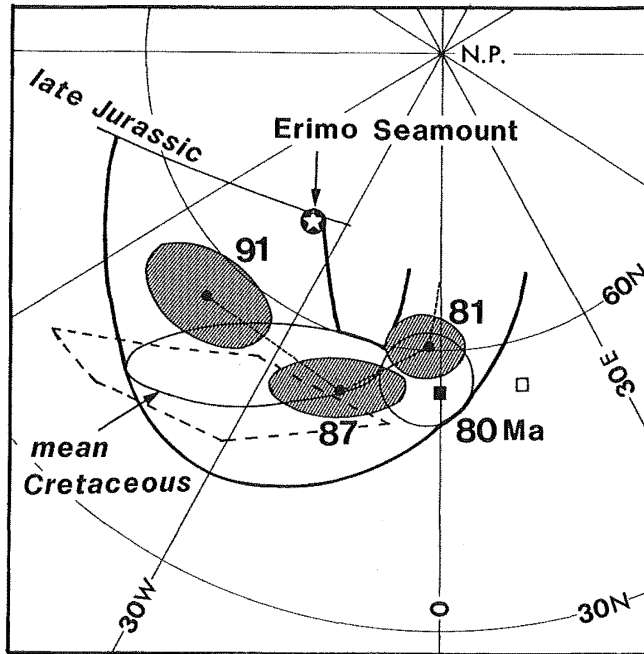


Fig. 3 Comparison of the VGP position of Erimo Seamount with apparent polar wander paths of the Pacific Plate. Recently proposed ages of Erimo Seamount are 100 to 120 Ma (Takigami et al., 1986; Cadet et al., 1987a,b). The star is the VGP position of Erimo Seamount by the method in which the contribution of the lineations was subtracted before the inversion. The open square is the VGP position from the planar regional field model. The solid square is the VGP position of Uyeda and Richards (1966). The shaded ellipses are the pole positions of the Pacific Plate proposed by Sager and Keating (1984). The bold curves are the polar wander path of Cox and Gordon (1984). The broken lines show the pole position estimated from the skewness of the magnetic lineations M1 to M10 by Larson and Chase (1972), but the validity of a pole position determined by the skewness is at present controversial (Cande, 1976; Raymond and LaBrecque, 1987).

References

- Cadet, J.-P., K.Kobayashi et al.(1987a) *Earth Planet. Sci. Lett.*, 83, 267.
 Cadet, J.-P., K.Kobayashi et al.(1987b) *Earth Planet. Sci. Lett.*, 83, 313.
 Cande, S.C. (1976) *Geophys. J. R. astr. Soc.*, 44, 547.
 Cox, A. and R.G. Gordon (1984) *Rev. Geophys. Space Phys.*, 22, 47.
 Larson, R.L. and C.G. Chase (1972) *Geol. Soc. Amer. Bull.*, 83, 3627.
 Raymond, C.A. and J.L. LaBrecque (1987) *J. Geophys. Res.*, 92, 8077.
 Sager, W.W. and B.H. Keating (1984) *J. Geophys. Res.*, 89, 11135.
 Takigami, Y., I. Kaneoka and T., Ishii (1986) *Abstracts of papers, International KAIKO conference on subduction zones*, 16.
 Uyeda, S. and M. Richards (1966) *Bull. Earthq. Res. Inst.*, 44, 179.
 Vacquier, V. and S. Uyeda (1967) *Bull. Earthq. Res. Inst.*, 45, 815.

(Submitted to *J. Geomag. Geoelectr.*)

MAGNETIC ANOMALY, CRUSTAL STRUCTURE AND LITHOSPHERE DESTRUCTION

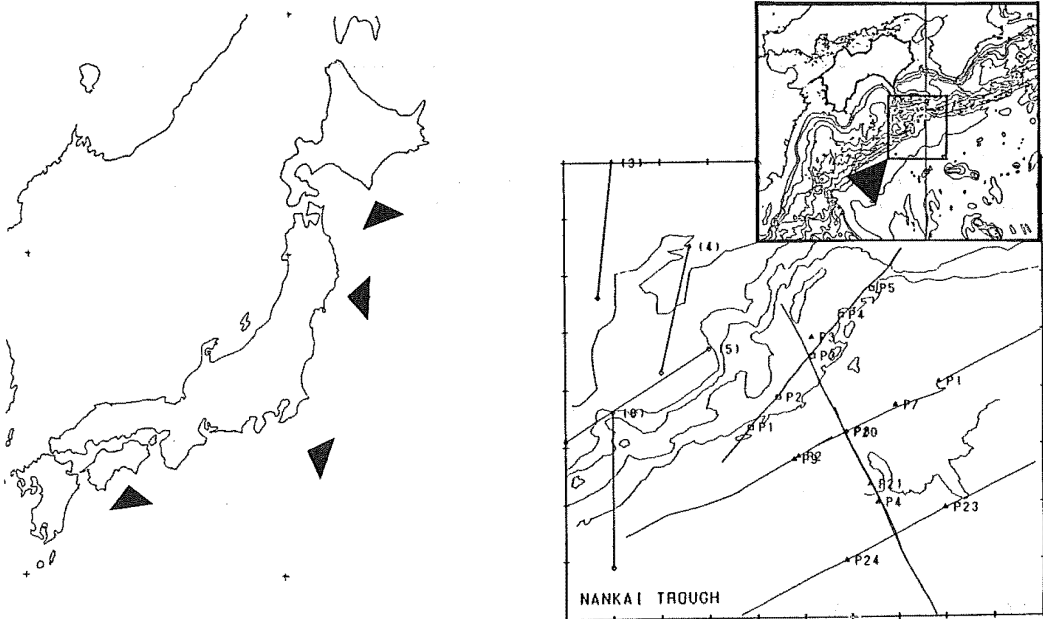
Hajimu KINOSHITA and Naoko MATSUDA

Department of Earth Sciences, Faculty of Science
Chiba University, Chiba 260

Seismic structures of subducting lithosphere around the Japanese island arc were studied in reference to geomagnetic anomaly patterns. The studied areas are shown by solid triangles of which the Nankai Trough is authors' primary concern. Recent seismic surveys conducted in this area (Fig.2) have revealed that the crustal thickening below continental shelves must be a result of accretion, i.e., scraping of top-most layers including basaltic (mostly altered) basement during subduction. Mechanical weakening of the basement is suggested by series of ODP surveys such as Hole 504B. This weathered basement can easily be scraped off by the coupling between obducting and subducting lithospheric bodies. Dipping angles of the subducting plate seem to be low in the strong coupling and vice versa. Magnetic lineation patterns of the subducting lithosphere may be destroyed either by geometrical structural disturbances or by thermal agitation beneath sedimentary covers. Present study will show which effect predominates in the Nankai Trough area.

Fig. 1 (left) Area of well studied seismic structure as well as magnetic anomaly patterns.

Fig. 2 (right) Nankai Trough area surveyed in detail by present authors.



Remarks: A full paper of the present study and discussions will appear either in Journal of Geomag. Geoelectr. or Tectonophysics.

CRUSTAL STRUCTURE AND MAGNETIC ANOMALY IN SOUTHERN PART OF
BOSO PENINSULA, CHIBA, JAPAN

Hajimu KINOSHITA and Rie MORIJIRI

Department of Earth Sciences, Faculty of Science, Chiba University, Chiba
and Toshiyasu NAGAO

Earthquake Research Institute, University of Tokyo, Tokyo

Geophysical structure of a line of ultramafic massive bodies which forms a boundary between Tertiary and Quaternary in the southern tip of Boso peninsula, Kanto, Japan is presented. Data of paleomagnetic, geomagnetic, gravimetric and seismic surveys were used to deduce the deep (surface to 10 km) structure. It was found that the ultrabasic belt is of deep sea origin (covered by thick lime stone layer) and the formation has been tilted by almost 90 degrees as a result of accretion to the Boso block in the late Tertiary era. Full descriptions on this subject will be given in a future issue of Journal of Geomag. Geoelectr.

Fig. 1 This indicates the surveyed area with geophysical data points.

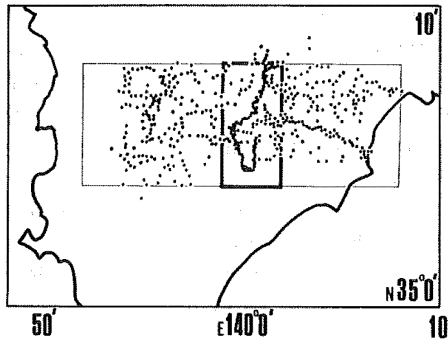
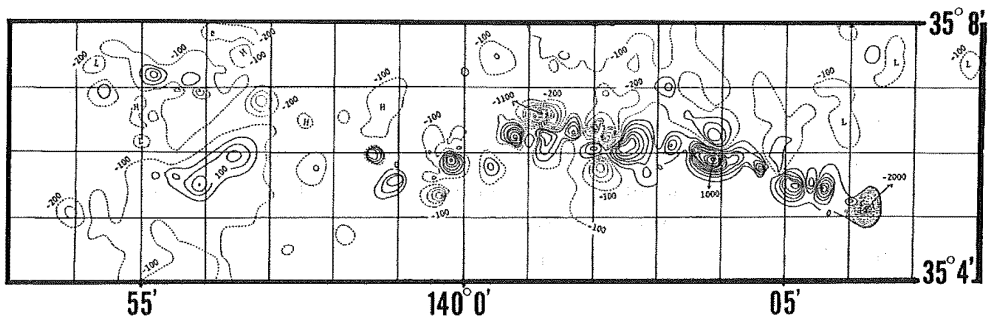


Fig. 2 (bottom) Magnetic anomaly patterns obtained by reducing field values referring those of Kano-zan Geodetic Station, Geographical Institute, Japan.



THE RIKITAKE TWO-DISK DYNAMO SYSTEM: STATISTICAL PROPERTIES AND GROWTH OF INSTABILITY

Masaru Kono and Masayuki Hoshi

Department of Applied Physics, Tokyo Institute of Technology
Ookayama 2-12-1, Meguro-ku, Tokyo 152, Japan

1. Introduction

Modeling the geomagnetic field based on complete hydromagnetic equations is a very difficult problem. Although such efforts have already gained some success, models directly comparable to the actual field behaviors may not be available for some time yet, because of the complexity and difficulty inherent in hydromagnetic problems. An alternate approach is to use some simplified systems which have well defined physical and/or stochastic properties and which can be studied with ease. A particularly interesting physical model is the two-disk dynamo of Rikitake (1958), because it displays not only oscillations but also occasional flippings of the coil current which is similar to the polarity reversals of the geomagnetic field. The Rikitake dynamo is governed by a set of very simple first-order differential equations, and yet, this model exhibits a wide variety of behaviors, from almost periodic to apparently chaotic or stochastic. Also, the equations contain a term representing the counteraction of the magnetic field on the motion, which is not included in kinematic dynamos (e.g., Bullard and Gellman, 1954).

As the differential equations of the Rikitake system are quite simple, it is easy to integrate them with sufficient accuracy. It is also possible to examine the system behavior in an exhaustive way, since the model contains only two parameters (μ , k). Rikitake (1958), Allan (1962), Cook and Roberts (1970), Shimizu and Honkura (1985), and Kono (1987) have already reported various characteristics of the two-disk dynamo. In the present study, we examine the statistical properties of the current intensity and reversal frequency in detail, and investigate how instability grows until polarity reversals take place.

2. The Rikitake Dynamo

Rikitake (1958) considered a system of two coupled disk dynamos, which is an extension of the homopolar dynamo of Bullard (1955). The system consists of two disks and two coils which are interconnected with each other. If the mechanical and electric properties of the two disks are identical, the non-dimensional electric currents x_1 and x_2 flowing in the two coils and the non-dimensional angular velocities y_1 and y_2 of the two disks satisfy the following differential equations.

$$\dot{x}_1 + \mu x_1 = x_2 y_1$$

$$\dot{x}_2 + \mu x_2 = x_1 y_2$$

$$\dot{y}_1 = \dot{y}_2 = 1 - x_1 x_2$$

where the dot indicates differentiation by the non-dimensional time, and μ is a non-dimensional parameter of the system representing the square root of the ratio of the mechanical time scale and electromagnetic time scale (Cook and Roberts, 1970). The equations contain four dependent variables x_1 , x_2 , y_1 , y_2 , but as y_1 and y_2 are linearly

related, the Rikitake dynamo has three degrees of freedom. If the time derivatives are set equal to zero, the normal (N) and reversed (R) steady state solutions can be obtained as $x_1 = \pm k$, $x_2 = \pm k^{-1}$, and $y_1 = \mu k^2$, $y_2 = \mu k^{-2}$, where k is an arbitrarily chosen constant depending on the initial condition (Rikitake, 1958).

In the following, we shall analyze the systematics of the Rikitake dynamo in order to gain some insight for understanding the very complicated process related to the generation of and variations in the geomagnetic field. We shall particularly concentrate on the manner by which the instability grows until polarity reversals are triggered.

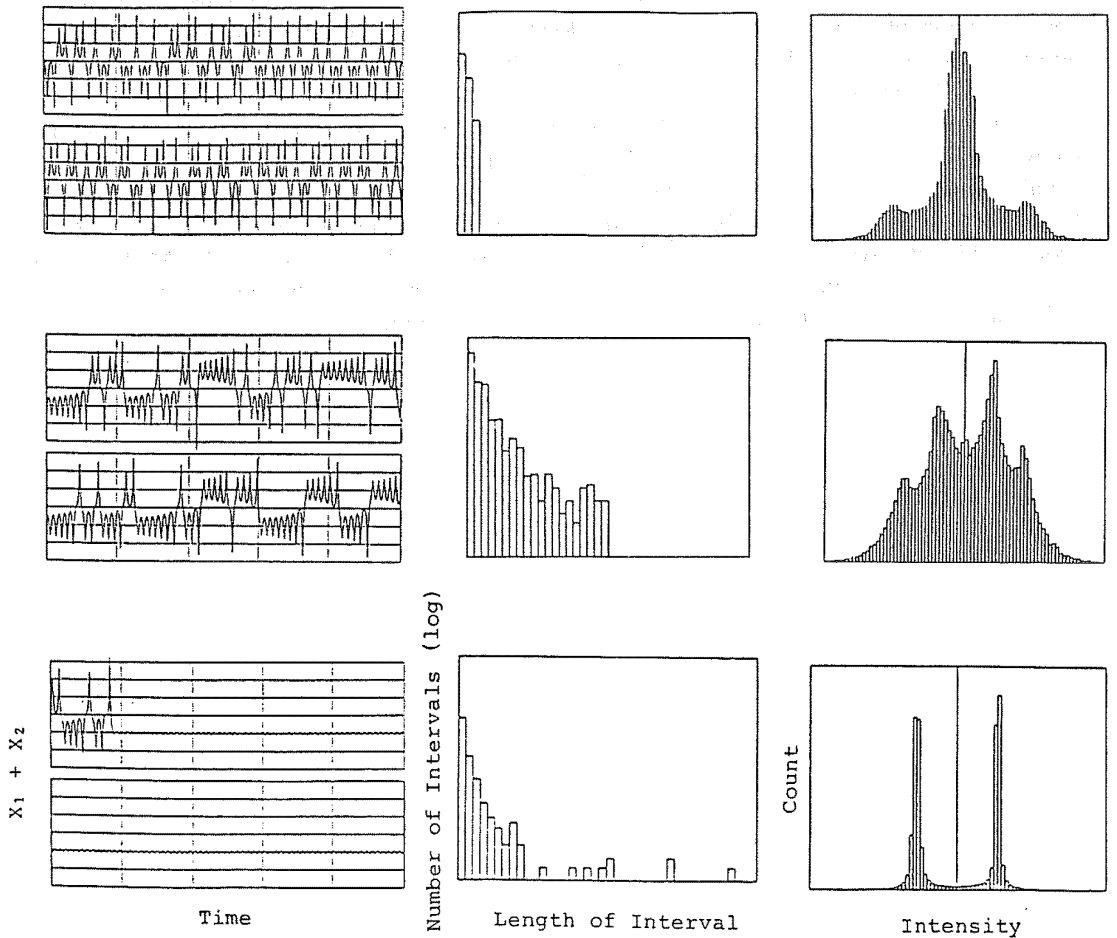


Fig. 1. Three types of polarity interval and current intensity distributions. The left panel on each row shows typical changes of the total current with time, and the center and left panels are the reversal and intensity statistics of each type. (Top) Type A, $k = 3$, $\mu = 3.0$; (middle) type B, $k = 2$, $\mu = 1.6$; (bottom) type C, $k = 3$, $\mu = 1.8$.

3. Statistical Properties of the Rikitake Dynamo

The behaviors of the Rikitake dynamo is controlled by the two parameters (μ , k). If k is kept constant and μ is changed, the system behavior changes accordingly. Following Kono (1987), we examined the distributions of the polarity intervals and of the field intensities, because they are well characterized for the actual geomagnetic field by the

paleomagnetic observations of the recent past (Cox 1968, 1969; Harland et al., 1982; Kono, 1971; McFadden and McElhinny, 1982). In the Rikitake dynamo, these distributions can be assigned to three different types. It is interesting that the change in the shape of distributions occur almost in parallel in polarity intervals and intensities. The parameter ranges corresponding to the three-peak distribution of the field intensity almost coincide with the range where reversals occur in one or two cycles of oscillations (Fig. 1, top). Likewise four-peak intensity distribution and truncated exponential distribution of polarity intervals share the similar parameter range (Fig. 1, middle). Ito's (1980) maximum entropy regime (MER) is characterized by the two highly concentrated peaks in the intensity distribution and by exponential distribution plus many longer intervals in the reversal statistics (Fig. 1, bottom). We may call these three typical distributions of polarity intervals and intensities as types A, B, and C.

The phase diagram of Ito (1980) is modified with the foregoing information and shown as Fig. 2. Correspondence of the types of polarity interval and intensity statistics is usually good as defined earlier. Discrepancies occur only near the transition between the types. It is seen that type A behavior appears near the chaotic/periodic boundary in (μ, k) space, while the type C behavior is in the center of the chaotic region (the MER of Ito), and type B between these two regions. The manner of change of the system characteristics is almost the same for different values of k , when the parameter μ is changed.

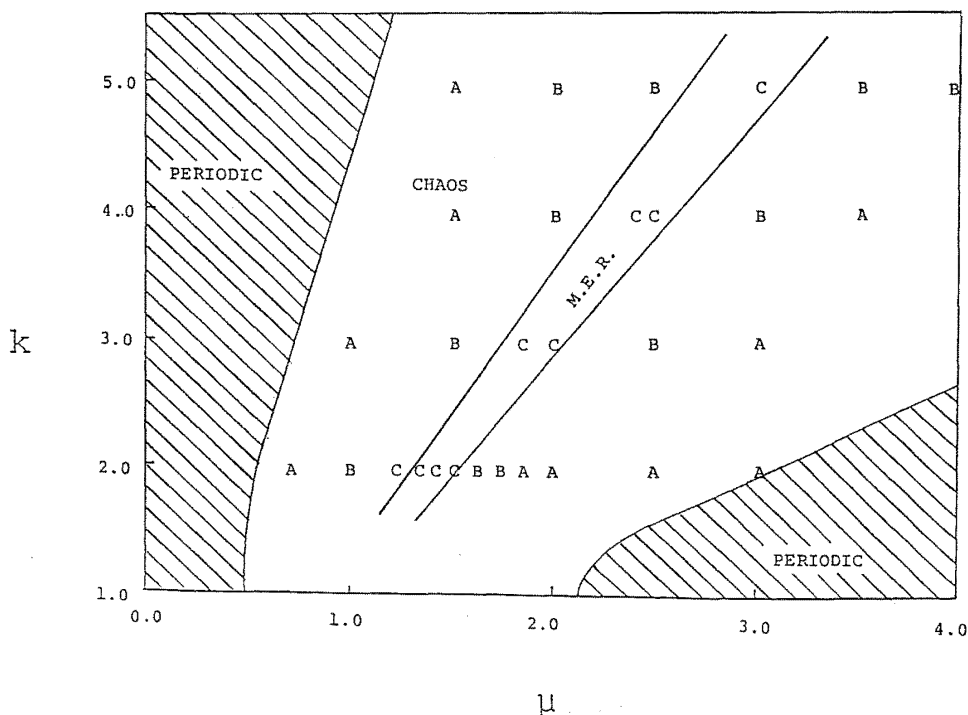


Fig. 2. Phase diagram of the Rikitake dynamo simplified from Ito (1980), with the regions corresponding to the three types of Fig. 1. The symbols are placed to indicate the parameters (μ, k) examined.

4. Growth of Instability Leading to Reversals

In the Rikitake dynamo, the intensity of the currents flowing in the coil (equivalently

the magnetic field) fluctuates about the steady state value (N or R states). The amplitude of oscillation always increases monotonically until the polarity reverses (Fig. 2). Fig. 3 shows changes in the extrema of the oscillation (peaks or troughs) as the time progresses, with the origin of the abscissa taken at the time when the total current $x_1 + x_2$ changes sign for the next time.

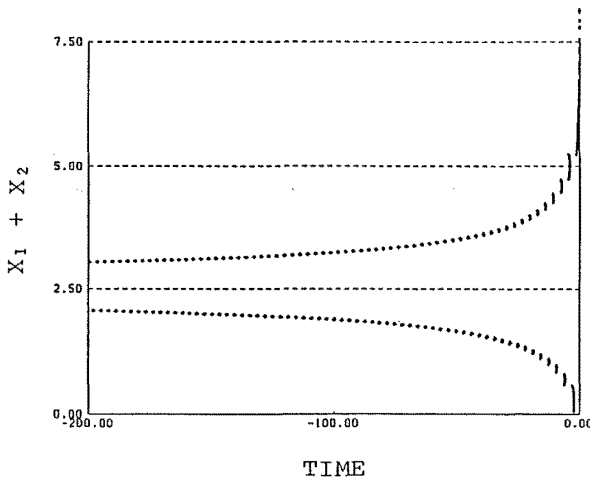


Fig. 3. Growth of the amplitude of oscillation of the total current $x_1 + x_2$, as shown by the change in the extremum values (peaks and troughs) with time for $k = 2$ and $\mu = 1.3$. The origin of the abscissa is placed at the time of the next reversal of the polarity. The points are separated in time by the period of oscillation. Note the rapid growth of the amplitude just before the reversal.

Fig. 4 illustrates the dependence of the growth rate of the amplitude of oscillation on the amplitude itself. When the amplitude is small, the growth rate is so small that the oscillation continues with almost the same amplitude for a very long period. As the amplitude increases, however, the growth rate becomes larger and larger until the oscillation is vigorous enough to cause polarity reversal and a new oscillation starts around the stationary state of the opposite polarity.

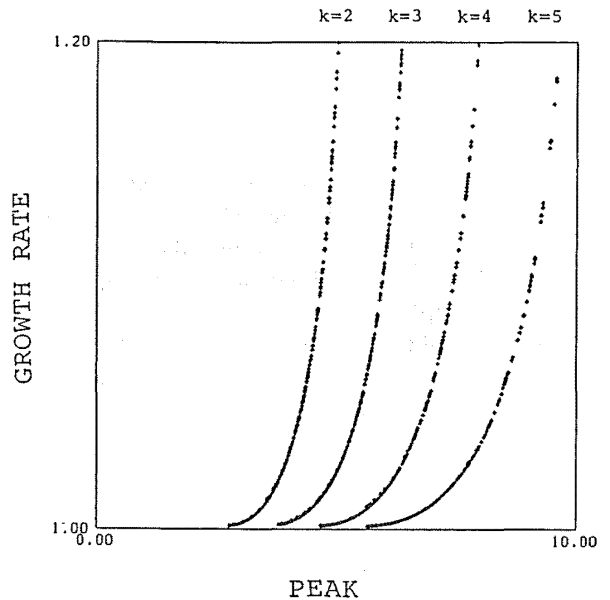


Fig. 4. Dependence of growth rate on the amplitude of oscillation. The peak amplitude and the growth rate are defined as $(x_1 + x_2)_{\max} - (k + k^{-1})$, and $(\text{peak})_{n+1}/(\text{peak})_n$, respectively.

Fig. 5 shows the correspondence between one extremum (peak or trough) and the next extremum (trough or peak) in the total current intensity, for different values of k . The data with different μ but with the same k lie on the common line except very near to the horizontal axis. The middle part of each curve is absent because states very near to the N or R steady state solutions cannot be approached even for the type C or the MER

parameters. The curves have nearly -45° slope near the N or R points, but have very steep gradients near the vertical axis. The former corresponds to the nearly sinusoidal oscillation when the amplitude is small, and the latter indicates that asymmetrical oscillations (sharp peaks and flat troughs) prevail at larger amplitude and that the growth of the peak is much faster than that of the trough for such circumstances.

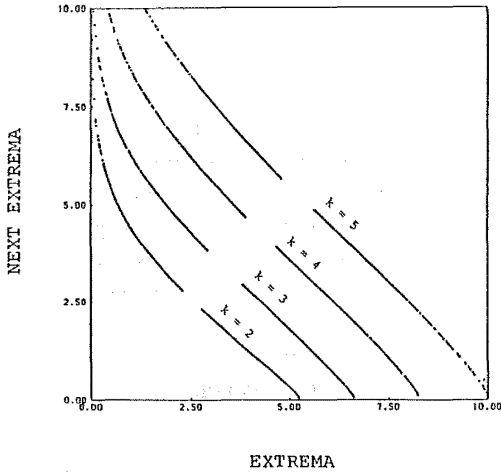


Fig. 5. Correspondence between the peak (trough) and the next trough (peak) of the oscillation of the current, for the typical cases of $k = 2, 3, 4, 5$. Data for the same k but different μ plot almost exactly the same, except at the rightmost part of each curve.

The evolution of the system can be traced by adding a subsidiary line inclined 45° to the coordinates and drawing lines connecting successive extrema (Fig. 6). In the case A, the growth rate of the amplitude is so small that successive trajectories almost coincide, indicating that the peaks and troughs do not change appreciably for quite a long time. On the other hand, the current grows more and more rapidly in the case B that a reversal occurs after only a few oscillations.

RIKITAKE DYNAMO $k=2.0 \mu=1.3$

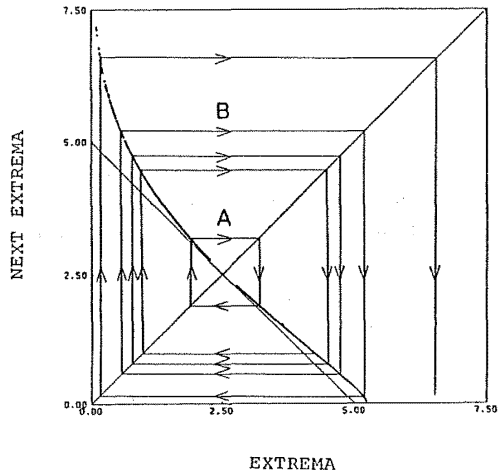


Fig. 6. Evolution of the oscillation with time. In case A, the growth rate is so small that the system repeats sinusoidal oscillation for a long time without appreciably increasing its amplitude. In contrast, the amplitude grows rapidly in case B, until the peak exceeds the threshold and polarity reversal occurs in the next cycle of oscillation.

Fig. 5 and 6 also show that there is some threshold in the last peak amplitude; when the peak exceeds this value the system reverses its polarity in the next cycle of oscillation. As the oscillation grows following a nearly common trend (Figs. 3-6), and as there is a threshold value after which the reversal takes place without fail, there is a definite relationship between the peak amplitude of oscillation and the time before the next reversal.

Cook and Roberts (1970) noted that the polarity interval will be very long if the last reversal occurred when the system is much removed from one of the stationary state, and

vice versa. This can be demonstrated by showing the dependence of the amplitude of oscillation *after* the reversal on the amplitude *before* the reversal (Fig. 7). The figure shows a definite dependence of the amplitude after reversal on the last amplitude of oscillation before reversal. It is remarkable that the first amplitude changes drastically when the last amplitude is large in the MER region ($k = 2$, $\mu = 1.3, 1.5$). This explains the reason why many long intervals can occur only in the MER region.

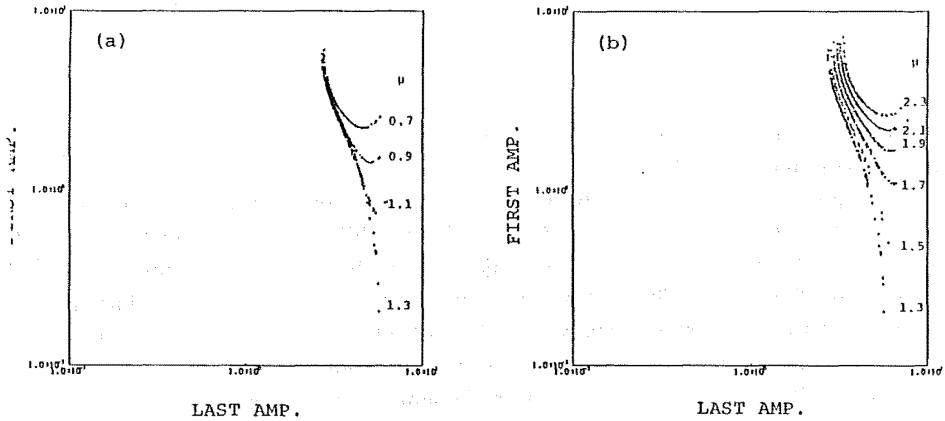


Fig. 7. The dependence of the first peak amplitude after reversal on the last peak amplitude before the reversal. $k = 2$. (a) $\mu = 0.7, 0.9, 1.1, 1.3$. (b) $\mu = 1.3, 1.5, 1.7, 1.9, 2.1, 2.3$.

5. Discussion

For very wide range of parameters (μ , k), the behavior of the two-disk dynamo is quite similar. The amplitude of the oscillation increases with time and then suddenly the reversal of polarity takes place. When the amplitude is small, oscillation is almost sinusoidal. With the increase in amplitude, however, the oscillation becomes more and more asymmetric; x_1 having sharp peaks and broad troughs and x_2 similarly distorted. As x_2 oscillates nearer to zero than x_1 , the sign of x_2 change first. At this stage, x_1 or the sum of x_1 and x_2 do not change sign. After a few more oscillations, however, both of them change sign at the same time and the system oscillates on the opposite side of zero. When the amplitude of the oscillation before reversal is large, the amplitude is small after reversal and the same polarity continues a long time because it takes long time for the amplitude to grow from smaller values (Figs. 4, 7).

The statistical distributions of the lengths of polarity intervals depends on the manner by which instability grows and eventually reversals take place. If the state near the N or R stationary points can be reached as in the case of type C, very long polarity intervals appears because the oscillation grows so slowly at first. In other cases, there is a sharp cutoff in the distribution because the state near the N or R is inhibited by the shape of the amplitude mapping function (Fig. 7). The distinction between type B and type A is not crucial; only states very far from the N or R points can be realized in type A (very short polarity intervals only), while intermediate states can be attained in type B (cutoff moves more to the longer intervals).

The intensity statistics, on the other hand, depends more on the manner of oscillation of the currents. The system oscillates almost sinusoidally if the amplitude is not too large

(Fig. 5). The density function of intensity for this period is derived from arcsine function, which is infinity at both ends of the oscillation amplitude and zero outside (Cox, 1970; Kono 1972). As the amplitude grows with time, the intensity distribution becomes the superposition of such density functions with varying amplitudes. Since the growth rate of the amplitude is small when the system is near the stationary point N or R, the distribution is dominated by the small amplitude oscillation, for which the two adjacent maxima of density function can not be discriminated. Such is the case for the type C distribution (Fig. 5c, d).

6. Conclusions

Our investigations clarified some important characteristics of the Rikitake dynamo. They are summarized below.

The system has two steady state solutions, corresponding to the normal (N) and reversed (R) states of the magnetic field. The instability grows as nearly sinusoidal oscillations around the N or R points. The trajectory in the phase space lies on the limit surface of Cook and Roberts (1970). When the amplitude increases, the oscillation deviates from sinusoidal shape, with sharp peaks and flat bottoms. x_2 , the smaller current is always the first one to oscillate beyond zero, while x_1 and the total current change polarity only after a few more oscillations when x_2 become sufficiently large in opposite polarity. In this sense it is the minor component of the system which triggers the reversal in the Rikitake dynamo. The stochastic model of Cox (1968) is similar in that the non-dipole component of the field triggers the reversal.

The manner of growth of oscillation amplitude is always the same and monotonic with time. There are certain limit in the peak amplitude for staying in the same polarity. When the peak exceeds this threshold value, polarity reversal takes place in the next oscillation cycle without fail. If a large amplitude was attained in the N (R) polarity before the reversal, the oscillation starts with small amplitude in the R (N) state and a very long polarity interval ensues, and vice versa (Cook and Roberts, 1970). The system is therefore quite deterministic in that the last amplitude *before* the reversal controls the oscillation *after* the reversal, and so almost everything of the next polarity interval. The apparently random behavior enters the system because the growth rate of amplitude is exceptionally large for the last oscillation before the reversal. A minute change in the variables some time before will cause a large difference in amplitude at the last moment, and therefore the next polarity interval will be quite different for such cases. It is typical of the chaotic system that an infinitesimal difference in the initial condition cause an arbitrarily large difference after sufficient time elapsed (Lorenz, 1963; May, 1976).

The statistical distributions of polarity intervals and field intensities reflect the manner with which the amplitude of oscillation grows, how near the steady state point (N or R) can be approached after reversal, and the threshold level of the peak amplitude. Both of them can be grouped into three types; (A) Three-peak intensity distribution with short polarity intervals only (one or two oscillation periods), (B) four-peak intensity distribution and exponential distribution for polarity intervals (truncated for longer intervals), and (C) sharp two-peak distribution for intensity and exponential distribution plus back ground of long intervals for polarity interval. Type C behavior occurs in the center of (μ, k) space surrounded by type B and then type A behaviors. The parameter range for type C behavior almost coincides with the MER region of Ito (1980).

Although a rich variety of behaviors can be produced in the Rikitake dynamo by changing (μ, k) , it is not possible to simulate the geomagnetic field to a satisfactory degree. The closest to the observed statistic properties of polarity intervals (Cox, 1968) and field

intensities (Kono, 1971) of the geomagnetic field are the models generated in the type C region. However, there are too many long polarity intervals in the reversal statistics and the intensity distribution is too much concentrated at the N and R mean intensities, which are very different from the paleomagnetically observed distributions. This confirms the result obtained earlier by Kono (1987).

References

- Allan, D.W., *Proc. Cambridge Phil. Soc.*, 58, 671-693, 1962.
Bullard, E.C., *Proc., Cambridge Phil. Soc.*, 51, 744-760, 1955.
Bullard, E.C., and H. Gellman, *Phil. Trans. Roy. Soc. Lond.*, A247, 213-278, 1954.
Cook, A.E., and P.H. Roberts, *Proc. Cambridge Phil. Soc.*, 68, 547-569, 1970.
Cox, A., *J. Geophys. Res.*, 73, 3247-3260, 1968.
Cox, A., *Science*, 163, 237-245, 1969.
Cox, A., *Geophys. J. Roy. Astron. Soc.*, 20, 253-269, 1970.
Harland, W.B., A.V. Cox, P.G. Llewellyn, C.A.G. Picton, A.G. Smith, and R. Walters, *A Geologic Time Scale*, pp. 63-84, Cambridge Univ. Press, London, 1982.
Ito, K., *Earth Planet. Sci. Lett.*, 51, 451-456, 1980.
Kono, M., *Earth Planet. Sci. Lett.*, 11, 10-17, 1971.
Kono, M., *Phys. Earth Planet. Inter.*, 5, 140-150, 1972.
Kono, M., *Geophys. Res. Lett.*, 14, 21-24, 1987.
Lorenz, E.N., *J. Atmos. Sci.*, 20, 130-141, 1963.
May, R.M., *Nature*, 261, 459-467, 1976.
McFadden, P.L., and M.W. McElhinny, *J. Geomag. Geoelectr.*, 34, 163-189, 1982.
Rikitake, T., *Proc. Cambridge Phil. Soc.*, 54, 89-105, 1958.

(Submitted to Journal of Geophysical Research)

NOBLE GAS SYSTEMATICS IN THE EARTH'S INTERIOR
-CLASSIFICATION OF NOBLE GAS COMPONENTS

Ichiro KANEOKA

Earthquake Research Institute, University of Tokyo,
Bunkyo-ku, Tokyo 113, Japan

1. Introduction

Compared with other isotopes, noble gas isotopes have several unique characteristics which make them as very useful indicators to infer the state of the Earth's interior. Since noble gases are chemically inert, the variation of isotopic ratios are controlled essentially by physical processes. The amounts of radiogenic components such as He-4 and Ar-40 are, however, controlled by both the amounts of parent elements and the time elapsed. Further, noble gases are relatively mobile compared with other elements. Especially He is most mobile among many elements except for hydrogen. Hence, He isotopes are easily homogenized in the Earth's interior. However, we can identify different He-3/He-4 ratios for samples from different geological circumstances of the magma sources, which becomes an important basis to infer the state of the Earth's interior. The Ar-40/Ar-36 ratio also indicates the different magma sources, because the ratios shows the integrated results of the K/Ar-36 ratio and the time since it retained Ar. This ratio also reflects the different history and condition of the magma sources. Thus the combination of the He-3/He-4 and Ar-40/Ar-36 ratios can be used as an effective tool to identify the magma sources (e.g., Kaneoka and Takaoka, 1980, 1985).

In order to identify the characteristics of magma sources in the mantle, several kinds of isotope combinations have been applied. The (Nd-143/Nd-144)-(Sr-87/Sr-86) diagram is now widely used since the development of this combinations (e.g., O'Nions et al., 1977). The (Pb-207/Pb-204)-(Pb-206/Pb-204) diagram has also been widely used, since both systematics are composed U and Pb isotopes (e.g., Tatsumoto, 1978). The (Hf-176/Hf-177)-(Sr-87/Sr-86) and the (Hf-176/Hf-177)-(Nd-143/Nd-144) diagrams are also developed (Patchett and Tatsumoto, 1980). With the accumulation of these data, it has been revealed that MORB (Mid-oceanic ridge basalt) and OIB (Oceanic island basalt) have different magma sources. Several models on the chemical structure of the mantle have been proposed on the basis of such data (e.g., Tatsumoto, 1978; Jacobsen and Wasserburg, 1979; O'Nions et al., 1979; Anderson, 1982). In these models, chemical models of the vertically layered mantles are most popular: one is the depleted mantle from which MORB is derived and the other is the fertile mantle from which mantle plumes would arise. On the other hand, some mantle models suggest that the fertile parts are distributed like spots in the depleted mantle (e.g., Davies, 1981; Zindler et al., 1984). However, these models are based mostly on the data for solid element isotopes such as Sr, Nd, Hf and Pb and they do not reflect the characteristics of the noble gas data, which would give important constraints on the chemical structure of the mantle.

Taking such a point into accounts, Kaneoka (1983) has tried to select the most probable one of the chemically layered model among the models proposed at that time. He has concluded that the OIB source, retaining the primordial components to some extent, should be located in the deeper part than the MORB source in the mantle. Based on the noble gas data, Allègre et al. (1983) have discussed the evolution of the Earth, implying the similar mantle structure. In the 1983 paper, Kaneoka has proposed the classi-

fication of noble gas data into several components and all observed data can be explained by mixing of these components. Such conjecture has been explained in more detail in Kaneoka and Takaoka(1985).

Below, such noble gas components are explained in more detail and their relationships with the geological circumstances are described.

2. The (He-3/He-4)-(Ar-40/Ar-36) diagram and classification of noble gas components

As introduced in the previous section, the combination of the He-3/He-4 and Ar-40/Ar-36 ratio gives characteristic features in defining each component in the Earth's interior. In Fig. 1, noble gas data for samples which would represent the present state of the Earth's interior are plotted. They include glassy parts of MORB, olivine and augite phenocrysts separated from recent lava flows, volcanic and natural gases. Since we cannot get direct information on the formation age of nodules in general case, nodules are excluded from this figure. In Fig. 1, we can identify that the observed data are scattered in limited regions according to their geological circumstances and they are schematically grouped in Fig. 2. For example, MORB shows relatively uniform He-3/He-4 ratios ($(1-1.4) \times 10^{-5}$)

with variable Ar-40/Ar-36 ratios. The variation in the Ar-40/Ar-36 ratio is commonly explained by contamination of the atmospheric component through air or sea water. If we assume that the typical MORB source has the Ar-40/Ar-36 ratio as assigned as M in Figs. 1 and 2, the mixing line between A (Atmospheric component) and M covers the observed data for MORB. Similar cases are observed for Icelandic gases. In this case, if we assume the typical end member as exemplified as P, most of the observed data can be explained as the result of mixing between P and A. Thus as shown in Fig. 2, all the observed data can be explained by mixing of at least four end members as defined from He and Ar systematics. They are P(Plume)-type, M(MORB)-type, A(Atmosphere)-type and C(Crust)-type (Kaneoka, 1983; Kaneoka and Takaoka, 1985). This does not always imply that only four end members exist in the Earth's interior. As stressed before, noble gases, especially He, are mobile and apt to be homogenized compared with other elements. Hence it should be noted that the He and Ar systematics still require the occurrence of different magma sources in the mantle as exemplified as P and M.

The M-type components are characterized by MORB, showing relatively uniform He-3/He-4 ratios together with relatively high Ar-40/Ar-36 ratios (more than 5,000). The P-type components are characterized by samples from some typical hot-spot areas such as Hawaii, Iceland and Reunion Islands,

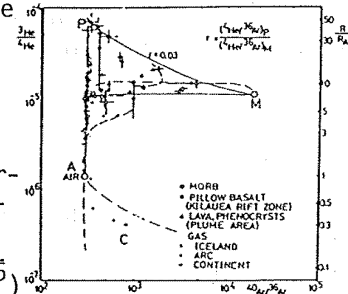


Fig. 1. The (He-3/He-4)-(Ar-40/Ar-36) diagram for samples which would represent the present state of the Earth's interior. P, M, A and C represent assigned end members for plume-, MORB-, atmosphere- and crust-type source materials, respectively. Solid lines indicate calculated mixing lines between each source. (After Kaneoka and Takaoka, 1985)

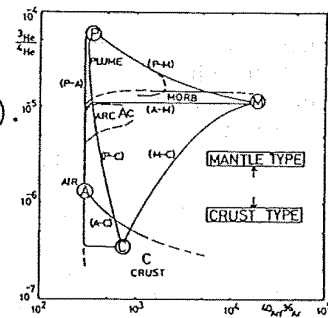


Fig. 2. Schematic diagram of mixing among several typical sources of noble gases in the (He-3/He-4)-(Ar-40/Ar-36) diagram. (After Kaneoka and Takaoka, 1985)

which show higher He-3/He-4 ratios and lower Ar-40/Ar-36 ratios (typically less than 1,000) than those of MORB. A-type components are characterized by the noble gas isotopes of the atmosphere, which are also similar to those of the sea water. C-type components are characterized by the typical crustal components, which have lower He-3/He-4 ratios than that of the A-type component and generally high Ar-40/Ar-36 ratios. However, C-type components are largely controlled by the geological history of the crust, including its formation age and degassing processes. Among these components, A-type component has unique values for the He-3/He-4 ratio (1.4×10^{-6}) and the Ar-40/Ar-36 ratio (295.5). As M-type and P-type components, the extreme values so far observed are selected as the end members for these components. The following values are adopted: P (He-3/He-4, 6×10^{-5} ; Ar-40/Ar-36, 350), M (He-3/He-4, 1.1×10^{-5} ; Ar-40/Ar-36, 20,000). They are assigned here to give just a measure for each component and may change to some extent with the accumulation of the data. Further it does not deny the occurrence of heterogeneity on local scale. The significant point is that at least two end members are required to explain the distribution of the data in the He and Ar systematics, which should exist on global scale.

In addition to these components, Ac(Arc)-type component may be raised as another one, which are characterized by the volcanic rocks and gases from the arc area and they show slightly lower He-3/He-4 ratios than those of MORB and relatively lower Ar-40/Ar-36 ratios, though the value is still larger than the A-type (Fig. 2). However, Ac-type values could be interpreted as a mixture of the M-, C- and A-type components, probably caused at the subduction area due to the addition of crustal components such as either continental crust or oceanic sediments to some extent. Hence we do not need to assign it as an end member in the mantle. If P-type and M-type materials are mixed as shown in Fig. 2, the resultant component would also be classified as Ac-type.

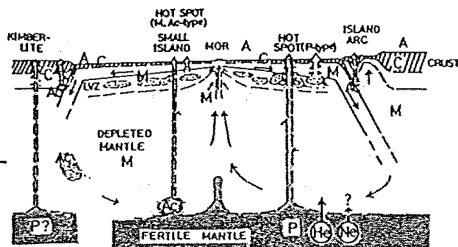
Compared with the M-type source, the P-type source should have higher He-3/U and lower K/Ar-36 ratios in order to explain the observed trend in Figs. 1 and 2. Since the M-type source is characterized by the depleted nature for incompatible elements including U and K, the P-type source contains larger amounts of U and K in general case. In Fig. 1, only recent samples which should indicate the present state of the Earth's interior are used. Hence these situations require that the P-type source should contain larger amounts of He-3 and Ar-36 than the M-type source. To explain such situation, Anderson(1985) has argued that such parts were formed due to the enriched processes in the mantle without degassing noble gases at a depth during the early history of the Earth and the present asthenosphere would correspond to such parts. However, Kaneoka(1983) has argued that the P-type component should be primordial and cannot be formed from the M-type component. In effect, to explain the occurrence of Ar-40 in the atmosphere, it is commonly admitted that the radiogenic Ar-40 derived from the K-40 in the Earth's interior was degassed through the history of the Earth. If we take this conjecture, it requires that radiogenic Ar-40 should have been degassed at least until 1-2 b.y. ago rather efficiently. Although we cannot identify the definite process to degas radiogenic Ar-40 so efficiently at present, we must admit that large parts of radiogenic Ar-40 should have been degassed from the Earth's interior. If it is, it is very difficult to imagine that only the asthenosphere could retain He and Ar as the enriched source. Generally, He has larger diffusion coefficient than Ar, indicating larger mobility than Ar. Hence it is more likely that the P-type source would be located in the deeper part than the M-type source and still retain primordial components. The degassing of radiogenic Ar-40 would have occurred mostly from the crust and the depleted (M-type) source.

are required to explain the present distribution of isotope data if we combine all the available data on solid element isotopes (e.g., Zindler et al., 1982). It should be mentioned, further, that the A-type source is not applicable to solid element isotopes, because it is characterized by the noble gas isotopes of the atmosphere and no solid elements exist in the atmosphere.

4. Noble gas components and the geological circumstances

In Fig. 5, the relationships among the noble gas components and the geological circumstances are shown schematically (Kaneoka and Takaoka, 1985). As shown in the previous section, these components are also correlated with solid element isotopes.

In this model, it is explained that the MORB source has a depleted character in incompatible elements as a result of extruding them to form crusts (especially continental crust). The fertile mantle, which contains primordial components, would exist below the depleted mantle and typical mantle plumes would arise from this layer.



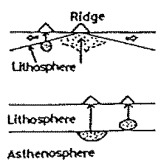
In Figs. 6(a) and 6(b), the relationships among each component and geological circumstances are schematically shown in more detail. As shown in Fig. 6(a), M-type materials are typically observed at a ridge. Small seamounts near the ridge would also have similar characteristics to MORB, because their source might have essentially no difference from that of MORB. For example, Zindler et al. (1984) have reported that the Sr-87/Sr-86 ratios of rocks of seamounts located near the East Pacific Rise are similar to those of MORB. Since it is assumed that the oceanic lithosphere and asthenosphere represent the M-type source, even a volcanic rock formed by the off-ridge volcanism would show the M-type characteristics, if it is derived from the asthenosphere. The thickening of the oceanic lithosphere can be explained by the addition of materials from the asthenosphere due to cooling of the uppermost region of the asthenosphere with time. Ultramafic nodules from the Hawaiian Islands show the M-type characteristics (e.g., Kaneoka and Takaoka, 1980). This may be explained as the result described above.

Fig. 5. Schematic diagram to indicate each type of noble-gas components in the Earth's interior. The arrows indicate the movement of materials on a global scale. LVZ indicates the low-velocity zone, which is probably partially melted. (Partly modified after Kaneoka and Takaoka, 1985)

(1984) have reported that the Sr-87/Sr-86 ratios of rocks of seamounts located near the East Pacific Rise are similar to those of MORB. Since it is assumed that the oceanic lithosphere and asthenosphere represent the M-type source, even a volcanic rock formed by the off-ridge volcanism would show the M-type characteristics, if it is derived from the asthenosphere.

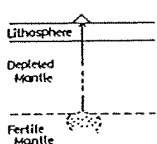
The thickening of the oceanic lithosphere can be explained by the addition of materials from the asthenosphere due to cooling of the uppermost region of the asthenosphere with time. Ultramafic nodules from the Hawaiian Islands show the M-type characteristics (e.g., Kaneoka and Takaoka, 1980). This may be explained as the result described above.

M(MORB) Type



$$\begin{aligned} {}^3\text{He}/{}^4\text{He}: & (6-10) R_A \\ & (1.0-1.4) \times 10^5 \\ {}^{87}\text{Sr}/{}^{86}\text{Sr}: & 0.7025 \\ & -0.7030 \\ {}^{143}\text{Nd}/{}^{144}\text{Nd}: & 0.5129 \\ & -0.5131 \end{aligned}$$

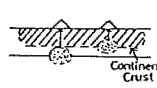
P (Plume) Type



$$\begin{aligned} {}^3\text{He}/{}^4\text{He}: & >10 R_A \\ & >1.6 \times 10^5 \\ {}^{87}\text{Sr}/{}^{86}\text{Sr}: & 0.7035 \\ & -0.7050 \\ {}^{143}\text{Nd}/{}^{144}\text{Nd}: & 0.5125 \\ & -0.5127 \end{aligned}$$

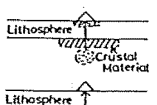
Fig. 6(a). M-type and P-type components and their geological circumstances.

C (Crust) Type



$$\begin{aligned} {}^3\text{He}/{}^4\text{He}: & < R_A \\ & < 1.4 \times 10^6 \\ {}^{87}\text{Sr}/{}^{86}\text{Sr}: & 2.0710 \\ {}^{143}\text{Nd}/{}^{144}\text{Nd}: & < 0.5126 \end{aligned}$$

Ac (Arc) Type



$$\begin{aligned} {}^3\text{He}/{}^4\text{He}: & (4-8) R_A \\ & (0.6-1.0) \times 10^5 \\ {}^{87}\text{Sr}/{}^{86}\text{Sr}: & 0.7040 \\ & -0.7060 \\ {}^{143}\text{Nd}/{}^{144}\text{Nd}: & 0.5124 \\ & -0.5126 \end{aligned}$$

Fig. 6(b). C-type and Ac-type components and their geological circumstances.

AUTHOR INDEX

ADACHI, Yasuhisa, H. Inokuchi, Y. Otofujii, N. Isezaki and K. Yaskawa	72
AKIMOTO, Takatoshi	see Kinoshita and Akimoto
BABA, Toshihiro	see Kodama and Baba
DANON, J.	see Funaki et al.
DOMEN, Haruo	36
FUJIWARA, Yoshiki, P. Gautam, M. Yoshida and Y. Katsui	7
FUNAHARA, Shoubu	see Otofujii et al.
FUNAKI, Minoru, I.Taguchi, J. Danon, and T. Nagata	1
FUNAKI, Minoru, M. Yoshida, and P.W. Vitanage	87
FURUTA, Toshio	see Kinoshita and Furuta
GAUTAM, Pitambar and M. Yoshida	68
GAUTAM, Pitambar	see Fujiwara et al.
HAYASHIDA, Akira and T. Yokoyama	27
HOSHI, Masayuki	see Kono and Hoshi
HYODO, Masayuki	see Katao et al.
IBARAGI, Kenzo	see Ueno et al.
INOKUCHI, Hiroo	see Adachi et al.
INOKUCHI, Hiroo	see Itota et al.
INOKUCHI, Hiroo	see Katao et al.
INOKUCHI, Hiroo	see Morinaga et al.
ISHIDA, Shiro	see Itota et al.
ISEZAKI, Nobuhiro	see Adachi et al.
ITOH, Yasuto	42
ITOTA, Chizu, H. Morinaga, H. Inokuchi, K. Yaskawa and S. Ishida	40
KAMINO, Masaki	see Morinaga et al.
KANEOKA, Ichiro	106
KATAO, Hiroshi, H. Morinaga, M. Hyodo, H. Inokuchi, J. Matsuda, and K. Yaskawa	75
KATSUI, Yoshio	see Fujiwara et al.
KIKAWA, Eiichi, M.Koyama and H. Kinoshita	24
KINOSHITA, Hajimu and N. Matsuda	96
KINOSHITA, Hajimu and T. Furuta	66
KINOSHITA, Hajimu, R. Morijiri, and T. Nagao	97
KINOSHITA, Hajimu and T. Akimoto	23
KINOSHITA, Hajimu	see Kikawa et al.
KODAMA, Kazuto and T. Baba	52
KONO, Masaru and M. Hoshi	98
KOYAMA, Masato	see Kikawa et al.
MATSUDA, Jun-ichi	see Katao et al.

P-type materials would only be observed on the surface when a plume is active enough to show its original characteristics. When a plume arises from a depth, it might be contaminated with the M-type materials during its ascent. Hence there is no reason to expect a priori that a lava flow from a hot spot would always show the characteristics of the P-type source. For example, in the Galapagos area, the He-3/He-4 ratios of the hydrothermals are similar to those of MORB (Lupton et al., 1977), though the place is assigned as a hot spot (Morgan, 1972). Since the area is close to the ridge, it might be affected by the activity of the ridge. Hence the apparent signature becomes M-type rather than P-type. On the other hand, as shown in the left-hand side of Fig. 5, the subducted lithosphere might not always be homogenized completely with the surrounding mantle materials. In such a case, the Ac-type material might be remained around the boundary region between the depleted mantle and the fertile mantle. When a plume arises through this material, it may be affected by this material and the observed values on the surface might show the Ac-type characteristics in some cases. Although Tristan da Cunha and Gough Islands are assigned to be hot spots (Morgan, 1972), their isotope signatures are similar to the Ac-type (e.g., Kurz et al., 1982). This may be explained by the processes stated above.

Ac-type materials are typically observed at the subduction areas, where the M-type materials are contaminated with C-type materials (continental crust and/or oceanic sediments). Although the Ac-type material can be defined from the isotope signatures, their source materials might be quite different in some cases. This situation is shown in Fig. 6(b).

As an example for the C-type component, natural gases from the old continent show generally very low He-3/He-4 ratios of less than 10^{-7} (e.g., Tolstikhin, 1978). The igneous rocks exposed on such a continent show much higher Sr-87/Sr-86 and lower Nd-143/Nd-144 ratios compared with P-type or M-type materials. Relatively old oceanic sediments might be classified into this component. Such cases are schematically shown in Fig. 6(b).

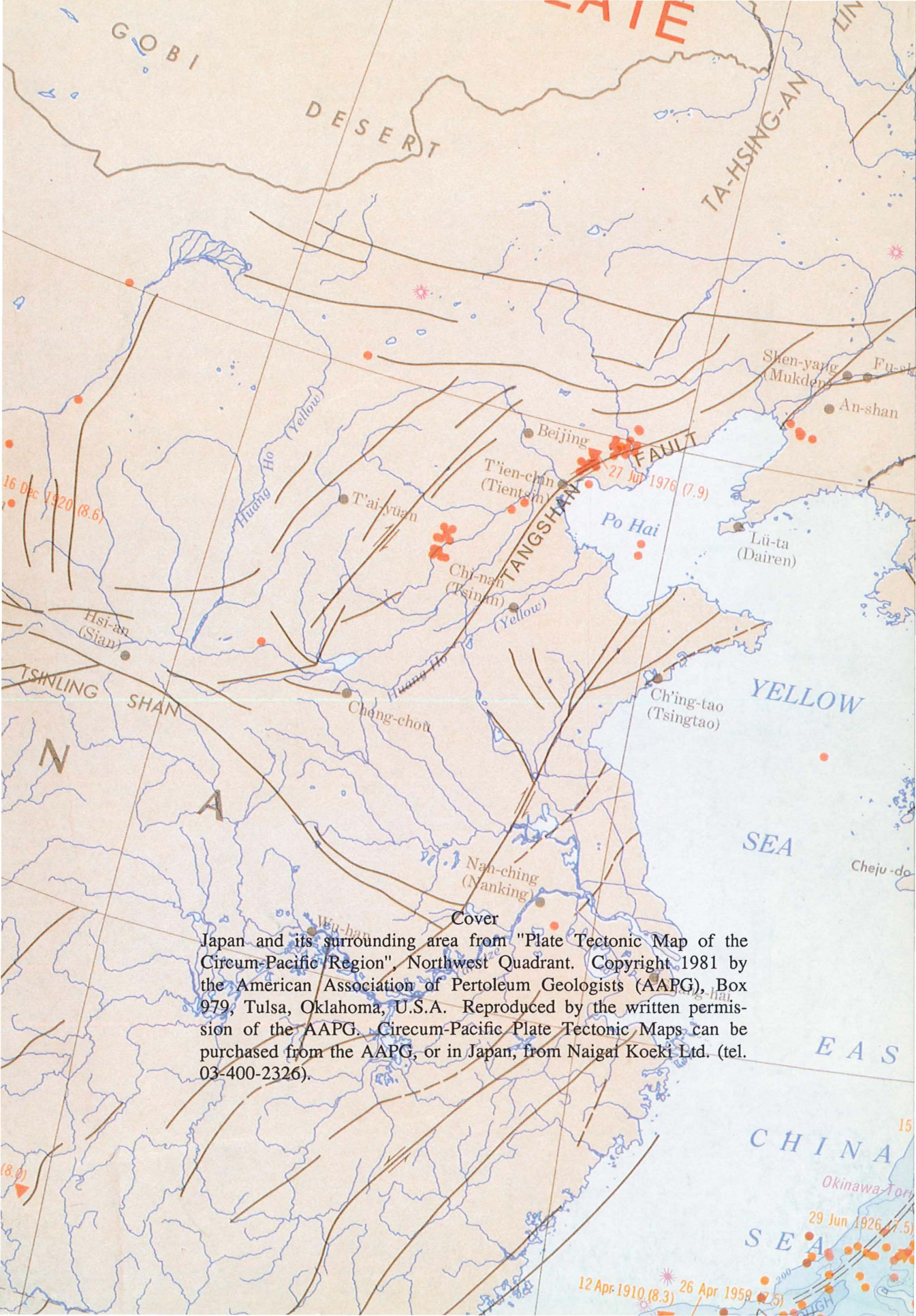
From the isotope data alone, we cannot assign the depth of the boundary between the depleted mantle and the fertile mantle. However if we take into accounts of other factors such as the concentrations of incompatible elements in each source, layering of the mantle based on the seismic data, the possible occurrence of magma ocean in the early history of the Earth and others, we might put the depth of about 650km as one of the possibilities for the depth of the boundary.

5. Other noble gas isotope characteristics of each component

Present classification of each component is based on He and Ar isotopes and the other noble gas isotopes are not used to define the component.

So far, no systematic variations are reported for Kr isotopes among each component except for the addition of fissiogenic components in U-enriched materials. Whereas, the occurrence of excess Xe-129 has been reported for MORB (e.g., Staudacher and Allègre, 1982), CO₂ well gases (e.g., Boulou and Manuel; Phinney et al., 1978) and some ultramafic nodules (e.g., Hennecke and Manuel, 1975; Kaneoka and Takaoka, 1978). The excess Xe-129 is generally attributed to the decay of extinct nuclide I-129 ($T_{1/2}=17$ m.y.), which means that the portion which contains the excess Xe-129 was never homogenized with the atmospheric components for more than about 4.3 b.y. Based on this systematics, Allègre et al. (1983) have argued that the depleted mantle was formed already more than 4.4 b.y. ago. Further, Staudacher (1987) has argued that the CO₂ well gases should be derived from a similar source to that of MORB. Whereas Ozima et al. (1985) have assigned the source of CO₂ well gases as a relatively primordial one

MATSUDA, Naoko	see Kinoshita and Matsuda	
MATSUDA, Takaaki	see Miki et al.	
MATSUO, Jun	see Otofujii et al.	
MIKI, Masako, T. Matsuda and Y. Otofujii	38
MORIJIRI, Rie	see Kinoshita et al.	
MORINAGA, Hayao, M. Kamino, H. Inokuchi and K. Yaskawa	13
MORINAGA, Hatao, H. Inokuchi and K. Yaskawa	18
MORINAGA, Hayao	see Itota et al.	
MORINAGA, Hayao	see Katao et al.	
MURATA, Fumiyuki	see Otofujii et al.	
NAGAO, Toshiyasu	see Kinoshita et al.	
NAGATA, T.	see Funaki et al.	
NEDACHI, Munetomo	see Ueno et al.	
NISHITANI, Tadashi and S. Tanoue	46
NISHIYAMA, Takashi	see Otofujii et al.	
OTOFUJII, Yo-ichiro	81
OTOFUJII, Yo-ichiro, S. Funahara, J. Matsuo, F. Murata, T. Nishiyama X. Zheng, and K. Yaskawa	79
OTOFUJII, Yo-ichiro	see Adachi et al.	
OTOFUJII, Yo-ichiro	see Miki et al.	
SUZUKI Ryoichi	see Ueno et al.	
TAGUCHI, T.	see Funaki et al.	
TANOUE, Seiji	see Nishitani and Tanoue	
TORII, Masayuki and H. Tsurudome	59
TSURUDOME, Hisashi	see Torii and Tsurudome	
UENO, Hiroto, M. Nedachi, Y. Urashima, K. Ibaragi and R. Suzuki	31
URASHIMA, Yukitoshi	see Ueno et al.	
VITANAGE, P.W.	see Funaki et al.	
YAMAZAKI, Toshitsugu	92
YASKAWA, Katsumi	see Adachi et al.	
YASKAWA, Katsumi	see Itota et al.	
YASKAWA, Katsumi	see Katao et al.	
YASKAWA, Katsumi	see Morinaga et al.	
YASKAWA, katsumi	see Otofujii et al.	
YOKOYAMA, Takuo	see Hayashida and Yokoyama	
YOSHIDA, Mitsuo	see Fujiwara et al.	
YOSHIDA, Mitsuo	see Gautam and Yoshida	
YOSHIDA, M.	see Funaki et al.	
ZHENG, Xilan	see Otofujii et al.	



Cover
 Japan and its surrounding area from "Plate Tectonic Map of the Circum-Pacific Region", Northwest Quadrant. Copyright 1981 by the American Association of Petroleum Geologists (AAPG), Box 979, Tulsa, Oklahoma, U.S.A. Reproduced by the written permission of the AAPG. Circum-Pacific Plate Tectonic Maps can be purchased from the AAPG, or in Japan, from Naigai Koeki Ltd. (tel. 03-400-2326).